STUDIES ON ELECTRICAL AND THERMAL PROPERTIES OF CERTAIN SELECTED PHOTONIC MATERIALS

THESIS SUBMITTED TO
THE COCHIN UNIVERSITY OF SCIENCE AND TECHNOLOGY
FOR THE AWARD OF THE DEGREE OF
DOCTOR OF PHILOSOPHY

EDWIN XAVIER

INTERNATIONAL SCHOOL OF PHOTONICS
COCHIN UNIVERSITY OF SCIENCE AND TECHNOLOGY
KOCHI - 682 022, INDIA

MARCH 1997

CERTIFICATE

Certified that the research work presented in this thesis is based on the original workdone by Mr. Edwin Xavier under my guidance in the International School of Photonics and initially in the Department of Physics, Cochin University of Science and Technology and has not been included in any other thesis submitted previously for the award of any degree.

Cochin - 682022
14 th March 1997

Prof.(Dr.) C.P.Girijavallabhan
(Supervising Teacher)
Director,
International School of Photonics
Cochin University of Science and
Technology,Cochin - 682022.

DIRECTOR
International School of Photonics
Cochin University of
Science & Technology
Cochin - 682 022

International School of Photonics
Cochin - 682022
Date .....
Cochin University of Science & Technology

DECLARATION

Certified that the work presented in this thesis is based on the original work done by me under the guidance of Prof. (Dr.) C.P. Girijavallabhan in the International School of Photonics and initially in the Department of Physics, Cochin University of Science and Technology, and has not been included in any other thesis submitted previously for the award of any degree.

Cochin - 682022
14 th March 1997

Edwin Xavier

PREFACE

Researchers have been engaged in developing newer and better materials which should have striking properties suitable for applications in different fields like industry and technology. An entirely modern research field called "Material Science" has emerged to develop noval materials with attractive structure and properties so as to enable the design and fabrication of new devices and systems. Along with the above mentioned experimental developments and discoveries, a large effort has gone into understanding of the properties of materials which include structural, electrical, magnetic, optical, thermal and mechanical behaviour. In this context characterization of these materials becomes extremely important as it throws light on the behavior of these substances under different conditions. Several tools and techniques have been employed in recent times for this purpose. Measurement of electrical and thermal properties acquire great importance in this scenario. Two key parameters viz: the electrical conductivity, dielectric constant give valuable informations on the properties and prospects of the sample under investigation. Photoacoustic technique is a comparatively noval approach and currently it has been used for the measurement of thermal and optical properties of many materials.

The conductivity of a solid dielectric depends mainly upon the mobility of ions and other charge carriers and on their concentration. A basic question in the measurement

of conductivity of dielectrics is whether the transport process is electronic or ionic. Because of the general similarity between the expressions for ionic conductivity and for electronic semiconduction in a dielectric, it is often difficult to distinguish experimentally between the two types of conduction mechanism. However, the activation energy calculation reveals the dominant factor responsible for conduction process. Phase transitions occurring in materials are also a striking phenomenon which have a direct impact on the electrical properties of solids. A phase transition leaves its own impressions on the key parameters like electrical conductivity and dielectric constant. The interest in the Photoacoustic (PA) effect as a new experimental tool to unravel the thermal and optical properties of solids grew appreciably in the last ten years. The basic mechanism of the photoacoustic effect is that a sample illuminated by modulated light and is heated periodically by nonradiative transitions following optical absorption. Indirectly these effects can be detected by taking the sample in an enclosed cell along with a sensitive microphone and measuring the sound wave generated in the coupling gas medium. The PA technique has been applied to a large range of problems, in particular to the study of the thermal properties of different materials. Using PA technique, thermal diffusivities of thin films, polycrystallines and single crystals have been determined precisely and such measurements provide the absolute values of thermal diffusivity of samples as a function of temperature. Among many techniques now available, the PA technique has been revived as a very useful and ideal technique for the thermal and spectroscopic investigation.

The present thesis attempts to summarise the work carried out in the above directions by the author during the past few years in the International School of Photonics and initially in the Department of Physics of Cochin University of Science and Technology.

The thesis contains 8 chapters which are divided into two parts **A** and **B**. Part A includes three chapters which describe the detailed investigations carried out in pure single crystals pressed pellets of Ammonium Dihydrogen Phosphate and Ammonium Iodate using dc electrical conductivity and dielectric constant measurements. Special attention has been paid to reveal the mechanisms of electrical conduction in various phases of these samples and those associated with different phase transitions occurring in them. Part B contains the remaining five chapters in which the details of the measurement of thermal diffusivity on Phthalocyanines, axis-wise measurement of thermal diffusivity in single crystals of Potassium Dihydrogen Phosphate ,thermal diffusivity of metallic thin films and the over all conclusions are presented.

In the first chapter a general introduction is provided to give an overview of the importance of the study of electrical conduction ,dielectric properties and phase transition in solids and their theoretical aspects. This chapter also describes, the technique generally employed to study the mechanisms of electrical conduction as well as the different experimental system employed for these investigations.

The investigations carried out on an important photonic materials viz: Ammonium Dihydrogen Phosphate single crystal in the temperature range 100 K to 400 K using dc electrical conductivity measurements are presented in the second

chapter. The results obtained show that this material undergoes a drastic change at 147 K with a hysteresis of 1.1 indicating a first order phase transition at this temperature unlike other ionic crystals in this category. The directional change which is observed for the first time in the conductivity plot undoubtfully confirm that, the crystal exhibit pyroelectric behaviour at the phase transition point. This observation is in good agreement with the possible coexistence of two phases at low temperature transition point in ADP crystals. Electrical conductivity at low temperature could be resulting from protonic motion in addition to a small contribution due to impurity dominated extrinsic conduction.

Chapter III presents the results of dc electrical conductivity and dielectric constant measurements carried out in Polycrystalline Ammonium Iodate in the temperature range 300 K to 420 K. Both the above properties exhibit anomalous variations at 363 K thereby confirming the occurrence of a first order phase transition in this material. The variation of dielectric constant as a function of temperature for different frequencies has also been investigated. The activation energy values in this material indicates that protonic conduction is the dominant mechanism responsible for the electrical conductivity of this material.

Chapter IV, which is listed in the Part B, gives a summary of photoacoustic theory in solids. Photoacoustic effect has been employed fairly extensively to obtain information on thermal properties of materials. A model which has been extensively used to explain the PA effect is that of Rosencwaig and Gersho here afterwards refered to as RG theory. Rosencwaig has given expressions for the pressure

amplitude as measured by the microphone which can then be simplified depending upon the thermal characteristics of the sample.

During the last decade, several methods have been developed to determine thermal diffusivities with high precision. The most widely used method is based on the photoacoustic effect. It includes both front surface excitation and rear surface excitation. The fifth chapter describes the thermal diffusivity measurements in metal free Phthalocyanines, Metal phthalocyanines and iodine doped Metal phthalocyanines using front surface excitation technique. Phthalocyanines and its metal complexes play a key role in the field of molecular semiconductors. Its structure corresponds to the porphyrins, of which class chlorophyll is a member. Recently Metal Phthalocyanines have emerged as a noval class of materials for optical, electrophotographic and photovoltaic applications. The are also expected to serve as active materials for molecular electronic devices such as electrochromic displays and chemical sensors. Recent reports shows that organic dyes such as phthalocyanines are very good material for optical data storage applications in the place of metallic substances because of their chemical stability and feasibility for synthetic engineering. Because of its high thermal and chemical stability, Phthalocyanines have become the focus of recent research. The results indicates that doping with iodine enhances the thermal diffusivity in a substantial manner in Metal Phthalocyanines. Photoacoustic technique provides a very convenient method for obtaining the thermal conductivities along the different crystallographic axes for small sample.

In the sixth chapter, axis wise measurements of thermal diffusivity carried out for the first time in single crystals of Potassium Dihydrogen Phosphate (KDP) have been described. The anisotropy in thermal conductivity of KDP crystal has been demonstrated using photoacoustic technique. It has been found that thermal diffusivity decreases with temperature along a/b as well as c- axes. Thermal diffusivity measurements in thin films using rear surface illumination method have been described in the seventh chapter. It describes the fabrication details and performance of the cell used for this purpose. Thin films of Indium ,Aluminium, Silver and CdS prepared from vacuum coating technique have been used for measurements. Thermal diffusivity values obtained using this cell shows close agreement with the previously reported values for standard materials.

The last chapter provides an over all summary and conclusion of the whole work presented in the thesis.

Part of the investigations contained in this thesis has been presented in conference or published / communicated in the form of following papers.

1. Electrical conductivity, Dielectric constant and phase transition in NH_4IO_3,
   Edwin Xavier, R.Navil Kumar and C.P.G.Vallabhan
   Solid State Ionics:Materials and applications, **1**, 711 (1992).

2. Investigation of low temperature phase transition in $NH_4H_2PO_4$ using dc conductivity measurements.
   Edwin Xavier, R.Navil Kumar and C.P.G.Vallabhan.
   Proceedings of the Solid State Symposium, BARC, Bombay,
   33C, 321 (1991).

3. Photoacoustic detection of the low temperature phase transition in $NH_4H_2PO_4$. Edwin Xavier, R.Navil Kumar and C.P.G.Vallabhan., Proceedings of the Solid State Symposium, BARC, Bombay, **33C**, 304, (1991).

4. Detection of low temperature phase transition in $(NH_4)_2Cr_2O_7$ using photoacoustic technique. R.Navil Kumar, Edwin Xavier and C.P.G.Vallabhan., Proceedings of the Solid State Symposium, BARC, Bombay, **33C**, 305 (1991).

5. Observation of high temperature phase transition in NH_4IO_3 and $NH_4IO_3Te(OH)_2$ by dielectric measurements, Leena .P.P., Edwin Xavier and C.P.G.Vallabhan. Proceedings of the Solid State Physics Symposium, Varanasi. **34 C**, 386 (1991)

6. A Photoacoustic cell for rear side illumination of thin films., Edwin Xavier and C.P.G.Vallabhan., Proceedings of National Symposium on Instrumentation CUSAT, Cochin, **C40** 23 (1991).

7. Electrical conductivity and Thermal diffusivity of Zinc Naphthalocyanine, Jayan Thomas, V.N.Sivasankara Pillai, Edwin Xavier and C.P.G.Vallabhan, Journal of Material Science Letters **15** , 151 (1996).

8. Photoacoustic measurements of thermal diffusivity in metal phthalocyanines, Edwin Xavier, C.P.G.Vallabhan, Jayan Thomas and V.N.Sivasankara Pillai, Journal of Matieral Science Letters (communicated.)

9. A Study of low temperature phase transition in $NH_4H_2PO_4$ using dc conductivity measurements. Edwin Xavier, and C. P.G.Vallabhan. Journal of Material Science (communicated.)

10. Thermal diffusivity measurement of Europium Diphthalocyanines using Photoacoustic technique.
Jayan Thomas, V.N.Sivasankara Pillai, Edwin Xavier and C .P. G. Vallabhan.
Proceedings of National Symposium on Current Trends in Coordination Chemistry, Cochin , **1**, 49 (1995).

11. Photoacoustic measurement of Thermal diffusivity in metal phthalocyanines,
Edwin Xavier C.P.G.Vallabhan, Jayan Thomas and V.N.Sivasankara Pillai.
Proceedings of the National Laser Symposium, Dehradun. **1**, 99 (1995).

ACKNOWLEDGEMENTS

The investigations presented in this thesis have been carried out under the guidance and supervision of Prof.(Dr.) C.P.Girijavallabhan, Director, International School of Photonics, Cochin University of Science and Technology. It is with great pleasure I express my sincere gratitude for his able guidance and competent advice throughout the course of this work.

I am thankful to Prof. K. Babu Joseph, Head of the Department of Physics, Cochin University of Science and Technology for providing necessary facilities to carry out this work in the earlier stage.

The immense help and encouragement I have received from all the members of the faculty of the International School of Photonics as well as the Department of Physics are gratefully acknowledged.

I am highly indebted to Prof. Antony Issac, the former Principal of St. Paul's College, Kalamassery, for giving me constant encouragement and inspiration throughout the period of this work.

I would like to thank Dr. Navil Kumar and Dr. N.S. santhakumari for their constant help and interest in this work.

The constant help and co-operation received from the technical, administrative and library staff are sincerely acknowledged. Special thanks goes to the staff of the University Science Instrumentation Centre for their timely help and advice in fabricating various parts of experimental systems.

I express my sincere thanks to all my colleagues Dr.Vidyalal, Dr. Rajasree, Mrs. Anieta Philip, Mr. Sankararaman, Mr.Harilal, Miss. Latha K.P. and Mr. Dileep Chandra for their whole hearted co-operation and help.

Finally, I would like to thank Dr. Jayan Thomas for his help and interest in this work.

Edwin Xavier

CONTENTS

PART - A Page No.

CHAPTER 1 : INTRODUCTION

PART - A

CHAPTER 1

INTRODUCTION .

1.1. ABSTRACT

This chapter presents an overview of ideas and concepts necessary for the exposition of the importance of the study of electrical properties of solids. It also describes a reasonably comprehensive theoretical basis of some of the thermodynamical aspects of phase transition process. The experimental techniques generally employed in the study of phase transitions are also specified in this section. The methods used to grow single crystals and the details of a metallic cell used for low and high temperature electrical measurements are also described in the present chapter.

1.2. A brief history of Photonic materials

Optics is an old and venerable subject involving the generation, propagation and detection of light. Three major developments, which have been achieved in the last thirty years, are responsible for the rejuvenation of optics and for its increasing importance in modern technology. These landmarks are the invention of the laser, the fabrication of low-loss optical fibers, and the introduction of semiconductor optical devices. As a result of these developments, new disciplines have emerged and new terms describing these disciplines have come into use: electro optics, optoelectronics, quantum electronics, quantum optics and light wave technology are some of the terms in this new technology. However, in recent years, the term photonics has become increasingly popular. This term, which was coined in analogy with electronics, reflects the growing tie between optics and electronics forged by the increasing role that semiconductor materials and devices play in optical systems. The term photonics is used broadly to encompass all of the aforementioned areas including the functions such as amplification, detection, frequency conversion, switching etc. in different regions of the electromagnetic spectrum.

The ancient achievements in developing materials inspire us to achieve new heights in the modern era especially when we consider many new elements which have been discovered and a variety of materials developed, by different combination of atoms and processes for use in our every day life and also for specific high technology applications. These include semiconductors used extensively in electronic devices and in all present day computers, superconductors, polymers, amorphous materials such as

amorphous silicon which is useful for solar cell applications, liquid crystals which are used in displays, quasi crystals, and more recently nanomaterials which could lead to technological breakthroughs such as nanostructured tunable lasers and materials where clusters rather than atoms would be the building blocks. All these developments have come from extensive and innovative research and from the progress in analytical and experimental techniques which are now developed to a level that even information with atomic resolution can be obtained using the high resolution electron and the scanning tunnelling microscopes (STM) and it has become possible to prepare structures atom by atom. Along with the above mentioned experimental developements and discoveries, a large amount of effort has gone into understanding of the properties of materials which include structural, electrical, magnetic, optical, thermal and mechanical behaviour. In the course of these experiments, researchers encountered certain interesting and important optoelectronic phenomena associated with materials, suitable for application in the field of photonics. Those materials are generally termed as " photonic materials" and the list of such materials is very lengthy. We have selected only a few of such materials, which are comparatively important, for our present investigation.

1.3. Importance of the study of electrical properties of the material.

Some of the electrical properties like electrical conductivity and dielectric constant have been used to characterize the materials and to study the phase transitions in them. The study of electrical conduction process in materials can yield a great deal of valuable information on the formation and migration of charge carriers in materials.

Basically electrical conductivity in materials is a defect controlled phenomenon and hence detailed investigation of the electrical properties of the materials is one of the best available methods for the study of defects concentration. Recently, the electrical conductivity and dielectric constant measurements have become accepted as a very sensitive method for the study of phase transition as well as for the study of defects in ammonium containing crystals [1-10]. Usually these electrical properties are investigated as a function of temperature or as a function of pressure.

1.4. Electrical conduction in dielectrics.

Knowledge of electrical conduction in materials is the fundamental basis for the development of the branch of physics called Material Science and Technology. Most of the solid state devices developed in the last three decades are based essentially on the motion of the electrons. After the discovery of fast sodium ion conduction in β-alumina and silver ion conduction in $MAg_4 I_5$(M=K,Rb,NH_4) in 1967 [11,12], ionic solids have been found numerous applications in fabricating solid state batteries, fuel cells, memory devices, display panels etc. Nowadays a large number of Physicists, material Scientist and Engineers are engaged to develop a high density solid state battery for vehicular traction and low density miniaturized batteries for device applications. In this respect, the role played by the superconducting materials is very important in the sense that, these materials are potentially important from the point of view of technical applications.

The foundations upon which our understanding of ionic conductivity are built were laid down before 1940 by the early work of Schottky [13],Wagner [14] and Mott and Littleton [15,16]. It was found that the transference of mass and charge occurring in alkali halide crystal is mainly by means of ionic processes. Later the subject of ionic conductivity was expounded at length by Lidiard [17-19], Fuller [20-25], Barr [26,27], Franklin [28] etc. In addition to these, some other notable works [29-35] can also be found in literature.

1.5. Simple theory of electrical conduction in dielectrics.

All materials conduct electricity to a greater or lesser extent, and all suffer some form of breakdown in a sufficiently strong electric field. For low field strengths the conduction process in most material is ohmic, but as the field strength is increased further some form of destructive irreversible conduction takes place. The conductivity of dielectrics may be either ionic or electronic or both. A basic question in measurements of the conductivity of dielectrics is whether the transport process is electronic or ionic. Because of the general similarity between the expressions for ionic conductivity and for electronic semi conduction in dielectrics, it is often difficult to distinguish experimentally between the two types of conduction. Ionic conductivity is simply due to the migration of positive or negative ions. This could arise in a dielectric in two different manners; in an ionic crystal such as an alkali halide the basic constituents are ions and physical imperfections alone can be responsible for mechanisms of current flow, while in a non ionic substance chemical imperfection

is required to supply the mobile species. The basic theoretical expression for all electrical conductivity is,

$$\sigma = \sum n_i e_i \mu_i \quad \text{----------} \quad (1.1)$$

where n_i is the density of carriers of the i^{th} species, and e_i and μ_i the corresponding charges and mobilities. In the usual analysis of experimental low field ionic conductivity, one write ,

$$\sigma = \sigma_0 \exp.(\Phi/kT) \text{----------} (1.2)$$

where σ_0 and Φ are experimentally determined (usually constants with in some given range of temperatures), k is Boltzmann's constant and T the absolute temperature. Since both the density and the mobility of the migrating species are usually temperature dependent, the single temperature dependent term in equation (1.2) combines the effect of temperature on both n_i and μ_i of equation (1.1). The field dependence of ionic mobility should be small, but the concentration of charge carriers could be strongly influenced by an electric field. The simplest understanding of electronic conduction in a solid dielectric arises from modifications to the quantum mechanical band theory of solids. This gives a picture of a dielectric in which a series of allowed electronic energy bands are completely occupied by electrons up to a certain level, and empty there after. The conduction band does not give rise to any conductivity since it contains no electrons, and neither

does the valence band conduct since there are no unoccupied states into which an electron can be accelerated by an applied field. This simple picture applies only to a perfect crystalline insulator at the absolute zero of temperature. But in real insulators at finite temperature, trapping levels are caused by the influence of foreign ions, vacant lattice positions, interstials etc. on the normal lattice field. In general only the conduction and valence levels are important in pure, strain free crystals at low temperatures. The relative importance of isolated levels increases with admixture of foreign ions, mechanical strain, and rise in temperature. In band theory the effect of an applied electric field is regarded as causing an acceleration of conduction electrons in the band; it may however be more correct to regard the electric field as causing transitions between adjacent but more or less localized states of the conducting electrons. This mechanism is referred to as hopping conduction, and the conducting electron is regarded as making its way through the dielectric in a series of discrete movements. Band conduction and hopping conduction are not regarded as the antithesis of each other; rather the latter is a more appropriate visualization than the former in the limiting case of narrow bands. These simple ideas of the electronic conductivity of dielectrics fail in a striking way for certain of the transition metal oxides. Regardless of the theoretical model which one may adopt to explain electrical conduction in the insulating transition metal oxides, the experimental data is adequately described in terms of an activation energy with the conductivity given by equation (1.2).,The basic theoretical steady state conduction equation is

$$j = \sigma E \text{ ---------- } (1.3)$$

where j is the current density, E, the electric field strength and σ the electrical conductivity defined by equation (1.1). The experimentally measured quantities are the current I and the voltage V. The simplest procedure to establish a connection between theory and experiment is to write,

$j = I/A$ and $E = V/d$ ----------(1.4)

where A is the cross sectional area and d, the thickness of the specimen. Since the breakdown path usually extends over only a tiny fraction of the cross sectional area, the current density in the break down channel is much higher than would be found by the application of equation (1.4) for prebreakdown current; it is therefore used for lack of anything better. The correct relation between voltage difference and field strength across the dielectric involves consideration of space charges.

1.6. Dielectric Constant.

The investigation of dielectric properties has provided an important approach to an understanding of the structure of matter, and, without some understanding of the relation of these properties to the structure of the materials, our extensive knowledge of dielectric behavior loses much of its significance. The so called static or low frequency dielectric constant will be examined first, since it has thus proved most useful in investigating structure and since understanding of the static constant is necessary for the treatment of the high frequency constant. The dielectric properties of a material are governed by the response of the material to an

applied electric field at the electronic, atomic, molecular and macroscopic levels. If an electric field is created in a dielectric material the dipole moments of separate kinetic elements or atomic groups will tend to orient in the field direction. If the external electric field is now removed then after a certain time the polarization of the sample will diminish to zero as a result of thermal motion of separate kinetic elements, and the system will return to its previous equilibrium state. Such a process of transition to equilibrium is called dielectric relaxation. It is characterized by the relaxation time τ. On the other hand if an alternating voltage is applied to the dielectric, the dielectric properties of the material will obviously depend on the relation between the frequency of the applied voltage ω and the dielectric relaxation time τ.The dielectric properties of the specimen can be characterized by the, complex dielectric constant,

$$\varepsilon^{*} = \varepsilon^{1} - i\,\varepsilon^{11} \text{ ---------- (1.5)}$$

where ε^{1} the real component of complex dielectric constant, and ε^{11} the imaginary component of complex dielectric constant (also called the dielectric loss factor),

The ratio $\varepsilon^{11} / \varepsilon^{1} = \tan\delta$----------(1.6)

is the dielectric loss tangent. It characterizes the phase shift between the alternating voltage applied to the capacitor between whose plates the sample is

placed and the current passing through the capacitor. If the dielectric relaxation can be described by a single relaxation time then,

$$\varepsilon^{1} = \varepsilon_{\alpha} + (\varepsilon_{0} - \varepsilon_{\alpha} / 1 + \omega^{2} \tau^{2}) \text{---------- (1.7)}$$

$$\varepsilon^{11} = (\varepsilon_{0} - \varepsilon_{\alpha})\, \omega\tau \,/\, (1 + \omega^{2} \tau^{2}) \text{- ----------(1.8)}$$

where ε_0 is the dielectric constant at $\omega = 0$.

ε_α, the dielectric constant at ω = infinity and,

$$\tan \delta = (\varepsilon_{0} - \varepsilon_{\alpha})\, \omega\tau \,/\, (\varepsilon_{0} + \omega^{2} \tau^{2}) \text{----------(1.9)}$$

If ε_0 the static dielectric constant, ε_r , the relative permittivity, ω, the angular frequency and tan δ the loss tangent, then, σ_{ac} can be found out by the equation,

$$\sigma_{ac} = \varepsilon_{0}\, \varepsilon_{r}\, \omega \tan \delta \text{----------(1.10)}$$

1.7. Protonic Conductors.

Protonic conductors assume significance in fuel cells, high energy density batteries and in sensors. This recent interest has initiated detailed investigation on thermally stable protonic conductors [36,37].The existence of proton as a conductor in a medium is not that simple as it appears to be. An unsolvated proton has a very small radius, such free protons are not found in materials under equilibrium

conditions. Hydrogen atom is covalently bond to electronegative atoms such as carbon, nitrogen or oxygen. Hydrogen has the rare capability for expanding its covalency forming additional bond (hydrogen bond) which is characterized by directional properties. Oscillations of the hydrogen atom in such situations would effectively lead to a shift in its equilibrium position. This is equivalent to the transport of a proton. Since the hydrogen bond has directional characteristics, transport of a proton across a hydrogen bond has different magnitudes along different crystal axes depending upon the lattice structure.

1.8. Mechanism of Proton Conduction.

1.8a. Liquid Transport.

Certain protonic conductors with layered structure contain intercalated water molecule. In these layered materials, water molecules present in the interlayer space form a liquid like network permitting high protonic conductivity [38]. In pellicular materials with absorbed moisture, the water present on the surface and in the interpellicular space can also act as a liquid transport medium [39].

1.8b. Proton Jump followed by reorientation of hydrogen bonds.

Proton jump is often possible by a process of tunneling through a hydrogen bond. In effect, a reorientation of the hydrogen bond occurs. This mechanism operates

in hydrated salts, ammonium salts and organic acids. The probable modes of transport are described below.

(i) Polyatomic ion migration (vehicle mechanism).

This conduction mechanism operates strongly in acidic media containing water where H_3O^+ species is dominantly present, e.g. H_3O^+ - β- alumina [40], phosphomolybdic acid etc. [41]. In these cases H_3O^+ species migrates, thus effectively transporting H^+ A layered configuration of the anions facilitates this type of vehicular transport. Since the transport involves migration of massive polyatomic ions, the activation energy of the process is fairly high.

(ii) Cooperative proton transfer (Grothus mechanism).

Conduction can also occur due to proton exchange across a continuous chain or network of hydrogen bonds. This occurs in some layered hydrates which are weakly acidic or basic. The activation energy in such cases will be due to the barrier for the reorientation of the hydrogen bond and will be low in magnitude.

1.9. Protonic Conduction in Ammonium Salts.

Electrical properties of ammonium salts such as NH_4Cl and NH_4Br have been extensively investigated by various workers [42-49]. Herrington and Staveley made a comparative study of the electrical conductivity of NH_4Cl, NH_4Br, NH_4I,$(NH_4)_2SnCl_6$ and NH_4PF_6. They concluded that protons play a dominant role in charge

transport in these ammonium salts. Later investigation on NH_4 Cl and NH_4 Br support the observations of Herrington and Staveley. Murti and Prasad [46] have probed phase transition using electrical conductivity measurements. They ascribed the excess conductivity observed at the phase transition to the release of protons from freely rotating ammonium ions. This well fit into the proton transport mechanism proposed by Herrington and Staveley .

A survey of the literature reveals that $NH_4H_2PO_4$ (ADP) is an ammonium compound thoroughly investigated by several research groups [51-56]. Harris and Vella [53] have unambiguously proved that ADP dissociates according to the scheme,

$$NH_4H_2PO_4 \longrightarrow NH_3 + H_3PO_4$$

This process was detected at all temperatures above 40^0 C. C.P.G.Vallabhan et.al. have investigated a number of ammonium salts like $(NH_4)_2SO_4$, $LiNH_4SO_4$, $NH_4H_2PO_4$, , $(NH_4)_3H(SO_4)_2$, $(NH_4)Cr_2O_7$ and $(NH_4)_2HPO_4$ by dc and ac electrical conductivity and ionic thermocurrent measurements [1-10].

1.10. Application of Protonic conductors.

An era of active research in solid state protonic conductors was opened up by the energy crisis in early seventies. From the energy point of view major application of solid state protonic conductors is as electrolytes in fuel cells meant for stand alone power systems, heavy duty automobile traction and electricity storage by the

hydrogen route. Other applications include hydrogen concentration cells, batteries and sensors.

1.11. Phase transition and its thermodynamical aspects.

Phase transitions are common occurrences in matter. The subject of phase transition is of vital interest to physicists, chemists, metallurgists and others involved in the study of solids. This cross disciplinary subject is not only of academic importance, but also of technological relevance. The field of phase transitions in solids is characterized by a huge amount of experimental materials and by a relative scarcity of satisfactory theories. From experience we find it simplest to characterize a phase transition as the manifestation of a certain singularity or discontinuity in the equation of state. To explain the properties of a material and to develop new materials, a basic understanding of phase transformation is required. A greater understanding of the structure and properties of materials undergoing phase transitions has resulted by the introduction of modern technique and highly sophisticated instruments.

The most fully developed theories of phase transitions are based on thermodynamics and in particular, on statistical thermodynamics. A given assembly of atoms or molecules in solids may be homogeneous or nonhomogeneous. The homogeneous parts of such an assembly called phases, each possessing its characteristic energy, temperature and entropy. An isolated phase is stable only when its energy or more generally, its free energy is a minimum for the specified

thermodynamic conditions. As the temperature, pressure, or any other variable like an electric or a magnetic field acting on a system is varied, the free energy of the system changes smoothly and continuously. Whenever such variations of free energy are associated with changes in structural details of the phase (atomic or electronic configurations), a phase transition is said to occur. Gibbs who was the first to give a rather complete analysis of transformations on this basis, by considering the function,

$$G = U - TS + PV \text{ ---------- } (1.11)$$

Where G is known as the Gibb's function [57]. An equilibrium between phase 1 and phase 2 at a given temperature T , and pressure P requires $G_1 - G_2 = 0$. Since the compressibility of solids is relatively small, one can assume $dV = 0$ and then the equilibrium condition can be expressed as $dF = 0$,where F is the Helmholtz free energy given by,

$$F = U - TS \text{ ---------- } (1.12)$$

It should be kept in mind however, that for solids, the use of F instead of G in the equilibrium requirement is only an approximation. An estimation of the free energy of a solid as a function of temperature can be obtained in the following manner.

From equation (1.12)

$$dF = - P\,dV - S\,dT \text{ ---------- } (1.13)$$

At constant pressure ,

$$F = F_0 - \int_0^T S.dT - P(V_T - V_0) \text{ ----------} (1.14)$$

On the other hand,

$$S = \int_0^T \left(\frac{C_P}{T}\right) dT \quad \text{---------- } (1.15)$$

and thús,

$$F = F_0 - P(V_T - V_0) - \int_0^T \left(\int_0^{T^{11}} \frac{C_P}{T^1}\, dT^1 \right) dT^{11} \text{-------} (1.16).$$

where V_T and V_0 are molar volumes at pressure P and F_0 is free energy at absolute zero equal to the internal energy U_0 at that temperature. Equation (1.15) gives the

absolute value of entropy S by assuming that S = 0 at T = 0 which is the Nernst heat postulate or the third law of thermodynamics [58]. For certain solids, this law appears not to be applicable because of orientation effects, order effects, isotopic composition etc. Such cases are metastable states which in proximity of absolute zero have no chance to reach true equilibrium because of vanishing mobility of atoms. For solids, the second term in equation (1.16) is very small. Therefore ,

$$F = A - \int_0^T \left(\int_0^{T^{11}} \frac{C_P}{T^1} dT^1 \right) dT^1 \text{ --------(1.17)}$$

where A is a constant. This formula is useful in discussing the influence of the lattice specific heat and of the electronic specific heat on phase transitions, such as $\alpha \rightarrow \gamma$ transition in iron [59] and it permits an understanding of the influence of alloying elements on this transition [60]. It can be used also to compare the free energy of solid phases if the specific heats are known experimentally or theoretically. The latter possibility is useful if Debye specific heat theory is applicable. At the transition temperature, the change in the total energy is

$$dU = T\,dS - P\,dV \text{ ---------- (1.18)}$$

which gives for the change of enthalpy,

$$dH = dU + P\,dV = T\,dS \text{ ---------(1.19)}$$

This relation enables one to obtain the entropy of transformation dS from the experimentally known heat of transformation at constant pressure, dH. Thus it is possible to find the transformation temperature provided we know the enthalpies and entropies of both phases as a function of temperature.

Further we have

$$S = (dG / dT)_P \text{ ----------(1.20)}$$

which gives,

$$G = H + T\,(dG / dT)_P \text{ ----------(1.21)}$$

and,

$$dG = dH + T\,\frac{d}{dT}(dG)_P \text{ ----------(1.22)}$$

is the Gibb's Helmholtz equation. The derivative in the equation (1.22) vanishes at absolute zero and thus $(dG)_T$ can be calculated from measured $(dH)_T$. Among the other thermodynamical formulas of importance for transformations, it is worth mentioning in particular,

$$(d\alpha / dP)_T = -(d\beta / dT)_P \text{ ----------(1.23)}$$

and the Maxwell relations:

$$(dS/dV)_T = (dP/dT)_V = \alpha / \beta \quad \text{-----(1.24)}$$

$$(dS/dP)_T = - (dV/dT)_V = - \alpha V \quad \text{----(1.25)}$$

where,

$$\alpha = 1/V \, (dV/dT)_P \quad \text{---------- (1.26)}$$

is the cubic thermal expansion coefficient and ,

$$\beta = - 1/V \, (dV/dP)_T \quad \text{----------(1.27)}$$

is the isothermal compressibility. These formulas apply to a single phase only. Differentiating the equation (1.25) one obtain,

$$(dC_P / dP)_T = - \alpha^2 TV - T(d\alpha / dT)_P V \quad \text{-------(1.28)}$$

in which for solids $(d\alpha / dT)_P$ is usually very small and thus approximately,

$$(dC_P / dV)_T \cong (\alpha^2 T / \beta) \quad \text{--------- (1.29)}$$

here,

$$C_P = T(dS/dT)_P = (dH/dT)_P \quad \text{-------(1.30)}$$

is the usual specific heat at constant pressure. From relation (1.24) one can deduce that at equilibrium between two phases 1 and 2,

$$dP/dT = (S_1 - S_2) / (V_1 - V_2) = (H_1 - H_2) / T(V_1 - V_2) \quad \text{----------(1.31)}$$

where the quantities S, V and H refer to one mole of a single component. This is the so called Clausius-Clapeyron relation which describes the effect of pressure on transitions. Equation (1.31) is very useful for explaining transformations like melting, change of crystal structure etc. Variation of Gibb's free energy, entropy, volume and order parameter with temperature in a first order phase transitions is shown in Fig. (1.1). Similarly, the variation of enthalpy, entropy, specific heat and order parameter with temperature in a second order phase transition is shown in Fig. (1.2).

An important consequences of the existence of relationships among the various thermodynamic quantities is the so called Gibb's phase rule

$$C = F + P - 2 \quad \text{----------} \quad (1.32)$$

in which C is the number of independent components, F is the number of degree of freedom and P is the number of phases. Degree of freedom are independently variable parameters such as temperature, pressure composition of phases etc. In applying this

rule to transitions in solids, containing more than one species of atoms or molecules, it should be kept in mind that if the two phases have the same chemical composition then C is equal to unity. Such conditions occur for instance, at a congruent melting point or at the critical temperature of order-disorder transitions [61-65].

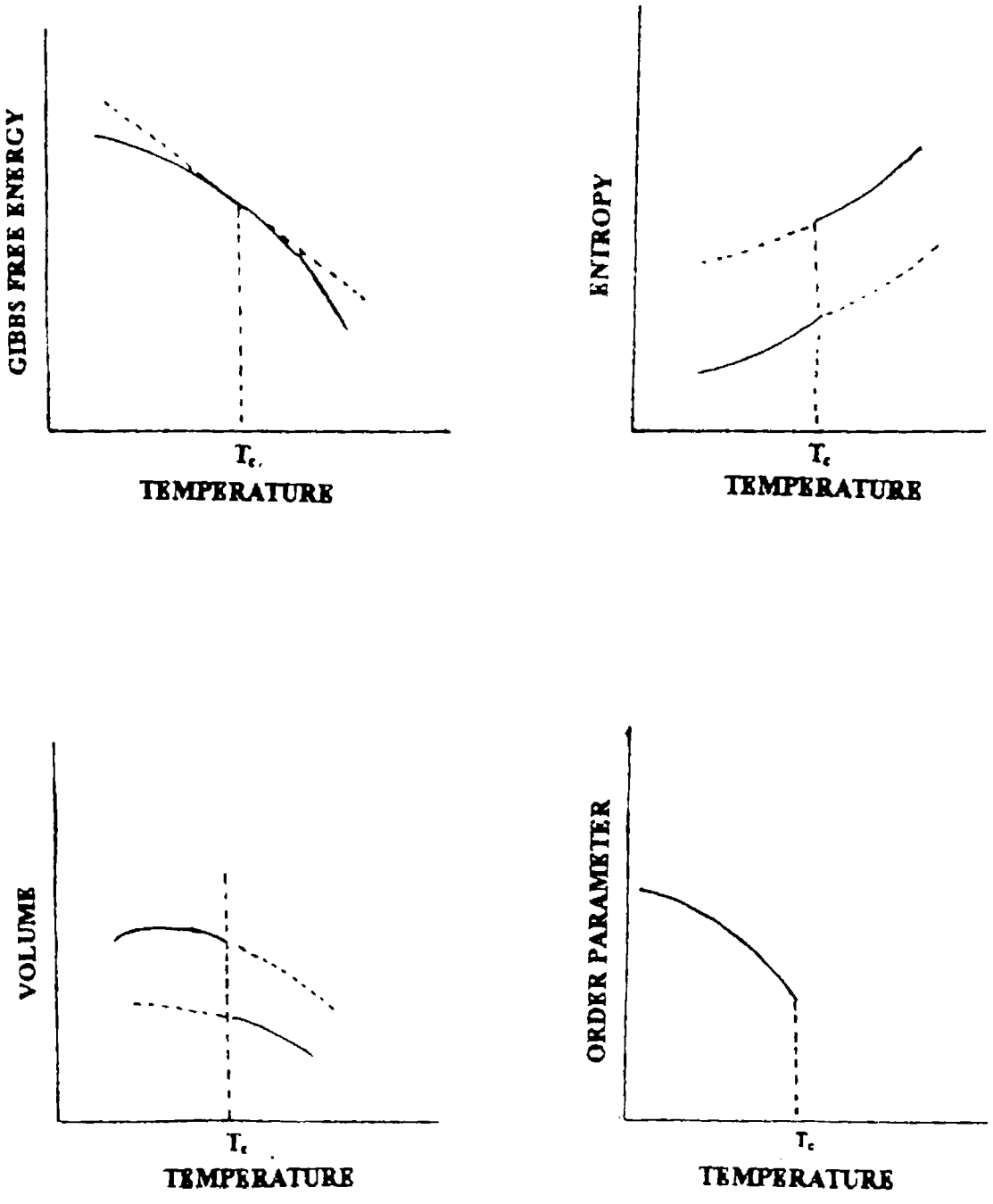

Fig.(1.1) Variation of Gibb's free energy, entropy, volume and order parameter with temperature in a first order phase transition.

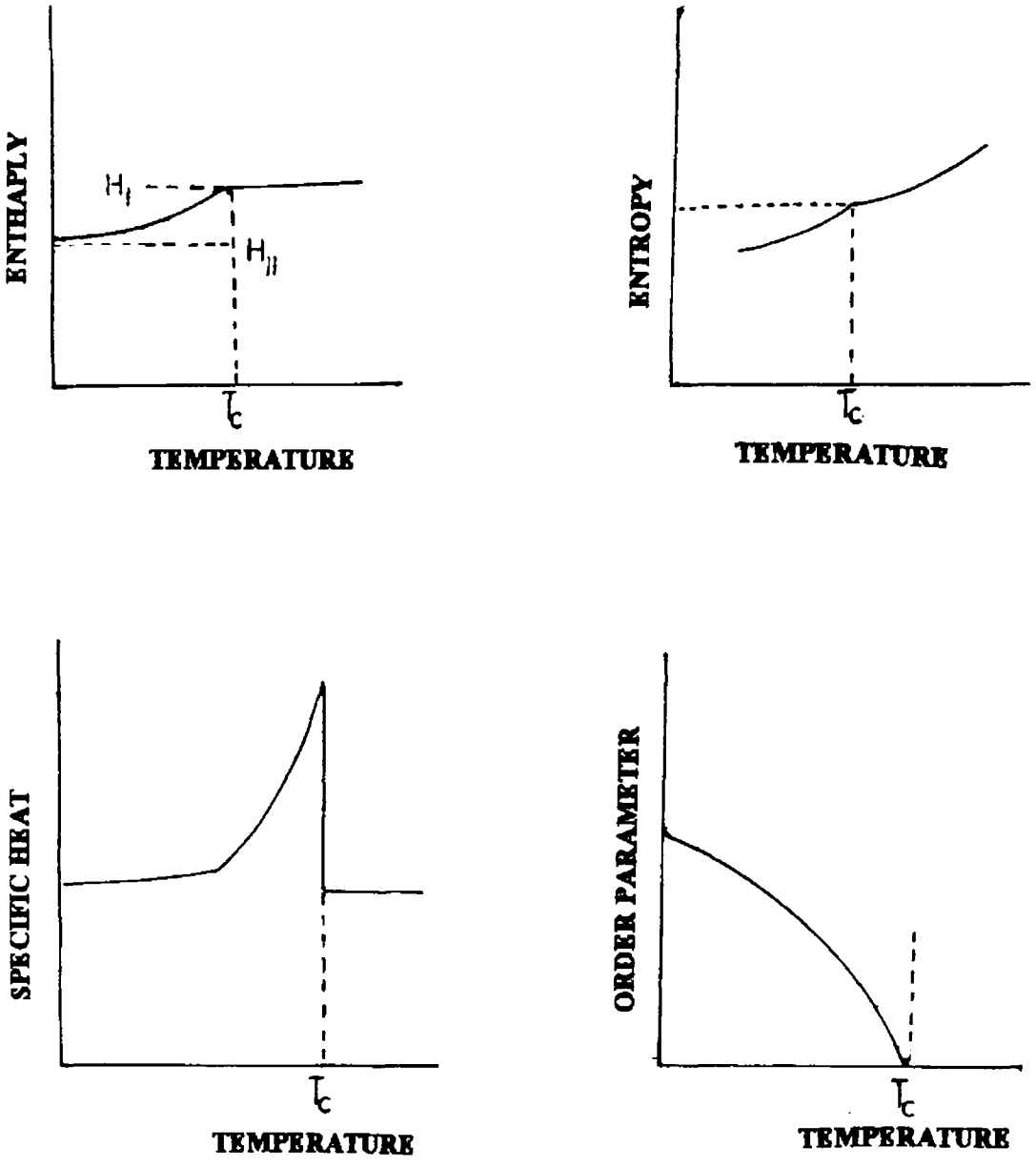

Fig. (1.2). Variation of enthalpy, entropy, specific heat and order parameter with temperature in a second order phase transition.

1.12. Higher order transitions.

Ehrenfest suggested a classification of transitions according to which a transition is of the n^{th} order when derivatives lower than the n^{th} derivative of the function G are continuous at the transition temperature while the n^{th} derivative is discontinues. Strictly speaking, a transition is a phase transformation only when it is of the first order but in accord with common usage the word phase will be used here in the broader sense. The applicability of Ehrenfest's criterion turned out to be limited not only because of experimental difficulties in establishing whether a certain quantity is continuous or not, but also because of the existence of various intermediate kinds of anomalies [66]. Fig.(1.3) illustrates the various kinds of transitions reported (67). The main difference between first order and anomalous first order transitions is that in the latter category each phase anticipates the change with approaching transformation temperature or transformation pressure. Instead of the simple second order transition one observes usually a "lambda" transformation in which near the transformation point both phases show a pronounced continuous change in the various thermodynamic quantities. This change is usually greater below than above the transition point. Finally ,the "diffuse" transformation is spread over an appreciable range of temperatures and pressures. Since thermodynamics is unable to give an artistic quantitative picture of second order transitions much effort has been directed towards obtaining a solution using purely statistical methods. These are based mostly on the so called Ising model in which two kinds of atoms (or two spin orientations) are distributed in a regular one, two, or three dimensional array. When a particular atom of one kind is substituted by an atom of the other kind (or one spin

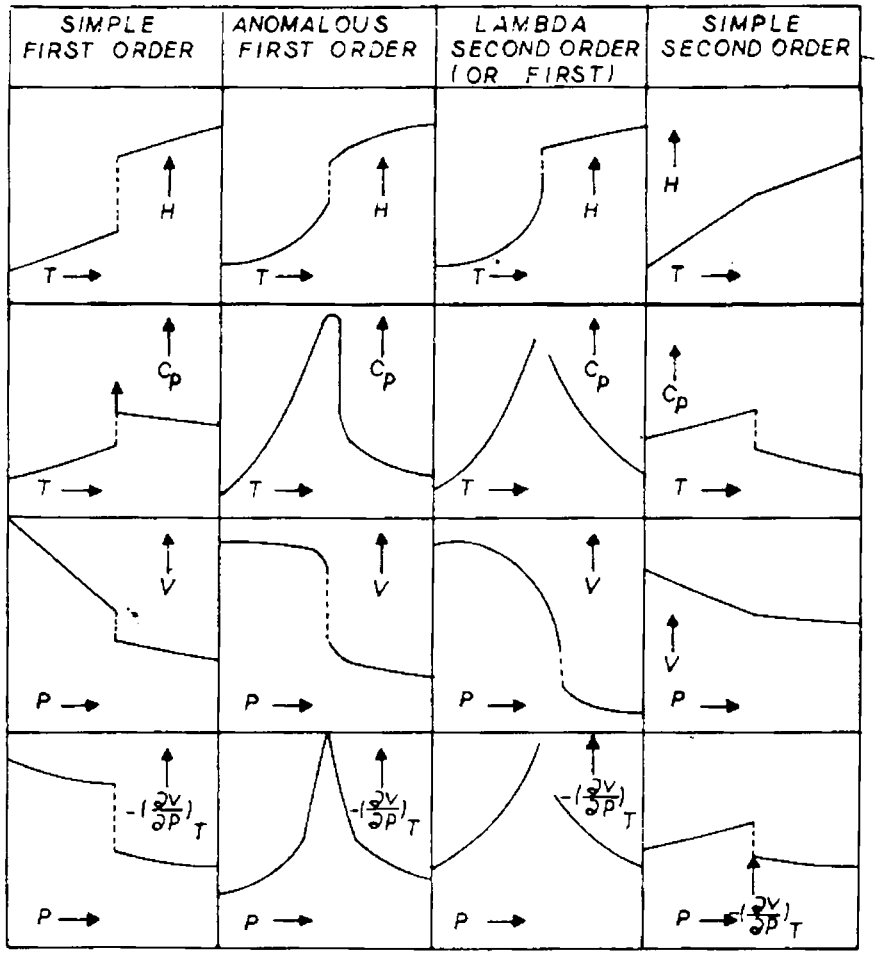

Fig. (1.3). Change in physical quantities at various kinds of transitions.

is reversed), then the energy changes by an amount which depends upon the kind of neighbors and upon their arrangement. This cooperative aspect of the phenomenon, which is characteristic of the second order transitions is implied by certain thermodynamic considerations.

1.13. Applications of phase transition.

A large number of application are already reported in the literature in which the phenomenon of phase transitions have been applied. The properties exhibited by certain liquid crystals are widely used for optical display, detection of temperature uniformity and impurities. Certain crystals can act as thermal switches during a phase transition. Metal-Insulator transition exhibited by certain oxides are of considerable interest from a technical standpoint.

Two important properties which change near T_C are softening of transverse optical mode before a displacive transition and temperature dependence of spontaneous polarization in ferroelectrics below T_C. These properties are used in dielectric and pyroelectric detectors. The applications of soft mode anomalies have been discussed by Fleury [68] The properties exhibited at the first order phase transition can be used for switching semiconductor-metal transitions. This could be employed in circuit breakers, voltage dividers or optical switches.

Ferroelectrics under going transition s are being widely used in practical applications. They are extensively used in high and ultra high capacitance capacitors, dynamic elements of memory and logical elements of electronic computers,

electromechanical converters, radiation modulators and regulators of the quality of optical quantum generators, IR detectors, ferroelectric energy converters, frequency multipliers etc. Ferroelectrics are also used in pulse generation circuits, device for controlling luminescence of electroluminophores, voltage and current stabilizers etc. Recently newer and better ferroelectric substances have been discovered so that we can expect a further widening of the field of application of ferroelectrics.

1.14. Techniques generally employed in the study of phase transformation

Several techniques are employed to investigate phase transitions depending on the nature of the solid and properties of interest. Phase transformations in solids are often accompanied by interesting changes in their physical properties. Hence, measurement of such physical quantities as a function of an external parameters like pressure or temperature is a direct way of investigating these phase transitions. Such studies are not only of technological importance but also of academic value in understanding the structural and mechanistic aspects of phase transitions. A large number of techniques are already reported in the literature and they include diffraction, thermal, optical, spectroscopic, magnetic, electrical, photoacoustic and ultrasonic measurements [69-80]. The availability of modern experimental methods employing highly sophisticated electronic techniques has brought out a quite large number of new transitions as well as transitions which have not been observed in earlier measurements.

1.14.1. Diffraction Technique

X-ray diffraction can conveniently be used to study the structural features of solids undergoing phase transition. Diffraction gives information in fourier form, which can be analysed in terms of the average spacings of lines and planes, symmetries of point groups, and the location of particular species of atoms, in different phases of the transition process. Electron diffraction techniques has certain special advantages, because of the wavelength of radiation used can be smaller than the distances to be resolved, and hence, it can be used for the study of superstructures and small domains. Neutron diffraction studies are most useful in studying the position of light atoms like hydrogen and in magnetic structure. The analysis of the powder neutron diffraction profiles [81] yields valuable structural informations.

1.14.2. Thermal measurements

Thermal measurements have been widely used to identify thermal and characteristic transitions. Differential thermal analysis (DTA), differential scanning calorimetry (DSC) and thermogravimetric analysis (TGA) provide valuable information regarding changes in various physical parameters associated with the phase transition. The heat capacity measurements using DSC and DTA technique give precise data on enthalpy changes and thermodynamic order of transition. The information on activation energies of transformation has also been obtained by fitting the DSC and DTA peak to first order kinetic equations [82,83]. Thermal hysteresis has also conveniently been studied by DTA and DSC. Being a dynamic technique DTA suffers from certain disadvantage compared to that of DSC. For example the heat capacity data and ΔH

values obtained by DTA are not reliable, whereas the values obtained from DSC being much more reliable than those of DTA.

1.14. 3. Optical Technique

The field if phase transition has experienced a period of extremely rapid growth since the development of lasers in the early 1960's. Optical methods particularly the light scattering has played an increasingly crucial role in the investigation of many types of phase transitions. The Optical microscope is a valuable tool for studying phase transformations, particularly with respect to the movement of boundaries, growth of nuclei and changes in grain size. Pressure transitions can also be studied by using an optical microscope and a diamond unvil press. Electron microscopic examination would give useful information on dislocations and structural aspects if the solid can be studied in the transition region . Optical Spectroscopy in the infrared , visible and ultravoilet regions has been used to study solids undergoing transitions. Laser Raman Spectroscopy has been particularly exploited in recent years to investigate phase transitions. In addition to neutron scattering , Raman Spectroscopy also yield direct information on soft modes in solids. X-ray and Ultraviolet photoelectron spectra of solids through their phase transitions can provide valuable informations on the changes in electronic structure. Positrón annihilation is a technique in which the phenomenon of e^- , e^+ recombination with consequent emission of γ-rays is used to study phase transitions in solids, since purity of the material plays a crucial role in transition , preparation , purification and characterisation of materials undoubtedly form an important part of phase transition studies. It is therefore

important that efforts are made to use the purest material possible while studying phase transitions. In this context, all the well- known techniques for the analysis and characterisation of materials like mass spectroscopy, Spectroscopy, atomic absorption spectroscopy and electron microscopic analysis have to be employed.

1.14. 4. Magnetic Properties and Resonance Techniques

Magnetic measurements give direct information regarding electron correlations and ligand field potentials. The Weiss molecular field approach gives the basis for understanding the temperature variation of magnetic susceptibility and magnetisation. Measurement of magnetic susceptibility and magnetisation as function of temperature, along with techniques like neutron diffraction , inelastic neutron scattering and Mossbauer spectroscopy provides information on magnetic moments, the nature of coupling, and magnetic order in solids. NMR Spectroscopy has been employed to study phase transitions of solids containing the appropriate nuclei, for example, V in VO_2 and V_2O_3 and Mn in $MnCr_2O_4$. Phase transitions in NaCN and Na H.S have been studied by NMR Spectroscopy, studies of hundred rotations of CH_3 or NH_4 groups and phase transitions in hydrogen bonded ferroelectric like KH_2PO_4 are other important applications of NMR Spectroscopy. ESR Spectra of solids undergoing transitions have been reported in the literature; a useful application of ESR Spectroscopy is to study a diamagnetic crystal doped with a paramagnetic ion (Mn^{2+} in KNO_3) in the region of the phase transition. NQR Spectroscopy has been employed to study phase transitions of halides (eg.; $CsPbCl_3$), nitrates and nitrites ($NaNO_3$ and

$NaNO_2$) containing nuclei like halogens, nitrogen and others (Nb in $KNbO_3$) with quadrapole moments. Ferromagnetic or antiferromagnetic resonance experiments also provide useful information on magnetically ordered solids. Excellent treatments on magnetism and chemical bond [84] and detailed studies of several magnetic transitions [85-110] on a variety of solids are available in the literature.

1.14.5. Electrical Measurements

The electrical properties like electrical conductivity, dielectic constant and thermo- electric power, hall effect , ionic thermo current measurements etc. have been used to characterise materials and to study the phase transitions in them. The study of electrical conduction process in materials can yield a great deal of information on the formation and migration of charge carriers in them. Basically electrical conductivity in materials is a defect controlled phenomenon and hence detailed investigation of the electrical properties of these materials is one of the best available methods for the study of defects in them. Usually these electrical properties are investigated as a function of temperature or as a function of pressure. Recently, the electrical conductivity (both dc and ac) , dielectric constant and ionic thermo current measurements have become accepted as a very sensitive method for the study of phase transitions as well as for the study of defects in ammonium containing crystals.

1.14.6. Photoacoustic Measurements

The Photoacoustic technique has been recently accepted as an important spectroscopic technique for condensed matter. The basic principle for the detection of

the Photoacoustic(PA) effect is the measurement of acoustic signal produced when a sample is placed in a sealed gas filled cell and illuminated by a chopped light beam. The generation and propagation of acoustic waves in the sample depend critically on the thermo-elastic and physical properties of the sample. In this way the detection of phase transitions is possible by using the sensitivity of the Photoacoustic Spectroscopy to follow the abrupt changes in the physical magnitudes associated with the phase transition. A detailed theoretical explanation will be given in chapter IV.

1.14.7. Ultrasonic Measurements

Ultrasonic measurement is an important tool for the investigation of structural phase transitions in solids. It is possible to get information on nature of phase transition by the measurement of the elastic response of this method. This elastic constant measurements are a very sensitive tool to locate transition points, to determine phase diagrams, and in certain special cases , to make statements about the order of phase transition. Further more, from the temperature variation of the elastic response functions the type of coupling between strain and order parameter can be deduced . Thus the coupling parameters and the characteristic variations of other important quantities can be derived. Ultrasonics thus offers an attractive method for investigations in the field of phase transitions[111-113].

1.15. Techniques and experimental system employed for the present investigation.

Among different techniques available, dc electrical conductivity and dielectric constant measurements have been selected as the ideal technique for the present

investigation. This is because the technique employed to study the electrical properties at or near phase transition are very important in the sense that these techniques are used to characterize materials which in turn can be used for technological applications. A brief description of the techniques and the procedures for measuring these properties have been presented in the following discussion.

1.15a . DC electrical conductivity.

Generally ammonium containing crystals show low value of conductivity at normal temperatures. At still lower temperature, the magnitudes are expected to be much lower and hence low current measuring instruments have to be used for conductivity measurements. For current measurements, highly sensitive electrometer (**Keithley model 642 and 617**), which can detect currents as low as 10^{-15} A, have been used.

The dc conductivity measurements were carried out in an ideal cell, whose description will be given later. The specimen is inserted in between the spring loaded electrodes. A dc potential of the order of 10 - 100 V is applied across the specimen from dry batteries or from a highly stabilized power supply. (A highly stabilized dc power out put ranging 100 to 100 V in steps of 50 mV is available from Keithley 617 electrometer). The current through the crystal is monitored using an electrometer. By making use of the magnitude of the current, area, thickness of the specimen, and the biasing voltage, conductivity can be evaluated. A schematic diagram of the

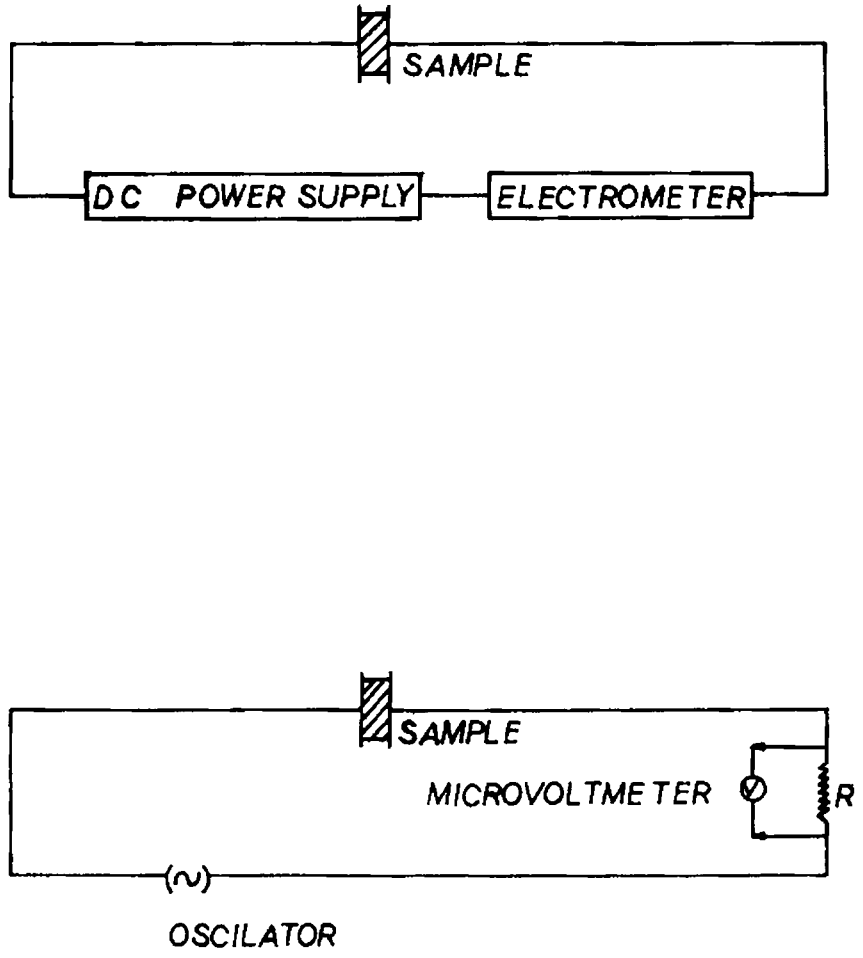

Fig. (1.4). Schematic diagram of the experimental set up used for the measurement of electrical conductivity.

Fig. (1.5). A photograph of the experimental set up used for the measurement of electrical conductivity.

measurement of electrical conductivity is shown in Fig. (1.4). Fig. (1.5) shows the photograph of the experimental set up.

1.15b. Dielectric constant measurements

The dielectric constant of all the samples studied here have been obtained by measuring the capacitance of a parallel plate condenser with the sample as the dielectric. The main disadvantage of this technique is that it is very difficult to isolate the capacitance due to the dielectric alone from the measured capacitance, as the total capacitance contains a component of lead and fringe capacitances. In the present investigation the method suggested by Ramasastry and Syamasundra Rao [69] have been accepted for accounting the effect of lead and fringe capacitances. The method relies upon measuring the total capacitance of a number of samples with varying A/d values (A being area and d, the thickness) and plotting a graph with A/d along X-axis and the measured capacitance along Y-axis. A straight line will be obtained, and the intercept of this will give the lead and fringe capacitances. **Hewlett Packard Impedance Analyzer model 4192A** was used for the measurement of capacitance C. Using this instrument, measurement could be effected in the frequency range 10 Hz to 13 MHz.

1.16. Method used for crystal growth

1.16.1. Growth from solution

Single crystal specimens used for the electrical measurements were grown from solution by slow evaporation at constant temperature. A saturated solution of the

material in an appropriate solvent is used for this process. When the solution becomes supersaturated the crystal will start to grow in solution. Materials which melt, decompose before melting or undergo a phase transformation between melting point and room temperature were grown using this technique. Depending on the nature of the solvent used, solution growth technique has been classified in to aqueous solution , molten salt(flux), metallic solution and hydro thermal growth. In the present studies only the aqueous solution technique has been used . For this we have used a constant temperature water bath having a stability of ±0.01°C in the temperature range 30-50°C. Fairly large single crystals of $NH_4 H_2 PO_4$ and KH_2PO_4were grown using this technique.

1.17. Preparation of samples for electrical measurements

The starting material used for the preparation of pure single crystals were obtained after five times recrystallization of the analar grade material using triply distilled water. Large single crystals grown from solution with good transparent nature were selected for the electrical and photoacoustic investigations. Samples of proper sizes were obtained by cutting slices from large single crystals and polishing with zero grade emery and ground glass. The polished faces of the specimens coated with silver conducting paint or vacuum evaporated electrodes were used for the electrical measurements. It is found that vacuum evaporated electrodes could give better electrical contacts, compared to that of silver paints. A photograph of the vacuum evaporation unit for metallic coatings is shown in Fig. (1.6).

Fig (1.6) A photograph of the vacuum coating unit

1.18. Shielded cell for electrical measurements

The reproducibility of electrical measurements on materials which have a tendency to absorb moisture depend to a large extent on the atmosphere in which the studies are carried out. It is observed that maintaining a dynamic vacuum in the sample cell and annealing the sample at an elevated temperature help to acquire reproducible data. Moreover, at sub ambient temperatures the samples used in the present investigations turn out to be highly resistive. This leads to small amplitude signals in ac techniques which are easily affected by electromagnetic pick up. For those reasons it became necessary to use a specially designed cell having the following features for electrical measurements.

(i) The cell must be capable of operating over a wide temperature range.

(ii) It must be capable of providing a linear heating rate with proper heater controls.

(iii) The measuring cell and leads must be electromagnetically shielded and earthed.

(iv) It must be possible to maintain a steady dynamic vacuum in the cell .

Depending upon the nature of measurement required, several cell designs have been described in the literature [70-76]. A Schematic diagram of the variable temperature cell used for the present study is shown in Fig. (1.7).

The cell assembly has a cylindrical nickel plated MS body which acts as an e.m. shield. The ends of the MS cylinder are permanently fitted with MS flanges which are provided with grooves to accommodate neoprene O-rings for vacuum sealing. One of the flanges rests on the bottom plate. The top cover plate carries insulated electrical terminals for heater, thermocouple and the leads for electrical measurements of the sample.

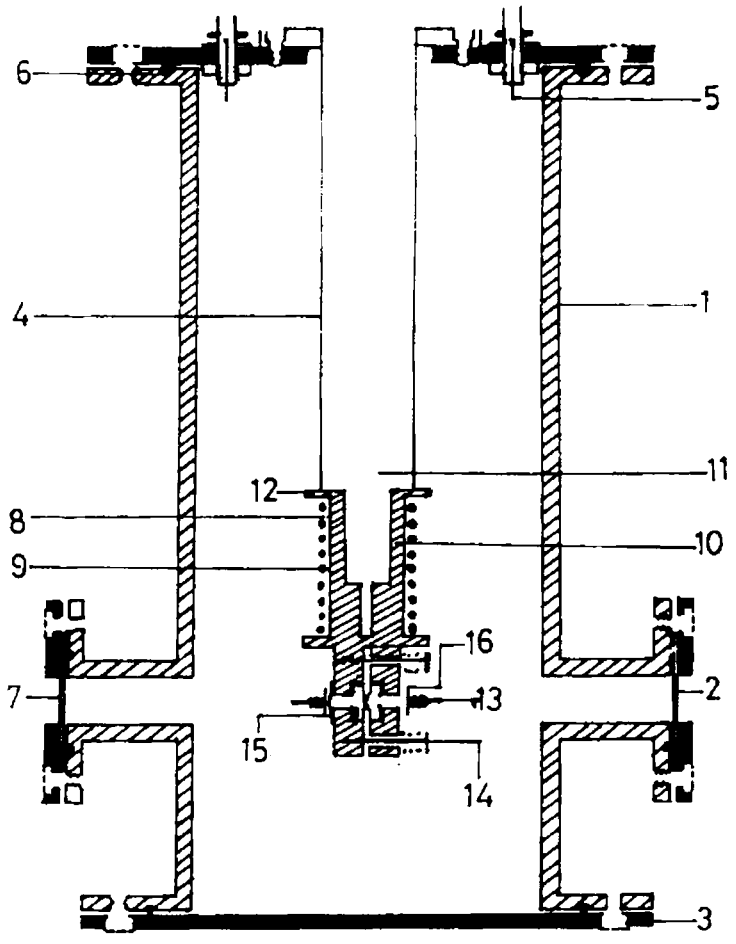

1. MS CHAMBER
2. GLASS WINDOW
3. MS FLANGE
4. SS PIPE
5. BNC
6. NEOPRINE O-RING
7. TO VACUUM PUMP
8. COPPER COLD FINGER
9. HEATER WINDINGS
10. MICA INSULATION
11. LN_2 CAVITY
12. SAMPLE HOLDER
13. COPPER ELECTRODES
14. SPRING LOADED SCREWS
15. TEFLON INSULATION
16. THERMOCOUPLE.

Fig. (1.7). Schematic diagram of the variable temperature cell used for electrical measurements.

The terminals for out put signals are provided with BNC connectors. The top cover carries a stainless steel tube into which liquid nitrogen can be poured. At the end of the SS tube a solid copper cylinder is brazed in. This act as a cold finger. The sample holder consist of a copper cylinder, one side of which is made in the form of a rectangular block as shown in the Fig. (1.7). The other end of the cylinder is bored to a depth such that the rectangular block is about 4 mm below the end of the bore. The outer portion of the drilled end is shaped in a suitable way to accommodate the heater windings. The rectangular block is provided with teflon insulated copper electrode of certain diameter at its centre. Another movable copper block of the same dimension fixed with teflon insulated copper electrode of a smaller diameter serves the purpose of the second electrode. This assembly is spring loaded on the static block such that the centers of the two electrodes are in a common axis. This configuration ensures rapid thermal equilibrium of the sample placed between the electrodes. The copper cold finger is provided with a heater winding which is also insulated by a thin mica sheet. The salient features of this cell are the following:

(i) Measurements can be made in the temperature range 80 to 450 K.

(ii) A dynamic vacuum down to 1 m torr can be maintained over the sample throughout the experiment.

(iii) By virtue of the special design of the liquid nitrogen holder, the consumption of liquid nitrogen is much lower than that in conventional commercial devices.

(iv) AC and DC electrical conductivities, dielectric constant and dielectric loss can be measured in the same cell with excellent sensitivity.

(v) Sample mounting and setting up the system for measurement can be accomplished rapidly.

1.19. REFERENCES.

[1]. U.Syamaprasad and C.P.G.Vallabhan, J.Phy.C:Solid State Phys.14 L 571 (1981).

[2]. U.Syamaprasad and C.P.G.Vallabhan, J.Phy.C:Solid State Phys.14 1865 (1981).

[3]. U.Syamaprasad and C.P.G.Vallabhan, Solid State Commun. 38, 555 (1981).

[4]. U.Syamaprasad and C.P.G.Vallabhan, Solid State Commun. 41,169 (1982).

[5]. U.Syamaprasad and C.P.G.Vallabhan, Phy.Lett.89A, 37 (1982).

[6]. U.Syamaprasad and C.P.G.Vallabhan, Phy.Rev.B. 26, 5941 (1982)

[7]. V.K.Subhadra, U.Syamaprasad and C.P.G.Vallabhan, J.Appl.Phys. 54, 2593 (1983).

[8]. R.Navil Kumar and C.P.G.Vallabhan, J.Phys.Condens. Matter. 1, 6095 (1989).

[9]. R.Navil Kumar and C.P.G.Vallabhan, Physica Status Solidi (a) 112, K113 (1989).

[10]. N.C.SanthaKumari and C.P.G.Vallabhan, Solid State Ionics 45,329 (1991).

[11]. B.B.Owens and G.R.Argue, Science 157, 308 (1967).

[12]. G.G.Bentle, J.Appl.Phys. 39, 4037 (1968).

[13]. W.Schottky, Z.Phy.Chem.Abt. B29, 335 (1935).

[14]. C.Wagner, Z.Phy.Chem.Abt. B38, 485 (1938).

[15]. N.F.Mott and M.J.Littleton, Trans.Faraday Soc. 34, 485 (1938).

[16]. N.F.Mott.and R.W.Gurney, "Electronic Process in Ionic Crystals", 2nd 12ed.;Oxford.

[17]. A.B.Lidiard, Handbuch der Physik, 20, 246 (1957).

[18]. A.B.Lidiard, Phys. Rev. 94, 29 (1954).

[19]. I.Boswara and A.B.Lidiard, Phil.Mag. 16, 805 (1967).

[20]. R.G.Fuller, C.L.Marguardt, M.H.Reilly and J.C.Wells Jr.,Phys Rev. 176, 1036 (1968).

[21]. R.G.Fuller, and H.B.Rosenstock, J.Phys Chem.Solids, 30, 2105 (1969).

[22]. R.G.Fuller and M.H.Reilly ,Phys Rev.Lett. 19, 113 (1967).

[23]. R.G.Fuller, Bull.Am.Phys Soc. 15, 384 (1970).

[24]. R.G.Fuller and M.H.Reilly J.Phys Chem.Solids. 30, 457 (1969).

[25]. R.G.Fuller and F.W.Pattern, J.Phys Chem.Solids. 30 539 (1970).

[26]. L.W.Barr and A.B.Lidiard, Defects in Ionic Crystals," Physical Chemistry an Advance Treatise",Vol.X, Academic Press, NewYork, (1970).

[27]. D.K.Dawson and L.w.Barr, Phys.Rev.Lett. 19, 844 (1967).

[28]. W.Franklin, Phys.Rev. 180, 682 (1969).

[29]. C.Ramasastry and Y.V.G.S.Murti, Proc.Roy.Soc. 305, 441 (1968).

[30]. F.A.Kroger, J.Chem.Phys. 51, 4025 (1969).

[31]. S.Chandra and J.Rolfe, Cana.J.Phys. 48, 397 (1970).

[32]. S.Chandra and J.Rolfe, Cana.J.Phys. 48, 412 (1970).

[33]. V.C.Nelson and R.J.Frianf, J.Phys.Chem.Solids. 31 825 (1970).

[34]. Y.V.G.S.Murti and P.S.Prasad, Proc.Nuclear Physics and Solid State Physics Symposium ,India, 17C, 67 (1974).

[35]. A.M.Karo and J.R.Hardy, Phys.Rev. B3 3418 (1971).,

[36]. Solid State Protonic Conductors III, ed.J.B.Goodenough, J.Jensen and A.Potier, Odense University Press, Denmark. (1985).

[37]. S.Chandra, Superionic Solids Principles and Applications, North Holand, Amsterdam (1981).

[38]. G.Alberti, M.Casciola and U.Costantino, in Solid State Protonic Conductors III, Ed.J.B.GoodEnOugh, J.Jensen and A.Potier, p. 215, Odense University Press, Denmark. (1985).,

[39]. W.A.England,M.G.Cross, A.Hammnett, P.J.Wiseman and I.B.Goodenough, Solid State Ionics. 1, 231 (1980).

[40]. G.C.Farrington and J.L.Briant, Mat.Res.Bull. 13, 763 (1978).,

[41]. O.Nakamura, T.Kodama, I.Ogino and Y.Miyake, Chem.Lett. 17 (1979).

[42]. F.A.Kroeger, J.Chem.Phys. 51 ,4025 (1969).

[43]. R.G.Fuller and P.W.Patten, J.Phys.Chem.Solids. 31, 1539 (1970).

[44]. A.Kessler, Solid State Commun. 12, 697 (1973).

[45]. Y.V.G.S. Murti and C.S.N.Murthy, J.Physique. 34, C9 (1973).

[46]. Y.V.G.S.Murti and P.S.Prasad, (a) Physica. 77, C9 (1974); (b) Solid State Commun. 15, 1619 (1974); (c) Physica 79B, 243 (1975).

[47]. F.Elkabanny, Appl.Phys.Commun. 6, 57 (1986).

[48]. Y.Berteit, A..Kessler and T.List, Z.Phys. B24, 15 (1976).

[49]. B.E.Taylor and A.L.Lasker, Physica Status Solidi (b). 101, 423 (1980).

[50]. T.M. Herrington and L.A.K.Staveley, J.Phys.Chem.Solids. 25, 921 (1964).

[51]. E.J.Murphy, J.Appl.Phys. 35, 2609 (1964).

[52]. J.M.Pollock and M.Sharan, J.Chem.Phys. 51, 3604 (1969).

[53]. L.B.Harris and G.J.Vella, J.Chem.Phys. 58, 4550 (1971).

[54]. S.Vasudevan and Ramaswamy, Ind. J.Pure and Appl.Phys. 23, 432 (1985).

[55]. S.C.Subharwal and B.Ghosh, Physica Status Solidi (a). 89, K83 (1985).

[56]. J.K.Rath and S.Radhakrishna. J.Mater.Sci.Lett. 6 929 (1987).

[57]. P.Ehrenfest, Proc.Amsterdam Acad. 36, 153 (1963).

[58]. A.B.Pippard, "Elements of Classical Thermodynamics" Cambridge University Press, 1966.

[59]. F.Seitz, " Modern Theory of solids", McGraw Hill, New York, 1940.

[60]. R.Smoluchowski, Metal Progr. 41, 363 (1942).

[61]. M.A..Krivoglaz and A.Smirnov, "Theory of order - disorder in alloys", McDonald, London, 1964.

[62]. H.Yamouchi and D.de Fontane, in " Order - Disorder Transformation in Alloys", H.Warlimont (Ed.), Springer - Verlag, Berlin, 1974, P- 148.

[63]. J.M. Cowley, J.Appl. Phys. 21, 24 (1950).

[64]. H.Lipson, in "Progress in Metal Physics", B.Chalmers (Ed.), Vol.2, Pergamon Press, NewYork, 1957.

[65]. B.H.Kear, T.Sims, N.S.Stoloff and J.H.Westbrook (Eds.), " Ordered Alloys, Structural Applications and Physical Mettallurgy", Clautiors Publishing Division Baton Range, 1979.

[66]. E.Baver, Changements de Phases, Soc.Chim.Phys. P-3, Paris, (1952).

[67]. J.E. Mayer and S.F.Streeter, J.Chem.Phys. 7, 1019 (1939)

[68]. P.A.Fleury in "Phase Transitions", H.Henisch, R.Roy and L.E.Cross (Ed.), Pergamon Press , New York, 1973.

[69]. Helen D.Megan, " Ferroelectricity in Crystals '',Methuen and Co., London, 1957.

[70]. C.N.R. Rao and M.Natarajan ,Crystal Structure Transformations in Binary Halides, NSRDS-NBS Monograph 41, Washington D.C., 1972.

[71]. C.N.R.Rao and G.V.Subba Rao, "Transition Metal Oxides : Crystal Chemistry , Phase Transition and Related Aspects ", NSRDS-NBS Monograph 49, Washington D.C., 1974.

[72]. C.N.R.Rao , B.Prakash and M.Natarajan, "Crystal Structure Transformation in Inorganic Nitrites, Nitrates and Chromates ",NSRDS-NBS Monograph 53, Washington D.C 1975.

[73]. C.N.R.Rao and B.Prakash, "Crystal Structure Transformations in Inorganic Sulphites, Phosphates, Perchlorates and Chromates ", NSRDS-NBS Monograph 56, Washington D.C 1975.

[74]. C.N.R.Rao and K.P.R.Pisharody, "Progress in Solid State Chemistry ", Pergamon Press, Oxford, Vol.10, 1975.

[75]. J.B.Goodenough and J.M.Longo, " Crystallographic and Magnetic Properties of Perovskite and Perovskite related Compounds ",landlot-Bornstein, New Series Group III, Vol.4a, Springer-Verlag, Berlin, 1970.

[76]. E.P.Papadakis, " Physical Acoustics ", W.P.Mason and R.N.Thruston(Ed.) , Vol.12, Academic Press, Newyork 1976.

[77]. R.Truell, C.Elbaum and B.B.Chik, " Ultrasonic Methods in Solid State Physics , Academic Press, Newyork 1969.

[78]. E.R.Fuller, A.V.Granato, J.Holder and E.R.Naimon, " Methods of Experimentel Physics ", R.V.Coleman(Ed.), Vol.11, Academic Press, Newyork, 1974.

[79]. You-han-Pao, " Optoacoustic Spectroscopy and Detection ", Academic Press , Newyork, 1977.

[80]. A.Rosencwaig , " Photoacoustics and Photoacoustic Spectroscopy ",John Wiley Newyork, 1980.

[81]. H.M.Hietveld, J.Appl. Cryst. 2, 65 (1969).

[82]. K.J.Rao and C.N.R.Rao J.Mat. Sci. 1, 238 (1966).

[83]. M.Natarajan, A.r.Das and C.N.R.Rao , Trans. Faraday Soc. 65, 3081 (1969).

[84]. J.B.Goodenough, " Magnetism and Chemical Bond ", John Wiley, Newyork, (1963).

[85]. E. Barthelemy , O.Gorochov and Mckinzie, Mat.Res. Bull. 8, 1401 (1973).

[86]. K.Dwight, N.Menyuk and J.A.Kafalas, Phys. Rev. B . 2, 3630 (1970).

[87]. B. Van. Laar, Phys. Rev. 156, 654 (1967).

[88]. D.K.Dwight, R.W.German, N. Menyuk and A.Wold, J.Appl.Phys. 33, 1341 (1962).

[89]. T.Shinjo and K.Kosuge , J. Phys. Soc. Japan. , 21, 2622 (1966).

[90]. P.H.Carr and S.Foner, J.Appl.Phys. 31 ,1960 (1960).

[91]. F.J.Morin, Phys. Rev. 78, 819 (1950).

[92]. W.S.Carter and K.W.H.Stevens, Proc. Phys. Soc. B 69, 1006 (1956) 76, 969 (1960).

[93]. D.R.Huffmann and R.L.Wild, Phys. Rev. 148, 526 (1966).

[94]. J.Chenavas, J.C.Joubert and M. Merzio, Solid State Commun. 9, 1057 (1971).

[95] D.S. Mcclure, "Excitons, Magnons and Photons in Molecular Crystals" , A.B.Zahlan(Ed.), Cambridge University Press, London, 1968.

[96]. W.J.L.Burgers, G.Dowling, J.Sakurai and R.A.Cowley, "Neutron Inelastic Scattering", Proceedings of IAEA Symp., Copenhagen, 2, 126 (1968).

[97]. J.B.Goodenough, Phys. Rev. 164, 785 (1967).

[98]. H.B.Mathur, " Solid State Chemistry ", C.N.R.Rao (Ed.), Markel Dekker, Newyork, 1974.

[99]. D.G. Wickham and W.J.Croft, J.Phys. Chem. Solids 7, 351 (1958).

[100]. T. Riste and L. Tenser, J.Phys. Chem. Solids . 19,117 (1961).

[101]. M.T.Evans, E.Warming and G.L.Squires, " Neutron Inelastic Scattering", Proceeding of IAEA Symp., Granoble, 1972.

[102]. W.Kudig, H. Bommel, G. Constabaris and R.H. Lindguist , Phys.Rev. 142, 327 (1966).

[103]. T.J.A.Popma, C.Hass and B. Van Laar, J. Phys. Chem.Solids. 32, 581 (1971).

[104]. H.F.Franzen, D.M.Strachen and R.G.Barnes, J. Solid State Chem. 7, 374 (1973).

[105]. J.P.Delamaire, H. Le Brasq and F. Marion, Acad. Sci. C 272, 2144 (1971).

[106]. F. Gronvold ,H. Heraldeson, B. Pedersen and T. Tufte, Rec. Chim. Min 6, 215 (1969).

[107]. C.B. Vanden Berg, Ferroelectrics: 4, 117 (1972).

[108]. A. B. De Vries and C.Hase, J. Phys. Chem. Solids. 34, 651 (1973).

[109]. J.B.Goodenough, J.Appl.Phys. 39, 403 (1968).

[110]. W.Kudig and R.S.Hargrove, Solid State Commun. 7, 223 (1969).

[111]. K.K.Kobayashi, J.Phys.Soc. Japan, 24, 497 (1968).

[112]. K.H.Michel and J. Nandts, Phys. Rev.Lett. 39, 212 (1977).

[113]. K.H.Michel and J. Nandts, J. Chem. Phys. 69, 547 (1977).

[114]. C.Ramasastry and Y.Syamasundara Rao, J.Phys.E: Sci.Instrum. 12, 1023 (1979).

[115]. R.D.Gretz, Rev.Sci.Instrum. 38, 112 (1967).

[116]. F.E.Card and J.J.Galen, Rev.Sci.Instrum. 32, 858 (1961).

[117]. V.Kopane and V.E.Shubin, Instrum.Exp.Tech. 19, 1228 (1976).

[118]. R.K.Chaudhary and L.Kishore, Cryogenics. 17, 419 (1977).

[119]. H.Abachi, J.Molenat and P.Malbrunot, J.Phys.E: Sci.Instrum. 12, 706 (1979).

[120]. H.Gobrecht and D.Hoffmann, J.Phys.Chem.Solids. 27 , 509 (1966).

[121]. E.B.Podgovsak and P.R.Moran, Phys.Rev.B. 8, 3405 (1973).

CHAPTER 2

A STUDY OF LOW TEMPERATURE PHASE TRANSITION IN AMMONIUM DIHYDROGEN PHOSPHATE USING DC ELECTRICAL CONDUCTIVITY MEASUREMENTS.

2.1. ABSTRACT.

Results of dc electrical conductivity measurements carried out on single crystals of tetragonal ammonium dihydrogen phosphate (ADP) along c-axis in the temperature range 100 K to 400 K have been presented. The log σ vs 10^3 /T plot obtained for this material shows anomalous variation at 147K with a hysteresis of 1.1 indicating that this material undergoes a first order phase transition at this temperature unlike other ionic crystals of this category. ADP is found to exhibit a clear pyroelectric behavior at the transition point. The mechanisms of electrical conduction process in this material are discussed along with that for phase transition. The activation energy values obtained from the straight line regions of the Ahrenius plot are also given.

2.2. INTRODUCTION

Studies on the properties of crystals containing ammonium groups have been of great interest in recent years in view of their optical, dielectric, ferroelectric and thermal behavior. The hydrogen bonds in these materials play a critical role in deciding many of these properties. The above mentioned properties have been studied extensively using various techniques such as NMR [1], EPR [2,3],IR [4],DTA [5] and neutron diffraction [6]. In this context it must be said that the measurements of the electrical properties like dc and ac conductivities also have yielded valuable informations about the transport processes and phase transitions occurring in these materials. ADP is a scientifically important photonic material used in the phenomenon of second harmonic generation. Second harmonic generation are now standard equipments for use with visible and IR lasers. Recently considerable advances have been achieved in harmonic generation, and in particular, ADP has sufficiently large nonlinear coefficients and high optical breakdown thresholds, it become an attractive material for the generation of higher order harmonics which is useful for obtaining laser radiation in the UV region with visible range lasers. Optical bistability has also been observed in ADP crystals. Optical bistability leading to bistable devices which are important in the digital circuit used in communications, signal processing and computing. They are also used as switches, logic gates and memory elements. Two wave mixing process occur in ADP can

be employed in real time holography. Wave mixing has numerous applications in optical data processing, including image amplification, the removal of image aberrations, cross correlation of images and optical interconnections.

ADP occupies a prominent position among the numerous isomorphous of potassium dihydrogen phosphate (KDP). It has been observed that the replacement of potassium ion by the ammonium group in KDP causes a radical change in the nature of the phase transition in ADP converting it into an antiferroelectric at low temperature [7]. Mason and Matthias have shown that this material undergoes a sharp first order antiferroelectric transition at 148 K accompanied by a discontinuous drop in dielectric susceptibility [8]. However, the dielectric and piezoelectric measurements show that the transition is not a ferroelectric one but an order disorder transition as was suggested by the specific heat measurements [9,10]. Since, the specific heat anomaly occurring at this transition is much larger than those observed in other ammonium containing materials, the above transition was believed to be due to the interaction of the distorted NH_4 ions which deviate from a spherically symmetrical configuration. X-ray studies by E.A.Wood show that the crystal structure change accompanying the transition in pure and deuterated ADP is caused by a quadratic distortion proportional to square and even powers of the spontaneous polarization. Hence below T_c , the structure is antiferroelectric. Several authors reported the temperature dependence of the thermal parameters extrapolated at T= 0 K. They obtained the following results; the P atom has a two-site distribution along the c- axis and the N atom along a(b) axis. The two-site distribution of the P and N atoms respectively means that the PO_4^{3-} and NH_4^+ ions have dipole moment that is parallel to the distribution direction [11]. Even though extensive investigations have been done to study this material near the well known transition using DSC and TGA, no attempt has hitherto been made to study the electrical

properties, particularly the dc electrical conductivity around this low temperature phase transition. In this paper we present the results of our studies on the low temperature electrical conductivity of ADP and discuss the implications of some of our findings.

2.3. EXPERIMENTAL

Single crystals of pure ADP were grown by slow evaporation from a saturated solution prepared with triply distilled water. Samples of the typical sizes 10 x10 x1 mm^3 were cut from large single crystals and the broad faces (C-axis) of the specimens were coated with silver using vacuum coating technique. Details of the cryostat, sample holder and temperature control and measurements have been described in chapter 1. DC conductivity data were obtained on single crystals of ADP using an electrometer (Keithley model 642) along with a constant voltage source. A potential difference of the order of 10 - 40 V has been applied across the specimen which was kept under vacuum conditions.

2.4. RESULTS

The dc electrical conductivity measurements carried out in single crystals of ADP along C-axis in the temperature range 100 K to 400 K are shown in Fig (2.1). The results were found to be very well reproducible for different heating and cooling runs. Curve denoted by (a) in Fig.(2.1). shows the log σ vs 10^3 /T for ADP in the cooling run whereas curve (b) represents the heating run. Conductivity plot shows a single unmistakable peak at 147 K on cooling the sample. In the heating

run it again occurs but is found to be shifted to a temperature of 148.1K. Paraelectric-antiferroelectric phase transition temperature determined by dielectric, NMR, EPR and DSC techniques for ammonium dihydrogen phosphate shows the thermal hysteresis of the transition to be close to 2^0 in all cases [12]. In the cooling run conductivity plot shows a sharp dip which is two orders of magnitude less compared to the one at 200 K whereas in the heating cycle it shows pronounced upward enhancement which is one order of magnitude greater than that observed at 200 K. This change in direction of the current peaks at the phase transition point is the most striking feature of the results of present measurements. It is also seen that below 300 K the log σ vs 10^3 /T can be divided into two straight line regions denoted as I and II which are characteristics of ionic crystals. The activation energy values obtained by making use of the respective straight line regions are 0.70 eV and 0.08 eV respectively. The inset of Fig. (2.1) shows the variation of current values as a function of temperature in the heating and cooling runs around this transition point. Fig. (2.2) shows the current I versus 10^3/ T plot for ADP in the cooling run and heating run (which are designated as (a) and (b) respectively) without applying any electric field across the sample.

2.5. DISCUSSION.

It is well known that ADP has a tetragonal structure with space group D_{2d}^{12} in the paraelectric phase and it undergoes an antiferroelectric transition to the orthorhombic structure with space group D_2^4 [13]. The tetragonal crystal structure was studied in detail by Ueda and Pepinsky [14,15]. The crystal lattice of ADP and

the four hydrogen bonds H_1 ,H_2 ,H_3 and H_4 associated with phosphate group P_0 and with ammonium group A in ADP are shown in Figs. (2.3), (2.4) and (2.5) respectively.

Their results show that the O----O distance of the hydrogen bonds connecting the neighboring PO_4 groups is 2.49A or 2.51A, smaller than the corresponding value for KDP which is 2.54A. Each nitrogen is surrounded by four oxygen atoms in the form of a flattened tetrahedron and the N---- O distance is 2.87A or 2.84A. It has been inferred from this small value of the N---- O distance that the formation of N---H---O hydrogen bonds may play an important role in the mechanism of phase transition. However, the sum of the ionic radii of NH_4^+ and O^{2-} is nearly equal to the observed N----O distance, leading to the conclusion that such bonds do not play any role in this phase transition mechanism. On the other hand, the experimental investigations conducted on the crystal using dielectric constant, specific heat and infrared absorption evidently show that the antiferroelectric ordering in ADP involves the protons in the hydrogen bonds linking the acid group $H_2PO_4^-$ [8,10]. The specific anomaly at T_c indicates a first order transition with a large isotopic effect on T_c for deuterated samples. This implies that hydrogen bond motions dominate the phase transition dynamics. However, the infrared studies show strong ammonium ion distortions occurring at T_c and this suggests that the NH_4 ion motions together with the acid group proton motions govern the phase transition dynamics which is fully in agreement with the NMR second moment calculations [16]. The polarized infrared reflectivity spectra of ADP in the paraelectric and antiferroelectric phase are reported for a wide spectral range, including the PO_4 and

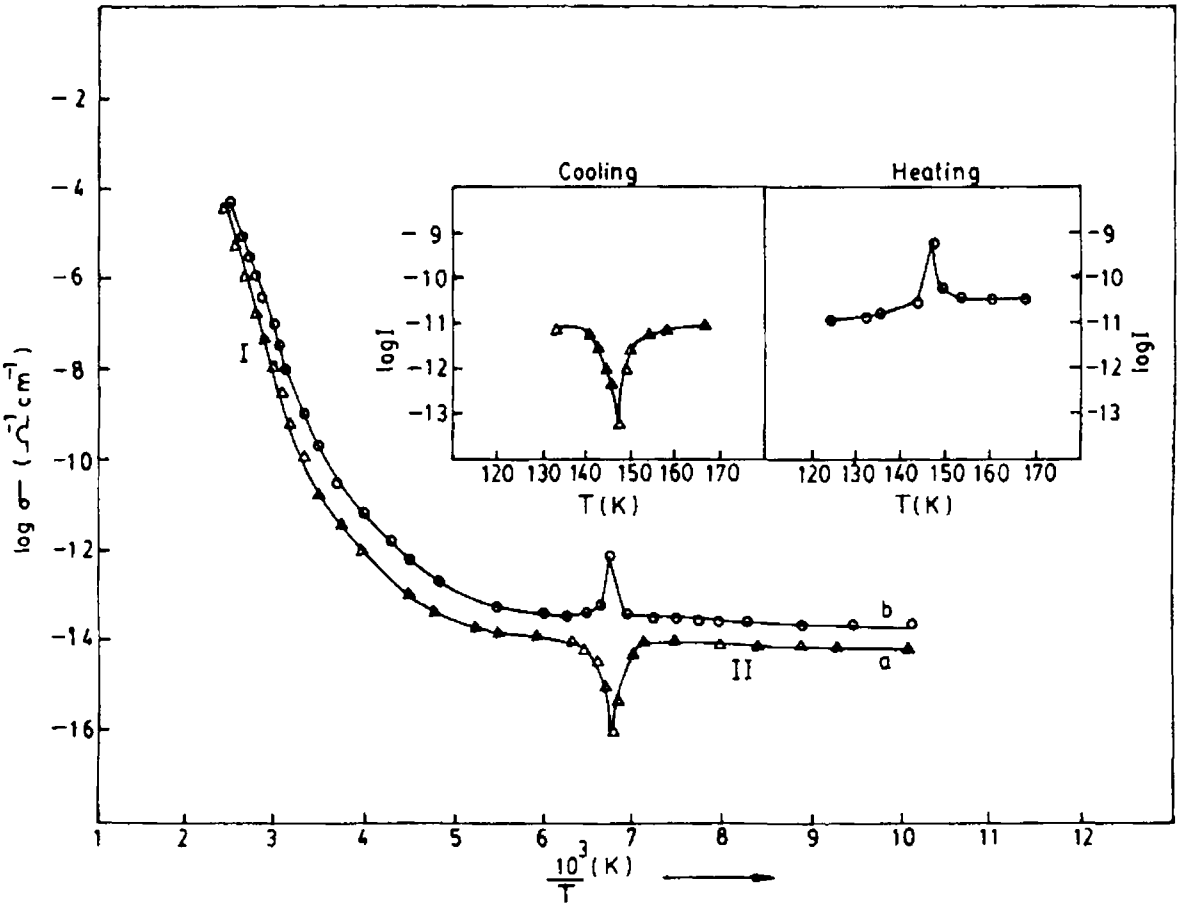

Fig. (2.1). Temperature dependence of dc electrical conductivity measurements of pure ADP single crystal (a) cooling (b) heating.

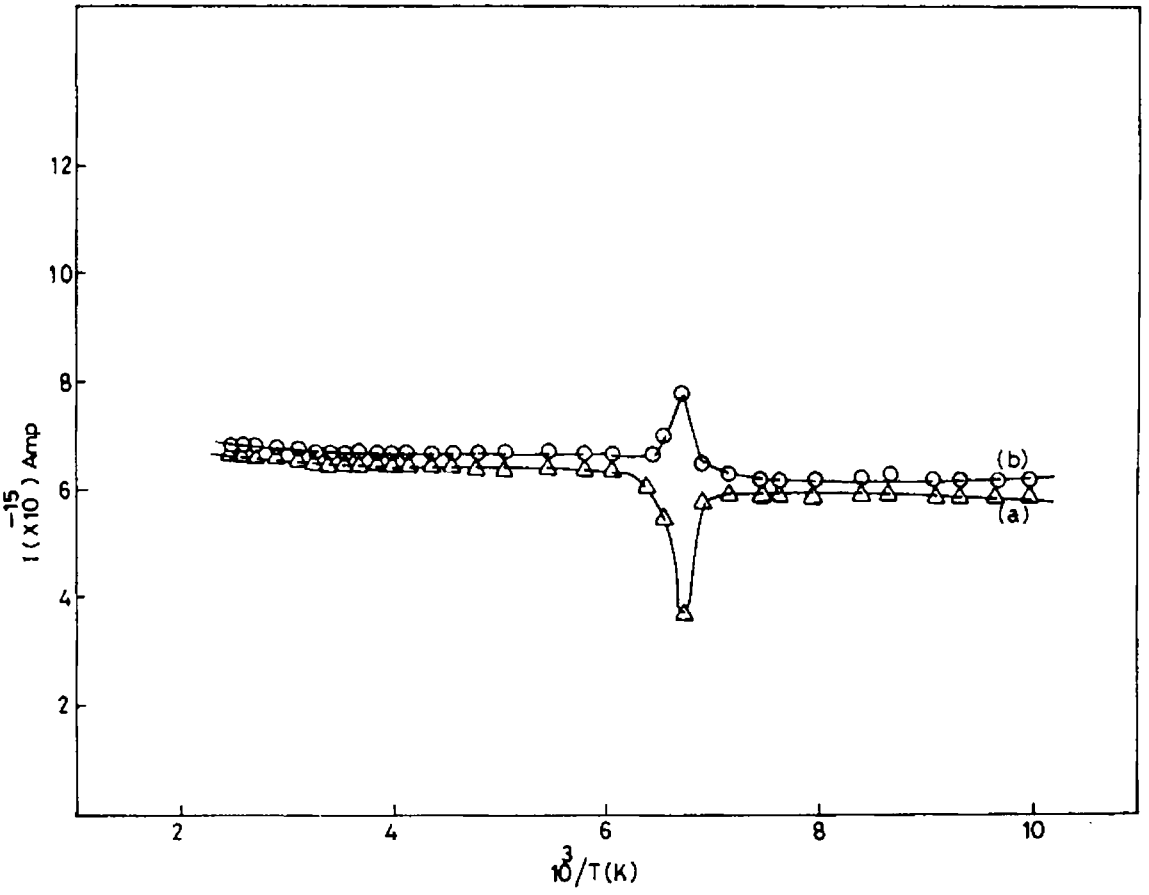

Fig. (2.2). Current I vs. 10^3 / T plot for ADP in the cooling (a) and heating (b) run without applying any electric field across the sample.

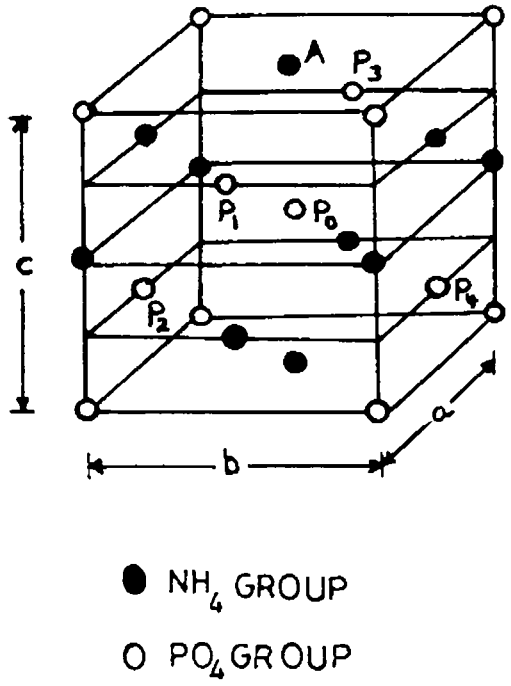

Fig. (2.3). The crystal lattice of ADP.

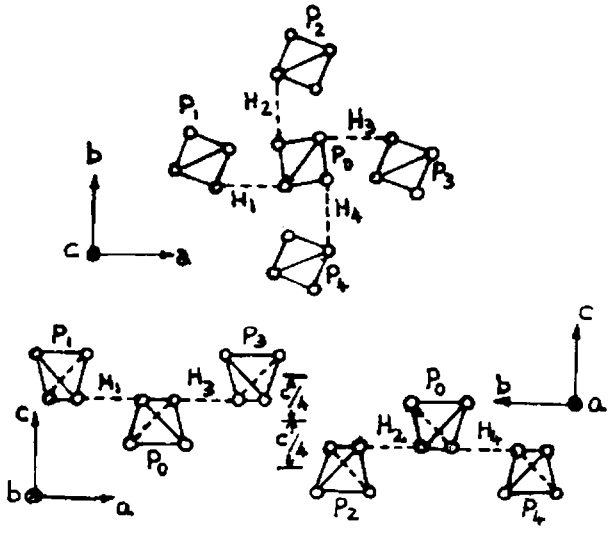

Fig. (2.4). The four hydrogen bonds H_1, H_2, H_3 and H_4, associated with phosphate group P_0

(a) view along c- axis (b) along b- axis (c) along a-axis.

The phosphate groups P_0 to P_4 are those shown in Fig.(2.3). Small circles are oxygens of the PO_4 groups.

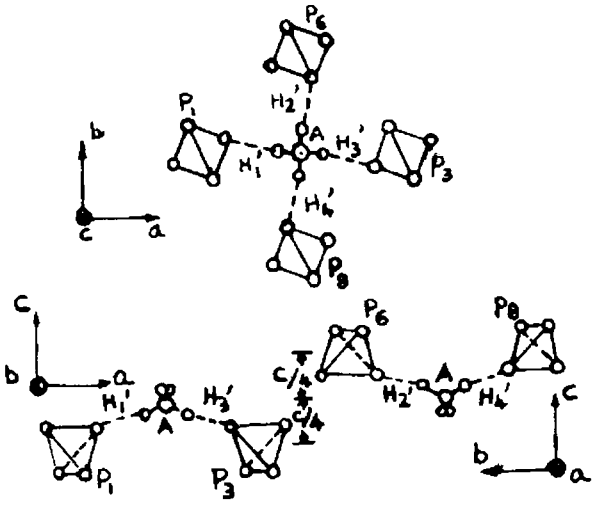

Fig. (2.5). The four hydrogen bonds H_1^1,H_2^1,H_3^1 and H_4^1 associated with ammonium groupA.

(a) view along c-axis (b) view along b-axis (c) view along a-axis.

The groups A, P_0, P_1 and P_3 are those shown in Fig. (2.3); P_6 and P_8 are at a distance c above P_2 and P_4 in Fig. (2.3), small circles are either oxygens of PO_4 groups or hydrogens of the NH_4 group A.

some of the NH_4 internal modes. Measurements were performed despite the shattering of the samples when undergoing the phase transition. Results evidence the disappearance just below T_c of a highly damped mode, which is observed in the whole paraelectric phase. This mode originates from intersite proton motions and is coupled with the brillouin zone-corner antiferroelectric instability. The other modes are only slightly affected by the phase transition, especially the NH_4 internal modes [17].

For ADP and its deuterated isomorphous DADP, the site symmetries of PO_4^{3-} (or $H_2PO_4^-$ or $D_2PO_4^-$) and NH_4^+ (or ND_4^+) ions have been reported to be C_2 in the paraelectric phase and C_1 in the antiferroelectric phase [15,16]. Although the order disorder mechanism is also expected for ADP and DADP in analogy with KDP, the site symmetry of the molecules or ions (PO_4 ,NH_4 and so on) in the paraelectric phase is different from that in the antiferroelectric phase. Consequently, the dipole moment produced by electric charges of ions and their distances in the paraelectric phase suggests that this phase has larger dipole moment at the transition point as the temperature decreases from 400 K to 100 K. According to the positional refinements of each atom in ADP by X ray diffraction study, each ammonium ion at the potassium position in KDP structure is shifted to the off center position by forming two shorter and longer bonds with four PO_4 tetrahedra at low temperature phase. When an oxygen is connected with the shorter N --- H --- O bond, it tends to keep the other proton off in the O --- H--- O bond and when with the larger N--- H--- O bond it tends to take the acid proton nearby. Thus the extra hydrogen bonds produce a distorted NH_4 ion lattice at low temperature causing a drastic change in the dipole moment. The

crystal invariably shatter on entry into the antiferroelectric phase because different domains get distorted in different directions. Several authors felt doubt about the coexistence of two phases at the low temperature transition point in the case of ADP crystals [5,6,20,21,22].

With reference to Fig.(2.1), although peaks appear during both cooling and heating runs in the conductivity plots the difference in direction of the peaks is particularly noteworthy. This observation undoubtfully confirm that, at the transition point the crystal shows pyroelectric behavior in addition to the antiferroelectric behavior. The corresponding pyroelectric field produced is directly proportional to the rate of heating of the sample. Hence this field get superposed over the externally applied field and produces peaks of different magnitude during cooling and heating runs, aiding the externally applied field in one case and acting in opposition in the other. Fig.(2.2) gives the recording of the peaks produced without applying any external electric field across the crystal at the transition point. The sharp and narrow nature of the peaks clearly distinguishes it from any ionic thermocurrent phenomenon. This explains the directional change observed in the conductivity plot at the transition point.

To elucidate the mechanism of electrical conduction process observed in ADP below 300 K, a brief discussion of the peculiar features of the PO_4 group in ammonium contain phosphates is required. Various types of defects observed in phosphate lattice is shown in Fig.(2.6). It is well known that in ADP type crystals the generally observed defects enhancing the electrical conduction processes are

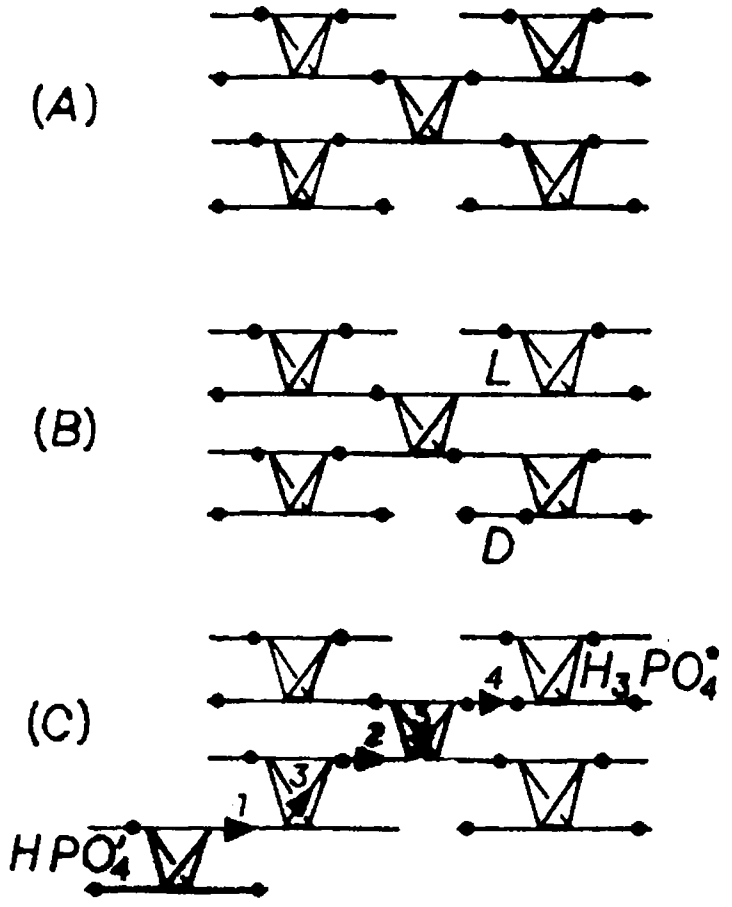

(A) Ammonium dihydrogen phosphate lattice

(B) L and D defects.

(C) Ionization defects.

Fig. (2.6). Various types of defects observed in phophate lattice.

the ionization defects viz: HPO_4 and H_3PO_4 produced as a result of the proton jumps from one phosphate group to the other along the same bond (intra bond jump) and the L and D defects (proton vacancy and doubly occupied proton positions) which are generated as a result of jumps of protons from one bond to another (interbond jump) of the same phosphate group. In ADP , in addition to the above defects there exists protonic defects associated with protons belonging to the NH_4 group (also known as A defects). In the extrinsic region above 285 K the conduction process is mainly due to the ionization defects and L and D defects corresponding to the activation energy value of 0.7 eV. In the temperature range below 285 K the small value of conductivity and activation energy (0.08 eV) observed could be due to the precipitation of the existing defects generated by the impurities in the conduction process.

2.6. CONCLUSION.

DC electrical conductivity measurements in single crystals of $NH_4 H_2 PO_4$ show anomalous variation at 147 K corresponding to a phase transition occurring in this material. The directional change observed in the conductivity plot undoubtfully confirm that, the crystal exhibit pyroelectric behavior at the phase transition point. This observation is in good agreement with the possible coexistence of two phases at low temperature transition point in ADP crystal. Electrical conductivity at low temperature could be mainly due to protonic motion in addition to a small contribution due to impurity dominated extrinsic conduction.

2.7. REFERENCES.

[1]. S.R.Kasturi and P.R.Moran, Phys.Rev.B, 12, 1874, (1975).

[2]. N.S.Dalal and C.A.McDowell, Phys.Rev.B, 5, 1074 (1972).,

[3]. N.S.Dalal and A.H. Reddoch, Abstracts of the International Symposium on Magnetic Resonance, 6th Banff, Alberta, Canada . p 241. (1977).

[4]. F.Brehat, B.Wyncke and H.Arbouz, J.phys.C: Solid State Phys. 19, 689 (1986).

[5]. G.M.Loiacono, Mater.Res.Bull. 5 , 775 (1970) .

[6]. J.Skalyo, B.C Frazer, G.Shirane and W.B.Daniels. ,J.Phys.Chem.Solids. 30 2045 (1969) .

[7]. T.Nagamia, Prog.Theor.Phys. 7 , 275 (1952) .

[8]. W.P.Mason and B.T.Mathias. Phys.Rev. 88 , 477 (1952).

[9]. E.V.Peshikov and N.N.Mukhtarova, Izv.Akad.Nank SSSR, Ser.Fiz., 35, 1939 (1971).

[10]. C.C.Stephson and A.C.Zettlemoyer. J.Am.Chem.Soc. 66 ,1405 (1944) .

[11]. T.Fukami, J.Phys.Soc.Jpn. 62 (6), 2182 (1993).

[12] S.R.Gough, J.A.Ripmeester, N.S.Dalal and A.H.Reddoch, J.Phy.Chem. 83(6), 664 (1979).

[13]. L.B.Harris and G.J.Vella. J.Chem.Phys. 58, 4550 (1973).

[14]. R.Ueda. J.Phys.Soc.Jpn. 3, 328 (1948).

[15]. L.Tenzer, B.C.Frazer and R.Pepinsky. Acta.Crystllogr.11, 505 (1958)

[16]. E.Wiener Avnear, S.Levin and I.Pelah. J.Chem.Phys. 52, 2891 (1970).

[17]. P.Simon, J.Phys. 50(24), P-3477 (1989).

[18]. M.Kasahara, M.Tokunaga and I.Tatsuzaki. J.Phys.Soc.Jpn. 55 , 367 (1986).

[19]. M.Kasahara and I.Tatsuzaki. Jpn.J.Appl.Phys. 24 , suppl.242, p - 920 (1985).

[20]. W.Kanzig, Ferroelectrics and antiferroelectrics in solid state physics, Advances in research and applications, Seitz and Turnbull, Ed.,Academic Press,New York, (1957).

[21]. G.A.Samara, Phys.Rev.Lett. 27, 103 (1971).

[22]. D.Grujic and S.Stamenkovic. Fizika (Zagreb) 481, Suppl. 298 (1976).

CHAPTER 3.

ELECTRICAL CONDUCTIVITY, DIELECTRIC CONSTANT AND PHASE TRANSITION IN NH_4IO_3

3.1. ABSTRACT.

DC electrical conductivity and dielectric constant measurements in the temperature range 300-420 K have been carried out in polycrystalline $NH_4 IO_3$. Both the above properties exhibit anomalous variations at 363 K thereby confirming the occurrence of a first order phase transition in this material. The variation of dielectric constant as a function of temperature for different frequencies has also been investigated. The mechanisms of the phase transition and of the electrical conduction process are discussed.

3.2. INTRODUCTION.

The search for new nonlinear photonic materials using the principle that molecules or ions of the form BO_x^{-n} tend to crystallise in acentric space groups when the B atom has a pair of nonbonded electrons, together with the need for a high refractive index in the material, has led to extensive studies on iodates AIO_3 (A = H, Li, Na, K, Rb, Cs and NH_4) [1]. Each of these materials is acentric, with large indices of refraction, and many are phase matchable and free from optical damage induced at high power densities. A very high acousto-optic figure of merit and large nonlinear optical coefficients have been estimated for NH_4 I O_3 [2]. The field of non-linear optics comprises many fascinating phenomena. Applications include the frequency doubling of a monochromatic wave (second harmonic generation), the mixing of two monochromatic waves to generate a third wave whose frequency is the sum or differences of the original waves (frequency conversion). Nonlinear optical effects (direct or indirect) may be used to make all optical switches. NH_4IO_3 crystals are transparent and optical examination shows them to be biaxial. Birefringence measurements along (010) and (100) directions results n_a-n_c = 0.082, n_b-n_c = 0.066 [2]. The availability of high optical quality single crystals, easily grown from aqueous solution, has led to considerable interest in this iodate.

Several authors have made detailed studies of the electrical properties and phase transitions in crystals containing ammonium ions by giving special attention to the protonic conduction process in them [36]. NH_4IO_3 is a very interesting material belonging to the above category of crystals. Keve et.al. have given detailed

informations about the crystal structure of NH_4 I O_3 [7]. They have also identified a high temperature phase transition in this material at about 358 K. It has been established that at 367 K crystals of ammonium iodate (phase A) transforms from pyroelectric point group m2m symmetry to a piezoelectric non-polar point group (phase B) [2,8,9]. The pyroelectric coefficient has been measured as $(3\pm1) \times 10^{-5}$ Cm^{-2} per ^{0} C., and the abrupt discontinuity in P_s at the transition to phase B is about 0.4×10^{-2} Cm^{-2}. The value of P_s calculated by the point charge method in ammonium iodate is strongly dependent on the charge assignment. The simplest model for NH_4IO_3 takes the charge on the tetrahedral NH_4 ion at the nitrogen atom and that on the distorted trigonal IO_3^- ion at the iodine atom. The latter assumption is partly justified by the lone pair of electrons that tends to compensate the charge distributed on the oxygen atoms [2]. However, no attempt has so far been made to study any of the electrical properties of NH_4IO_3. In this chapter a detailed investigations of the temperature dependent variations of dc electrical conductivity and dielectric constant in polycrystalline ammonium iodate have been presented. We have confirmed and accurately identified the high temperature phase transition in this substance and evaluated the activation parameters for the electrical conduction in different temperature ranges.

3.3. EXPERIMENTAL.

Ammonium Iodate is prepared by adding high purity ammonium hydroxide to a solution of analar grade iodic acid dissolved in triply distilled water. The precipitate obtained for both the samples are filtered and washed to remove

excess of ammonia [7]. Pellets of 8mm diameter and 1.5mm thickness were prepared from the powdered samples. The broad faces of the pellets were coated with quick drying silver conducting paint which served as the electrodes. The sample holder and the chamber used for the measurement of electrical properties were similar to those described in chapter 1. All the measurements were made in a dynamic vacuum of 10^{-3}Torr in the temperature range 300 to 420 K.

In the measurement of dc conductivity, a steady dc bias of 10-100 V was applied across the specimen and the current was measured using a programmable electrometer (Keithley Model 617). The capacitance was measured as a function of frequency as well as temperature using LF Impedence Analyser (Hewlett Packard Model 4192A). Dielectric constant was calculated from the measured values of capacitance after eliminating the lead and fringe capacitances using standard methods [10].

3.4. RESULTS.

Results of dc electrical conductivity measurements carried out in pressed pellet of ammonium iodate sample are shown in Fig.(3.1). The result was found to be well reproducible for different samples. The logσ vs. 10^3 / T plot obtained for this material in the temperature range 300 K to 420 K shows two straight line regions (denoted by I and II) characteristic of ionic crystals. These two straight line regions fit well into the equation $\sigma = \sigma_0 \exp.(-E/kT)$ where σ is the dc conductivity, σ_0 is a constant, k is the Boltzmann's constant and E is the activation energy. The activation energies obtained from the two straight line regions are 1.07 eV and 0.478 eV

respectively for the region I and II. The sudden jump in the conductivity resulting in a λ- shaped anomaly at 363K indicates a phase transition. The result of dielectric measurements carried out in polycrystalline ammonium iodate at 1 kHz in the temperature range 300 K to 420 K is shown in Fig. (3.2). The dielectric constant ε against T plot gives abrupt variations at exactly the same temperature at which the conductivity anomaly occurs. The dielectric constant increases gradually from its room temperature value of 27 and reaches a maximum of 31.6 at 363K. The variation of dielectric constant as a function of temperature for different frequencies has also been displayed in Fig.(3.3). It is observed that in each curve dielectric constant varies slowly up to 360 K. Above this temperature the variations are rapid and an abrupt change occurs at 363 K, confirming the occurrence of a phase transition at this temperature. It is also observed that dielectric constant value increases as frequency increases.

3.5. DISCUSSION.

The previous studies that have been reported by several workers on ammonium containing crystals have unmistakably shown that anomalous variations in the conductivity and dielectric constants of the type observed here are almost always associated with structural, orientational or order disorder transitions occurring in these materials at specific temperatures [6,9,11]. Ammonium Iodate is potentially a ferroelectric substance and the mechanism of electrical conduction and that of phase transition can be explained by considering the structural aspects of this material.

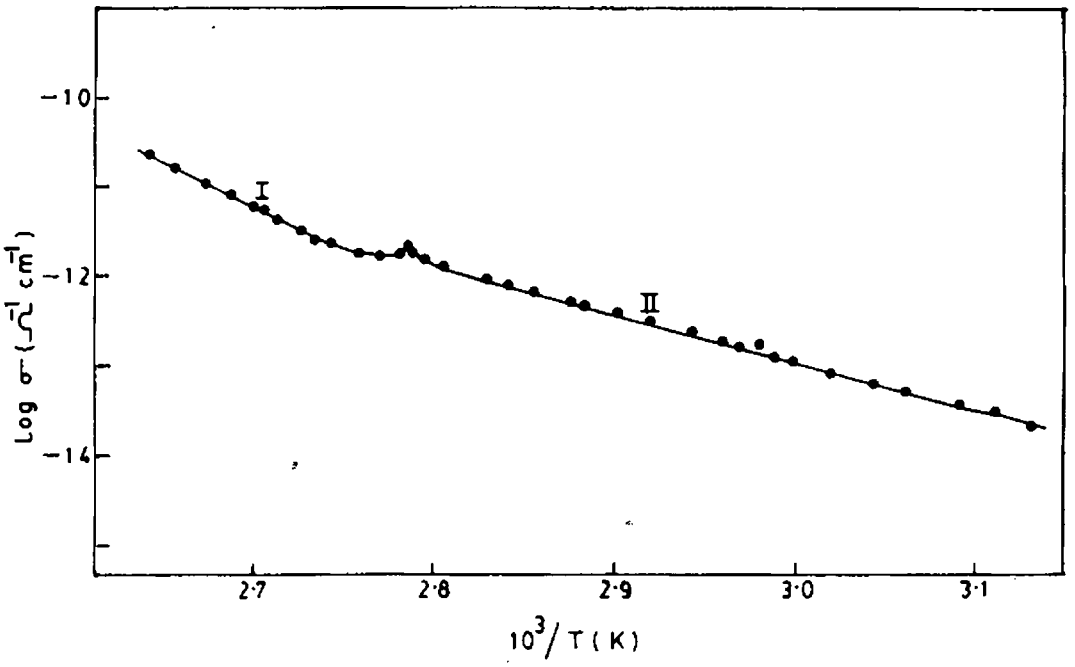

Fig. (3.1) DC conductivity plots for NH_4IO_3 in the temperature range 300 K to 420 K.

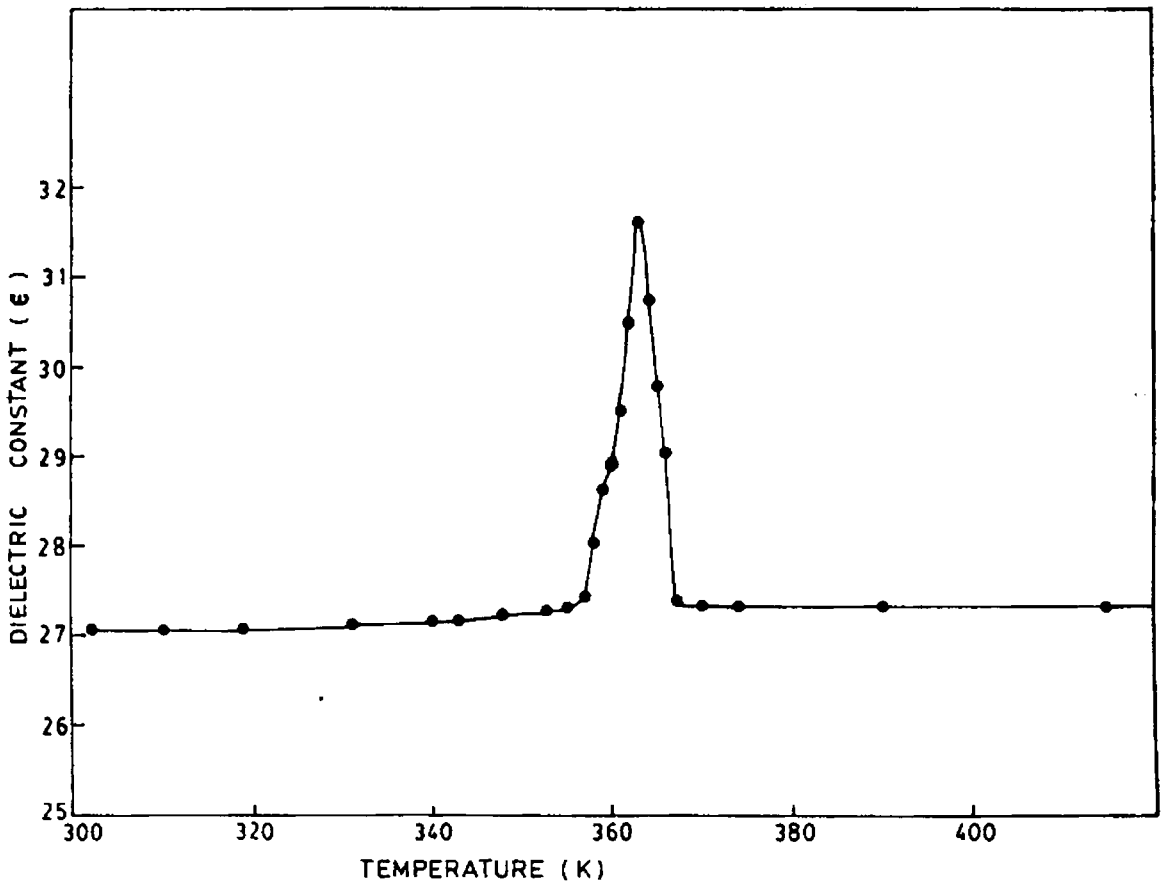

Fig. (3.2). Dielectric constant of NH_4IO_3 as a function of temperature at a constant frequency 1 kHz.

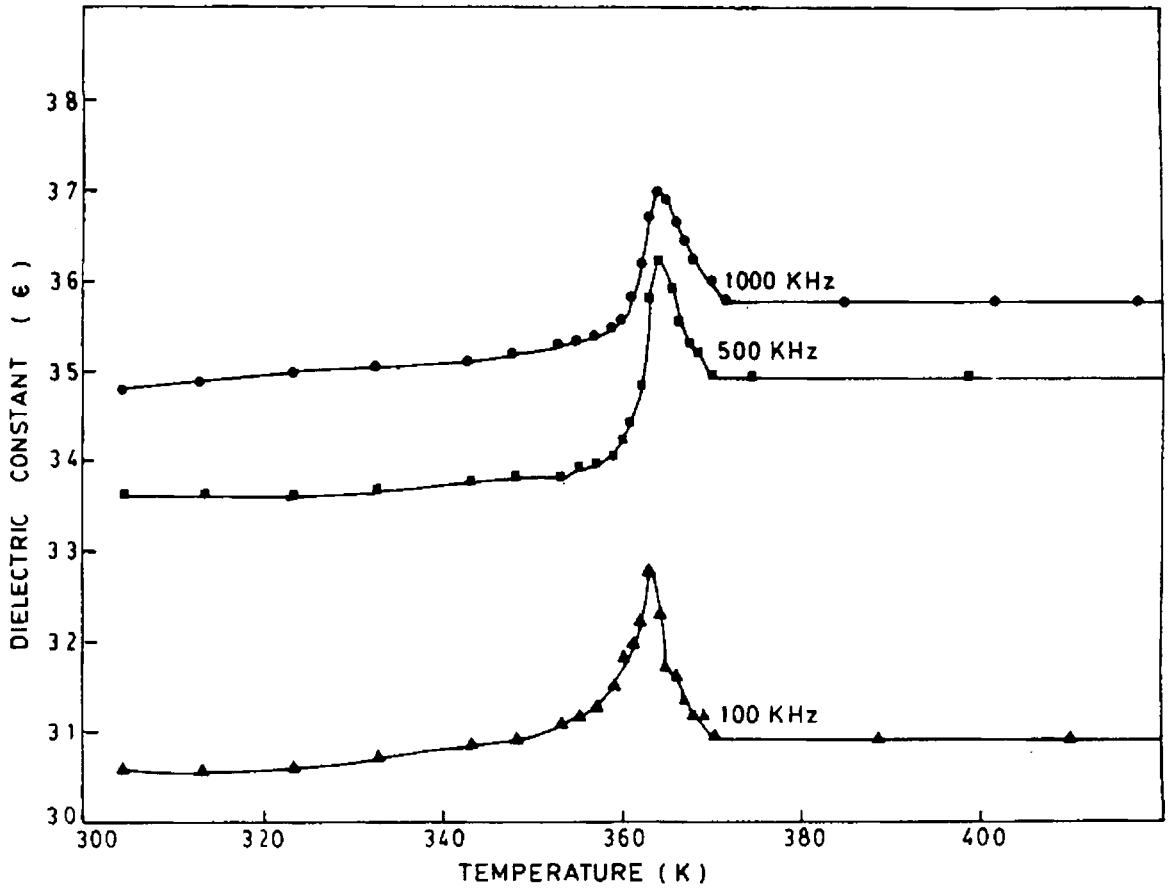

Fig. (3.3). Dielectric constant of NH_4IO_3 as a function of temperature at different frequencies.

Ammonium Iodate is pyroelectric at room temperature and it crystallises in the orthorhombic system with space group $P_c\ 2_1\ n$ and four formulas in the unit cell. The lattice constants of this orthorhombic crystal, measured on a modified version of Bond's precision lattice constant diffractometer are a = 6.4115±0.0005, b = 9.1706±0.0005 and c =6.3740 ± 0.0005 A at 297 K [12,13]. The crystal structure of $NH_4\ I\ O_3$ consists of distorted triangular pyramidal IO_3^- ions and NH_4^+ ions arranged in chains parallel to the b-axis and a-axis [see Figs.(3.4) and (3.5)]. Idealised view of $NH_4\ I\ O_3$ structure showing resemblance to perovskite is also shown in Fig.(3.6). Successive IO_3^- ions are in close proximity, giving the iodine atom a highly distorted octahedral environment (Fig.3.7), with three short (mean of 1.802A) and three long (mean of 2.808A) iodine - oxygen distances. It is thus possible to consider the structure as a highly distorted perovskite arrangement. The IO_3^- ions and NH_4^+ ions form chains parallel to the polar axis (b-axis). A reduction in the barrier to re-orientation of IO_3^- ions and of the spontaneous polarization in the pre-transition temperature interval 335-367 K could be due to an anomalous expansion of the crystal and a change in the system of hydrogen bonds [14]. This is confirmed by investigations of the infrared spectrum of an NH_4IO_3 crystal where an increase in the anion symmetry is attributed to an increase in the local symmetry of the ions because of reorientational motion and a change in the system of the intermolecular hydrogen bonds[15]. The N ------ O distances are less than 3A indicative of weak hydrogen bonding with highly distorted perovskite structure which is potentially a ferroelastic one. This weak hydrogen bonding gives rise large number of protonic defects at high temperatures as has been shown in a number of salts

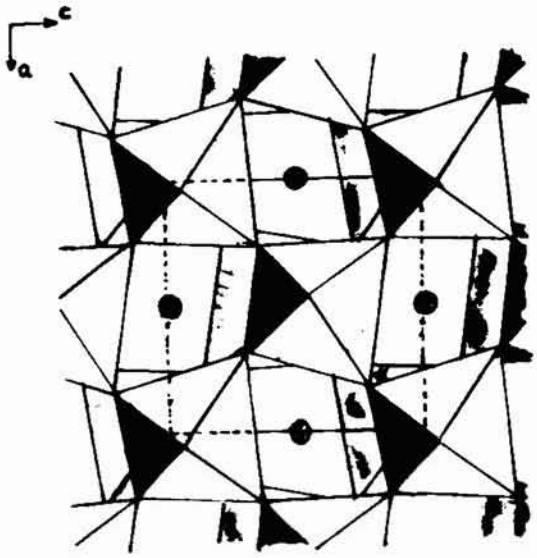

Fig. (3.4). Iodine- Oxygen octahedra viewed along polar b-axis. Hatched circles represent ammonium ions and black triangles the base of the pyramidal IO_3 group (with short I-O distances)

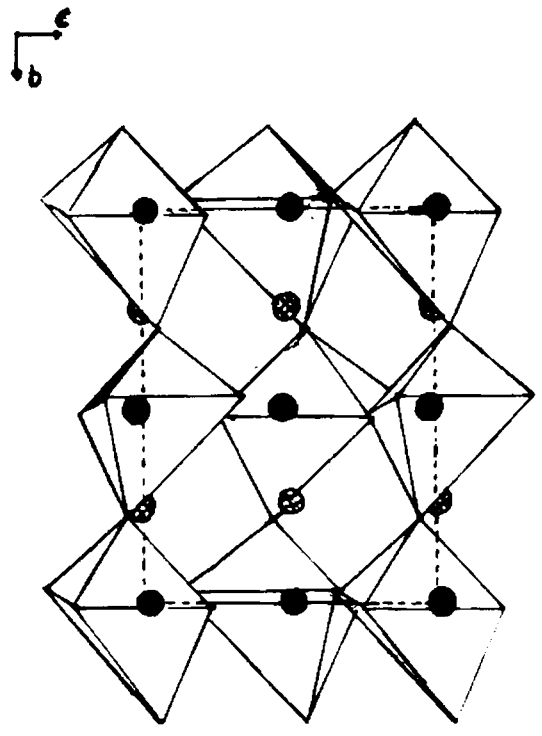

Fig. (3.5). Iodine- Oxygen octahedra viewed along a-axis.

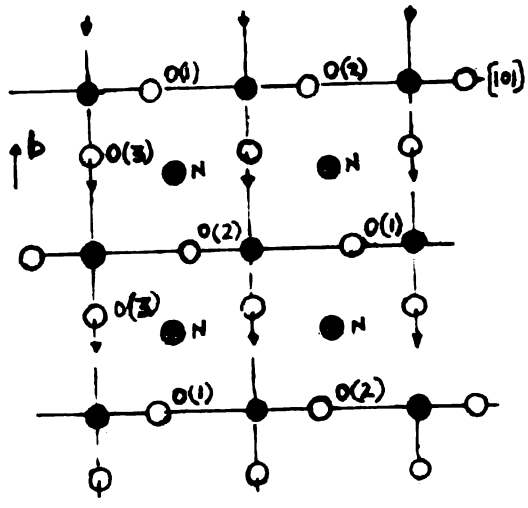

Fig. (3.6). Idealised view of NH_4IO_3 structure showing resemblance to perovskite, and motion of O (3) to reverse polarity. Black circles represent iodine atoms, hatched circle ammonium ions.

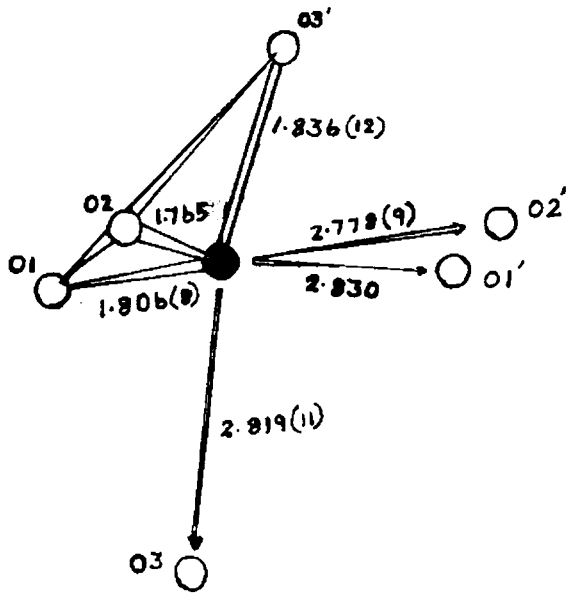

Fig. (3.7). Distorted octahedral oxygen environment of iodine atom, showing three short and three long I-O distances.

containing ammonium group [6,11]. The activation energy values obtained show the existence of a protonic conduction in this material in the temperature region studied here.

The anomalous change in the dielectric constant at the transition point is attributed to the reorientation of NH_4^+ ions in a slightly different hindered potential barrier and this is fully in agreement with the results of spin lattice relaxation time (τ_1) measurements [16]. Such a motion of NH_4^+ group will make a major contribution to the orientational polarizability which explains the high value of dielectric constant at the transition point. However, the τ_1 vs. temperature plot does not change appreciably above the transition point. This indicates that the structure of NH_4IO_3 does not change drastically in going through the phase transition.

3.6. CONCLUSION.

DC electrical conductivity and dielectric constant measurements in pressed pellets of NH_4IO_3 show anomalous variation at 363 K, corresponding to a phase transition occurring in this material. The activation energy values in this material indicate that protonic conduction is the dominant mechanism responsible for the electrical conductivity of this material.

3.7. REFERENCES.

[1]. J.A.Bergman Jr., G.D.Boyd, A.Ashkind and S.K.Kurtz, J.Appl.Phys. 40, 2860 (1969).

[2]. G.R.Crane, J.g.Bergman.Jr.and A.M.Glass, J.Am.Ceram.Soc. 52, 655 (1969).

[3]. E.J.Murphy, J.Appl.Phys. 35, 2604 (1964).

[4]. B.E.Taylor and A.L.Lasker, Phys.Stat.Sol.(b)101, 423 (1980).

[5]. U.Syamaprasad and C.P.G.Vallabhan, Phys.Lett. 89A, 37 (1982).

[6]. R.Navil and C.P.G.Vallabhan, J.Phys.: Condens.Matter.1, 6095(1989).

[7]. E.T.Keve, S.C.Abrahams and J.L.Bernstein, J.Chem.Phys. 54, 2556 (1971).

[8]. E.Salji, Acta.Crystallogr.Sect.A30, 518, (1974).

[9]. T.Oka, T.Mitsui, J.Shiroishi and S.Sawada, J.Phys.Soc.Jpn. 40, 913 (1976).

[10]. C.Ramasastry and Y.Syamasundra Rao, J Phys.E (Scientific Instruments) 12, 1023 (1979).

[11]. U.Syamaprasad and C.P.G.Vallabhan, JPhys.C. 14, L865 (1981).

[12]. R.L.Barns, Mater.Res.Bull. 2, 273 (1967).

[13]. W.L.Bond, Acta. Cryst. 13, 814 (1960).

[14]. D.F.Balsa, A.I.Barabash and E.A.Shadchin, Sov.Phys.Solid State. 27, 1414 (1985).

[15]. A.I.Barabash and G.A. Puchkovskaya, ' Abstracts of papers presented in Second All-Union Conf. On Physico Chemical Basis of Technology of Ferroelectrics and Related Materials' Nauka, Moscow, p-24 (1983).

[16]. R.K.Shenoy and J.Ramakrishna, Ferroelectrics. 48, 309 (1983).

PART -B

CHAPTER-4

INTRODUCTION

4.1. Photoacoustic effect and Photoacoustic Spectroscopy

Spectroscopy can be defined as the study of the interaction of energy with matter, in its broadest sense. Because of its versatility, range, and non destructive nature, Optical spectroscopy remains a widely used and most important tool for investigating and characterizing the properties of matter. Conventional optical Spectroscopies tend to fall in to two major categories, viz; transmission Spectroscopy and reflection Spectroscopy.[1]. There're, however, several instances where conventional Optical Spectroscopic methods are quite inadequate for the complete analysis of the interaction of optical radiation with matter. Such a situation arises when one is attempting to measure the very small change in the intensity of a strong, essentially unattenuated , transmitted signal, both in the case of weakly absorbing and optically opaque materials. Over the years several techniques have been developed to permit optical investigation of highly scattering and opaque substances. The most common among them are diffuse reflectance Spectroscopy [2], attenuated total reflection method [3], internal reflection method[4] and Raman Scattering [5]. All these techniques have proven to be very useful ; yet each suffers from serious limitations. In particular, each method is applicable to only a relatively small category

of materials, each is useful only over a small wavelength range , and the data obtained are often difficult to interpret. Thus another optical technique which yields sufficient information regarding the interacting photons rather than non-interacting photons has successfully been developed in recent times , to study those materials that are unsuitable for the conventional transmission or reflection methodologies, and this is called **Photoacoustic Spectroscopy or PAS** [6-8].

In Photoacoustic Spectroscopy , the sample to be studied is often placed in a closed cell or chamber. For the case of gases and liquids , the sample generally fills the entire chamber. In the case of solids the sample fills only a portion of the chamber, and the rest of the chamber is filled with a non-absorbing gas such as air. In addition, chamber also contains a microphone. The sample is illuminated with a monochromatic light that either passes through an electromechanical chopper or is intensity modulated in some other fashion. If any of the incident photons are absorbed by the sample, internal energy levels within the sample are excited . Upon subsequent deexcitation of these energy levels, all or part of the absorbed photon energy is then transformed into heat energy through non radiative deexcitation process. In a gas this heat energy appears as kinetic energy of the gas molecules, while in a solid or liquid , it appears as vibrational energy of atoms or ions. Since the incident radiation is intensity modulated, the internal heating of the sample is also modulated at the same frequency.

Since Photoacoustics measures the internal heating of the sample, it clearly is a form of calorimetry, as well as a form of Optical Spectroscopy. The periodic heating of the sample from the absorption of the optical radiation results in a periodic heat flow from the sample to the gas, which itself doesn't absorb the optical radiation. This

inturn produces pressure and volume changes in the gas that drive the microphone, the output of which can be suitably amplified and directed. This technique is extremely sensitive and therefore offers the detection of pressure variation corresponding to $\cong 10^{-6}$ °C rise of temperature at the sample-gas interface.

The advantages of Photoacoustics as a form of Spectroscopy are evident from the very nature of the technique. The striking advantage is that , since absorption of optical or electromagnetic radiation is required for the generation of the PA signal, light that is transmitted or elastically scattered by the sample doesn't interfere with the inherently absorptive PAS measurements. This enable one to work with essentially transparent media of highly light scattering materials such as powders, amorphous solids, gels and colloids. Another advantage is the capability of obtaining optical absorption spectra on materials that are completely opaque to transmitted light since the technique doesn't depend on the detection of photons. Furthermore, studies over a wide range of optical and electromagnetic wavelengths are possible with the same detector system, because the sample itself constitutes the electromagnetic radiation detector and no photoelectric device is required. This provides the experimental procedure to become more simple and straight forward. The only limitations are that the source be sufficiently energetic and that whatever windows are used in the system be reasonably transparent to the radiation.

Since the Photoacoustic technique involves the processes as optical absorption, non radiative relaxation and thermal diffusion in a material, this method can be effectively used to study the optical absorption co-efficient, quantum yield, lifetime of excited states and thermal diffusivity of the material with high precision [9].

Furthermore, the study of optical absorption and thermal diffusion at various layers of the sample has opened up a new branch of science namely Photoacoustic Microscopy (PAM). This new and promising technique provides the identification of flaws and defects in a material from the detailed analysis of heat flow through the material [10]. In particular, PAM appears to hold considerable promise both as a general analytical tool and as a dedicated process - control instrument for the Semiconductor industry [11].

With its various Spectroscopic and non- Spectroscopic attributes, PA techniques have already found many important applications in the research and characterisation of materials. A more detailed account of the applications of PA effect is presented in the following section.

4.2. Theory of Photoacoustic effect in solids.

The term Photoacoustic effect (PA) usually refers to the generation of acoustic waves by a sample by the interaction with a modulated electromagnetic radiation. The concept based on Photoacoustic effects and Spectroscopy was first reported by Alexander Graham Bell in 1880 [12]. Eventhough the PA effect was discovered more than a century ago, this field was dormant until 1938 when Veingerov in Russia made a microphone for the study of gases [13]. After that there had been some work during the thirties and forties to study infrared absorption in gas samples to evaluate the concentration of different species in gas mixtures, and to study deexcitation and energy transfer processes in gases [14-18]. In recent times the PA effect is being

successfully employed in various branches of Physics, Chemistry, Biology, Engineering and Medicine as an ultra sensitive detection and diagnostic tool.

Several theoretical models have been put forward for explaining the PA effect in the 19th century itself. Bell suggested that this effect was due to a cyclic expulsion and readsorption of air contained within the sample when it is heated with an intermittent light source. At about the same period Lord Rayleigh explained that this signal was primarily from a thermally induced mechanical vibration of the solid [19]. Another explanation put forward by Mercandier was that the sound is due to the vibrating movement , determined by the alternating heating and cooling produced by the intermittent radiation, principally in the gaseous layer adhering to the solid surface [20]. A more or less similar kind of explanation was also given by Precee [21]. None of the theories advanced in these early years could explain the PA effect satisfactorily.

The present understanding of the PA effect in solids is based on modern theories developed during the seventies. The first attempt to develop an exact quantitative theory was made in 1973 by Parker [22]. While conducting experiments with gases he noticed a sound apparently emanating from the cell windows. This led Parker to derive the theoretical expression for PA signal by which many of the salient features of the more general theories could be established. This was followed by the pioneering works of Rosencwaig and co-workers which resulted in enormous upraise of interest in this field.

The general theory of Photoacoustic effect in solids developed by Rosencwaig and Gersho, now commonly referred to as RG theory, has been found to be very successful in interpreting most of the experimental observations [23,24]. This theory

reveals that in a gas microphone set up for the measurement of PA signal, the signal apparently depends both on the generation of acoustic pressure disturbance at the sample- gas interface and on the transport of this disturbances through the gas to the microphone. The generation of surface pressure disturbance inturn depends on the period of temperature fluctuation at the sample - gas interface . Therefore RG theory could exactly predict the temperature variation in the gas medium which directly depends on the absorption of light by the sample. This theory could thus trigger a world - wide rebirth of interest in PA method and since then, there has been a real boom in the growth of this field.

In the following years , Bennett and Forman [25] gave a theory for nearly transparent sample based on linearised hydrodynamic equations which included both acoustic and thermal diffusion terms. Bennett claims that the acoustic term is dominant in the intermediate frequency range which is the one currently encountered experimentally. McDonald and Wetsel [26] have extended the RG theory to include mechanical vibration of the sample. This is particularly important for liquid samples. This infact led Quimby [27] to make appropriate changes in the RG theory by making use of the three dimensional heat flow at relatively low chopping frequencies. In 1982, Guli [28] formulated a theory based on thermo-elastic considerations in the sample which is in agreement with RG theory. However, these refinements did not change the basic results of the RG theory under most of the experimental conditions.

4.3. Rosencwaig -Gersho Theory

The significant feature of RG theory is its simplicity and straight forwardness in its approach to provide a basic understanding of the various physical processes in the generation of PA signal. This treatment is essentially based on the thermal diffusion through the sample which in turn produces the acoustic signal. Most of the experimental observations on PA studies can be interpreted on the basis of this theory.

RG theory starts with a one dimensional analysis of the generation of PA signal in a simple cylindrical cell as shown in Fig.(4.1). The sample is considered to be in the form of a disc having a diameter equal to the cell diameter and thickness l_s . The sample is mounted in such a way that its rear surface is in perfect contact with a poor thermal conductor of thickness l_b .The gas column which is the coupling medium between the sample and the microphone, has a length l_g. It is also assumed that the gas and the backing material are not absorbers of light .

The intensity of a monochromatic light beam modulated at a frequency ω incident on the sample is given by

$$I = \frac{I_0}{2}(1 + \cos\omega t) \text{ ----------(4.1)}$$

Where I_0 is the incident intensity of the light flux. If the absorption coefficient of the sample is β for the wavelength λ , then the heat density H produced at a point 'x' due to light absorbed at this point in the solid is given by ,

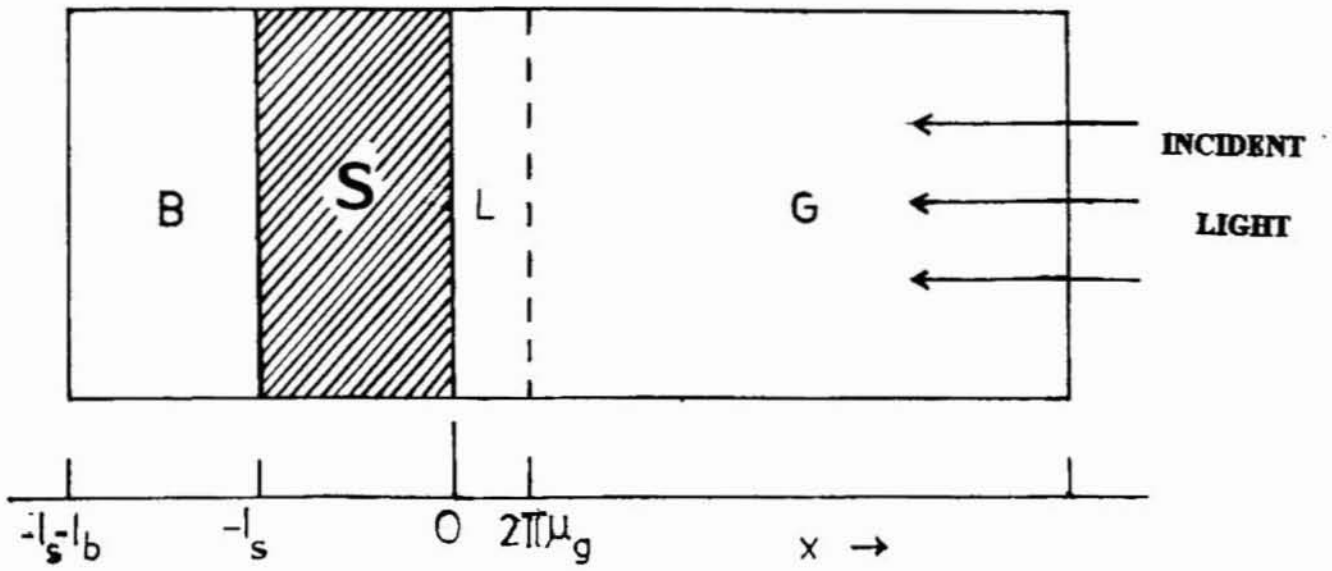

B - BACKING MATERIAL

S - SAMPLE

L - BOUNDARY LAYER OF GAS

G - GAS COLUMN.

Fig. (4.1). Schematic diagram of a cylindrical PA cell.

$$H = \frac{\beta}{2} Io\,[\exp(\beta x)]\,(1+\cos\omega t) \text{ ----------(4.2)}$$

where 'x' takes negative values since the solid extends from x = 0 to x = $-l_s$ with the light intensity at x = 0 . Note also from Fig. (4.1) that the gas column extends from x = 0 to x = l_g and the backing from x = $-l_s$ to x = $-(l_s + l_b)$.

4.3.1. Temperature Distribution

The heat generated in the sample represented by equation (4.2) warms up the sample , gas and backing by an amount $\theta(x,t)$ above the ambient temperature T_0 . There fore , the rise in temperature can be expressed as

$$\theta(x,t) = T(x,t) - T_0 \text{ ----------(4.3)}$$

As soon as the heat is generated in the sample due to the absorption of light ,it starts conducting to the gas and backing and the amount of heat transfer depends on the thermal conductivity of these media. Therefore, the thermal diffusion equation for the sample taking into account the distributed heat source due to illumination can be written as

$$\frac{\partial^2\theta_s}{\partial x^2} - \frac{1}{\alpha_s}\frac{\partial\theta_s}{\partial t} + A\,e^{\beta x}(1+e^{i\omega t}) = 0 \text{ ----(4.4)}$$

with $A = \frac{\beta I_0}{2K_s}\eta$ for $-l_s \le x \le 0$

where Ks is the thermal conductivity of the sample, α_s thermal diffusivity of the sample given by

$$\alpha_s = \frac{K_s}{\rho_s C_p} \quad \text{------(4.5)}$$

Cp , being the specific heat capacity of the sample at constant pressure and ρ_s the density of the sample. η is the efficiency at which the absorbed light at wavelength λ is converted into heat through non-radiative deexcitation processes. The value of η is taken as unity, a reasonable assumption for most solids at room temperature.

The last term in the equation (4.4) represents the heat generated in the sample. Since the heat generated in the sample is transferred to the air and the backing material, the temperature rise in these media will be entirely due to the heat transfer from the sample. The thermal diffusion equations for the gas and the backing material are respectively given by,

$$\frac{\partial^2 \theta_g}{\partial x^2} - \frac{1}{\alpha_g}\frac{\partial \theta_g}{\partial t} = 0 \quad \text{------(4.6)}$$

Where $0 \leq x \leq l_g$ and

$$\frac{\partial^2 \theta_b}{\partial x^2} - \frac{1}{\alpha_b}\frac{\partial \theta_b}{\partial t} = 0 \text{--------(4.7)}$$

where $-(l_s + l_b) \leq x \leq -l_s$

The real part of the complex valued solution $\theta(x, t)$ of equations (4.4), (4.6) and(4.7) is the solution of physical interest and represents the temperature in the cell relative to ambient, as a function of position and time .

The general solution for $\theta_s(x,t)$ in the sample neglecting transients can be written as

$$\theta_s(x,t) = b_1 + b_2 + b_3 e^{\beta x} + [U e^{\sigma_s x} + V e^{-\sigma_s x} - E e^{\beta x}] e^{i\omega t} \quad --(4.8)$$

where $-l_s \leq x \leq 0$

Similarly in the gas medium,

$$\theta_g(x,t) = (1 - \frac{x}{l_g}) F + \theta_0 e^{-\sigma_g x + i\omega t} \quad ---(4.9)$$

where $0 \leq x \leq l_g$

and the temperature at the backing material is

$$\theta_b(x,t) = \frac{1}{l_b}(x + l_s + l_b) W_0 + W e^{\sigma_b (x+l_s) + i\omega t} \quad ---(4.10)$$

where $-(l_s + l_b) \leq x \leq -l_s$.

Here, W, U, V, E and θ_0 are complex valued constants, b_1,b_2, b_3, W_0 and F are real valued constants, and $\sigma = (1 + i)a$, where 'a' is the thermal diffusion coefficient represented by $a = [\frac{\omega}{2\alpha}]^{\frac{1}{2}}$

θ_0 and W represent the complex amplitudes of the periodic temperature at the sample - gas boundary (x =0) and the sample - backing boundary ($x = l_s$) respectively.

The term with amplitude U represents a temperature wave propagating to the left and V represents a temperature wave propagating in the opposite direction in the sample. These waves will be effectively attenuated when they start propagating through the gas medium. The distance up to which these waves can propagate through the gas medium without any appreciable change in its amplitude is approximately one wavelength of this wave which is represented by

$$\lambda_g = 2\pi \mu_g \quad -----(4.11)$$

where μ_g is the thermal diffusion length in the gas. The quantities E and b_3 are given by

$$b_3 = -\frac{I_0}{2\beta K_s} \quad \text{and} \quad E = \frac{\beta I_0}{2K_s(\beta^2 - \sigma_s^2)}$$

In order to solve the thermal diffusion equations, it is necessary to apply proper boundary conditions. Here the boundary conditions for the temperature and heat flux at the sample surface are given by

$$\theta_g\,(0,t) \;=\; \theta_s\,(0,\,t) \quad \text{-------(4.12)}$$

$$\theta_b\,(-l_s,t) \;=\; \theta_s\,(-l_s,t) \quad \text{-------(4.13)}$$

Similarly,

$$K_g \frac{\partial\theta_g\,(0,t)}{\partial x} \;=\; K_s \frac{\partial\theta_s\,(0,t)}{\partial x} \quad \text{------(4.14)}$$

$$K_b \frac{\partial\theta_b\,(-l_s,t)}{\partial x} \;=\; K_s \frac{\partial\theta_s\,(-l_s,t)}{\partial x} \quad \text{------(4.15)}$$

Using the above conditions in the equations (4.8), (4.9), (4.10), the constants can be determined and those solutions are essential for evaluating the temperature distribution in the cell in terms of optical, thermal and geometric parameters of the system. Therefore, the temperature at the sample gas interface (at x = 0) is given by

$$\theta_0 \;=\; \frac{\beta I_0}{2K_s(\beta^2 - \sigma_s^2)} \frac{\left[(r-1)(b+1)e^{\sigma_s l_s} - (r+1)(b-1)e^{-\sigma_s l_s} + 2(b-r)e^{-\beta l_s}\right]}{\left[(g+1)(b+1)e^{\sigma_s l_s} - (g-1)(b-1)e^{-\sigma_s l_s}\right]}$$

---------- (4.16)

Where $b = \dfrac{K_b\,a_b}{K_s\,a_s}$; $g = \dfrac{K_g\,a_g}{K_s\,a_s}$; $r = \dfrac{(1-i)\beta}{2a_s}$

$$\sigma_s \;=\; (1+i)\,a_s$$

From the above relations it is evident that a_s, a_g and a_b play an important role on the heat transfer process in the sample, gas and backing material respectively. The thermal diffusion coefficient

$$a = \frac{1}{\mu} = \left(\frac{\pi f \rho C_p}{K}\right)^{\frac{1}{2}} \text{----------(4.17)}$$

where μ is the thermal diffusion length, f represents the modulation frequency, ρ denotes the density, Cp is the specific heat and K is the thermal conductivity. Therefore the thermal diffusion length in a medium is inversely proportional to the square root of the modulation frequency which means that at higher chopping frequencies, the amount of heat transferred from the inner layer of the sample to the gas medium is much less. This causes a decrease in PA signal at higher chopping frequencies.

4.3.2. Production of Acoustic Signal.

The periodic temperature variation at the sample surface as governed by equation (4.16) causes thermal waves to diffuse into the gas. This periodic diffusion process produces a periodic temperature variation in the gas as is given by the ac component of the solution (4.9)

$$\theta_{ac}(x,t) = \theta_0 \, e^{-\sigma_g x + i\omega t} \text{----------(4.18)}$$

The term $e^{-\sigma_g x}$ denotes the damping of temperature wave when it propagates through the gas medium. The time dependent component of the temperature in the gas (eqn.4.18) attenuates rapidly to zero with increasing distance from the surface of the solid. Since the thermal diffusion coefficient a_g represents the wave number of the temperature diffusion wave, the corresponding wavelength in the gas medium is

$\lambda_g = 2\pi/a_g = 2\pi\mu_g$

Consequently at a distance of $2\pi\mu_g$ which corresponds to one wavelength of acoustic wave in the gas medium, (where μ_g is the thermal diffusion length in the gas), the periodic temperature variation in the gas is assumed to be fully damped out. Thus the spatially averaged temperature of the gas with in this boundary layer as a function of time can be determined by

$$\bar{\theta}(t) = \frac{1}{2\pi\mu_g} \int_0^{2\pi\mu_g} \theta_{ac}(x,t)\, dx \qquad \text{----------(4.19)}$$

$$\bar{\theta}(t) = \frac{1}{2\pi\mu_g} \int_0^{2\pi\mu_g} \theta_0\, e^{-\sigma_g x + i\omega t}\, dx \qquad \text{----------(4.20)}$$

$$\theta(t) = \frac{1}{2\sqrt{2}\,\pi}\, \theta_0\, e^{i(\omega t - \pi/4)} \qquad \text{----------(4.21)}$$

using the relations $\sigma_g = \frac{(1+i)}{\mu_g}$ and $(1+i) = \sqrt{2}\, e^{i\frac{\pi}{4}}$

and the approximation made was $e^{-2\pi} << 1$.

Because of the periodic heating, this boundary layer of gas expands and contracts periodically and thus can be thought of as an acoustic piston on the rest of the gas column, producing an acoustic signal that travels through the entire gas column. The displacement of this gas piston due to the periodic heating can be estimated by the ideal gas law as,

$$\partial x(t) = 2\pi\mu_g \frac{\theta(t)}{T_0} \text{----------(4.22)}$$

Substituting the values from equation (4.21) for θ (t),

$$\partial x(t) = \frac{\theta_0 \mu_g}{\sqrt{2}\, T_0} e^{i(\omega t - \frac{\pi}{4})} \text{----------(4.23)}$$

where To is the temperature at the sample surface. This displacement of the acoustic piston therefore makes an adiabatic change in the gas pressure. Thus the corresponding acoustic pressure in the cell due to the displacement of this gas piston is derived from the adiabatic gas law

$$PV^{\gamma} = \text{Constant.} \text{----------(4.24)}$$

Where P is the pressure, V is the gas volume in the cell and γ is the ratio of specific heats of the gas. Then the incremental pressure is given by,

$$P(t) = \frac{\gamma P_0}{V_0}\delta V = \frac{\gamma P_0}{l_g}\delta x(t) \text{----------(4.25)}$$

where Po and Vo are the ambient pressureand volume respectively.

Therefore substituting values for δx (t) from equation (4.23)

$$P(t) = \frac{\gamma P_0 \theta_0}{\sqrt{2}\, l_g\, a_g\, T_0}\, e^{i(\omega t - \frac{\pi}{4})} \text{----------(4.26)}$$

where

$$\frac{\gamma P_0 \theta_0}{\sqrt{2}\, l_g\, a_g\, T_0} = Q \text{----------(4.27)}$$

Q specifies the complex envelope of the sinusoidal pressure variation in the gas medium which is detected by microphone placed in the cavity.

Thus the actual physical pressure variation Δ P(t) is given by the real part of the δP(t) as

$$\Delta P(t) = Q_1 \cos(\omega t - \frac{\pi}{4}) - Q_2 \sin(\omega t - \frac{\pi}{4}) \text{----------(4.28)}$$

$$\Delta P(t) = q \cos(\omega t - \psi - \frac{\pi}{4}) \text{----------(4.29).}$$

where Q_1 and Q_2 are the real and imaginary parts of Q, and q and Ψ are the amplitude and phase of Q, that is ,

$Q = Q_1 + iQ_2 = q\, e^{-i\Psi}$ ----------(4.30).

Explicit formula for Q is obtained by combining (4.16) and (4.26)

$$Q = \frac{\beta I_0 \gamma P_0}{2\sqrt{2} K_s T_0 l_g a_g (\beta^2 - \sigma_s^2)} \frac{\left[(r-1)(b+1)e^{\sigma_s l_s} - (r+1)(b-1)e^{-\sigma_s l_s} + 2(b-r)e^{-\beta l_s}\right]}{\left[(g+1)(b+1)e^{\sigma_s l_s} - (g-1)(b-1)e^{-\sigma_s l_s}\right]}$$

----------(4.31).

Equation (4.31) gives the amplitude and phase of the acoustic pressure wave generated in the cell by photoacoustic effect. Because of the complexity of equation (4.31), it is somewhat difficult to interpret the results obtained. However, a physical insight may be gained by examining special cases where the expression for Q becomes relatively simple. Rosencwaig and Gersho considered its application to a variety of special cases. In all these special cases the prominent term is nothing but optical absorption coefficient l_β defined by $l_\beta = 1/\beta$ where β is the optical absorption coefficient. The special cases mainly treat with the relative magnitude of l_β with respect to the sample thickness l_s and the variation of thermal diffusion length of the sample μ_s with respect to the sample thickness l_s. According to these conditions sample can be classified into mainly two groups. They are optically transparent samples in which the optical absorption length exceeds the sample thickness and optically opaque samples in which the optical absorption length must be smaller than the sample thickness. The sample can be again divided into two categories by considering its thermal properties. They are thermally thin samples in which the thermal diffusion length exceeds the sample thickness and thermally thick samples in which thermal diffusion length is smaller than the sample thickness.

A clear physical insight into the PA process can be easily obtained by choosing these special conditions. These conditions and their significances are discussed in the following section.

4.4. Special cases

4.4.1 Optically Transparent Solids ($l_\beta > l_s$)

In this case light is absorbed throughout the length of the sample and part of the light is transmitted through the sample. Hence also three special cases are to be considered depending on the thermal diffusion length and length of the solid sample.

(a) Thermally thin Solids

This is the case when $\mu_s >> l_s$ and $\mu_s >> l_\beta$ so that $e^{-\beta l_s} \cong (1 - \beta l_s)$;

$e^{\pm\sigma_s l_s} \cong 1$, $|r| >$

in equation (4.31). Therefore Q can be expressed as

$$Q = \frac{Y}{2a_g a_b K_b}(\beta - 2a_s b - i\beta) \cong \frac{(1-i)\beta l_s}{2a_g}\left(\frac{\mu_b}{K_b}\right) \text{----------(4.32)}$$

where $Y = \frac{\gamma P_0 I_0}{2\sqrt{2}T_0 l_g}$ ----------(4.33).

It is evident from the above expression that the acoustic signal is proportional to βl_s and since $\frac{\mu_b}{a_g}$ is proportional to ω^{-1} , Q has an inverse chopping frequency dependence. For this case where $\mu_s << l_s$, the thermal properties of the backing material play an important role on the PA signal.

(b) Thermally thin Solids.

Here we set $\mu_s > l_s$ and $\mu_s < l_\beta$ so that $e^{-\beta l_s} \cong (1 - \beta l_s)$, $e^{\pm\sigma_s l_s} \cong (1 \pm \sigma_s l_s)$ and $|r| <$ in equation (4.31). Therefore,

$$Q \cong \frac{(1 - i)\beta l_s}{2 a_g}\left(\frac{\mu_b}{K_b}\right) Y \text{ ----------(4.34).}$$

The acoustic signal is again proportional to βl_s which varies as ω^{-1} and also depends on the thermal properties of the backing material.

c) Thermally Thick Solids.

Here, $\mu_s < l_s$ and $\mu_s << l_\beta$. Therefore $e^{-\beta l_s} \cong (1 - \beta l_s)$, $e^{-\sigma_s l_s} = 0$ and $|r| << 1$

The acoustic signal then becomes

$$Q \cong \frac{-i\beta\mu_s}{2a_g}\left(\frac{\mu_s}{K_s}\right) Y \text{ ----------(4.35).}$$

Here, the signal is proportional to $\beta\mu_s$ rather than βl_s. That is, only the light absorbed within the first thermal diffusion length contributes to the signal, inspite of the fact that light is being absorbed throughout the length l_s of the solid. Also, since $\mu_s < l_s$, the thermal properties of the backing material do not have any influence on the

signal and it mainly depends on the thermal properties of the sample itself. Since the equation contains $\mu_s^2\,\mu_g$, the frequency dependence of Q in equation (4.35) varies as $\omega^{\frac{-3}{2}}$.

The above mentioned optically transparent sample demonstrate a unique capability of PA technique which enable one to obtain a depth profile of the optical absorption within a sample.

4.4.2 Optically Opaque Solids ($l_\beta << l_s$)

In this case most of the light is absorbed within a distance that is small compared to l_s, and consequently no light is transmitted. Here also depending on the sample geometry and thermal diffusion length there exist three special cases which are described below.

(a) Thermally Thin Solids.

Here, $\mu_s >> l_s$ and $\mu_s >> l_\beta$ and using the approximations $e^{-\beta l_s} \cong 0$; $e^{\pm\sigma_s l_s} \cong 1$, $|r| >>$ in equation (4.31), the expression for Q is obtained as

$$Q \cong \frac{(1-i)}{2\,a_g}\left(\frac{\mu_b}{K_b}\right) Y \text{ ----------(4.36).}$$

In this case , the acoustic signal is independent of β . This would be the case for a very black absorber such as carbon black. Since the sample possesses large absorption coefficient the acoustic signal is quite strong. The signal depends on the thermal properties of the backing material because the heat generated in the sample can

be transferred to the backing material owing to its large diffusion length. Here also the signal varies as ω^{-1}.

(b). Thermally Thick Solids.

In this case, $\mu_s < l_s$ and $\mu_s > l_\beta$. And setting $e^{-\beta l_s} \cong 0$, $e^{-\sigma_s l_s} = 0$ and

$|r| > 1$. in equation (4.31),

$$Q \cong \frac{(1-i)}{2a_g}\left(\frac{\mu_s}{K_s}\right) Y \text{----------(4.37).}$$

Equation (4.37) is similar to (4.36) except that the thermal parameters of the backing material are now replaced by those of the sample. Also, the acoustic signal is independent of β and varies as ω^{-1}.

(c). Thermally Thick Solids.

Here the condition is $\mu_s << l_s$ and $\mu_s < l_\beta$. Consequently $e^{-\beta l_s} \cong 0$

$e^{-\sigma_s l_s} = 0$ and $|r| < 1$.

Therefore by incorporating these simplifications, the final expression (4.31) then becomes

$$Q \cong \frac{-i\beta\mu_s}{2a_g}\left(\frac{\mu_s}{K_s}\right) Y \text{----------(4.38).}$$

This is a very interesting and important case because eventhough the sample is optically opaque, it is not photoacoustically opaque as long as $\mu_s < l_\beta$, that is the acoustic signal is proportional to β. The signal also depends upon the thermal properties of the sample and varies as $\omega^{-3/2}$. The complete illustration of these special cases has been schematically represented in Fig.(4.2).

One of the most obvious and important predictions of the theory is that the photoacoustic signal is always linearly proportional to the power of the incident photon beam, and that this dependence holds for any sample or cell geometry.

The essence of the RG theory as summarised in equations (4.33) to (4.38) have successfully been verified by several workers [29-32]. Further improvements to the theory have been made later by treating the transport of the acoustic signal in the gas more exactly with Navier-Stokes Equation [25,26,33]. Mcdonald and Wetsel [26] extended the theory to include the effect of thermally induced mechanical vibrations of the sample by solving coupled equations for thermal and acoustic waves in both the sample and gas. Although these refinements did not change the basic concept of the RG theory for most experimental conditions, they were able to account for observed deviations from the RG theory at very low modulation frequencies.

4.5. Applications of the Photoacoustic Effect

Since the PA signal is a combination of two fundamental processes; the absorption of photons and the thermal propagation within the sample, the application of PA effect can be classified mainly into two classes. The first one essentially deals

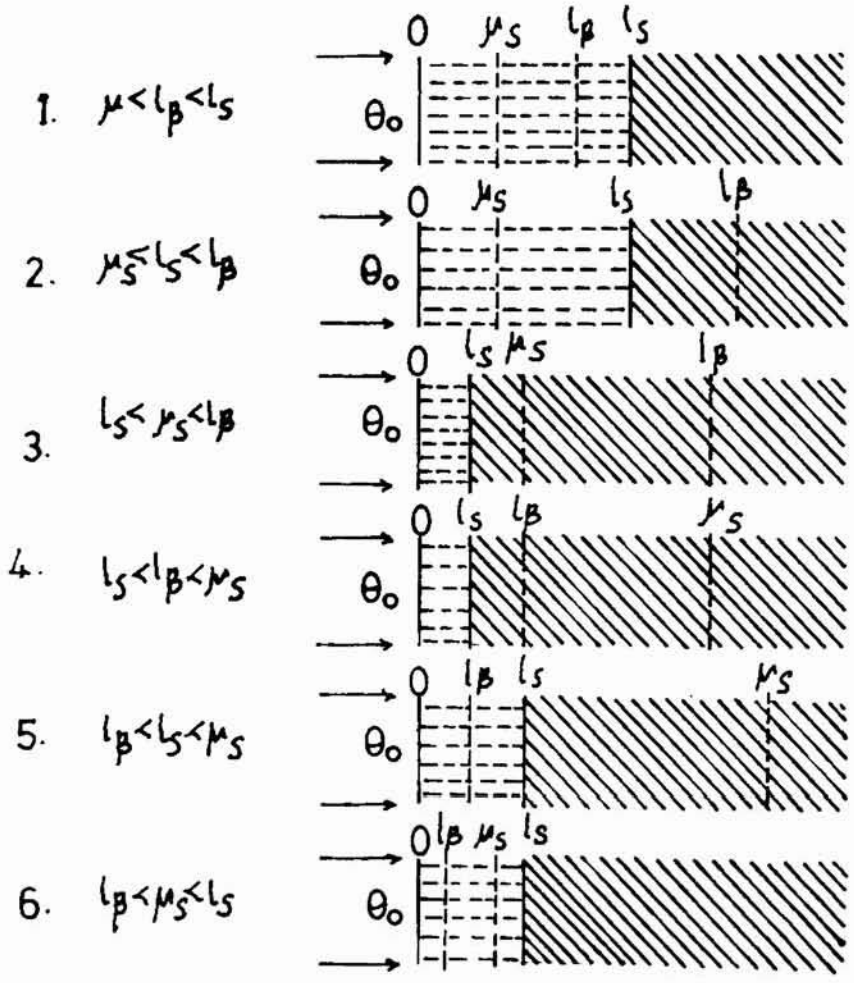

Fig. (4.2). Various cases of thermal piston in PA generation, depending on the relative magnitude of the sample, thermal diffusion length μ_s, optical absorption length l_β and sample thickness l_s.

properties with the spectroscopic applications and the second one is the study of thermal and acoustic es of materials. The range and variety of applications are so wide and there has been a considerable amount of developments in these applications of the PA technique in various branches of science and technology during the past few years. The following paragraphs explains only some of the important application of the PA effect.

Spectroscopy is perhaps the most striking application of the PA effect. It offers a powerful technique to study the absorption spectra of different samples such as solids, liquids and gases. Furthermore, it opens the possibility to obtain good optical absorption data of materials that are essentially transparent or completely opaque to incident light [34,35]. PA spectroscopy also offers important applications in research and analysis of inorganic, organic and biological solids and semisolids [6,35-37].

After the advent of laser PA systems, absorption measurement sensitivity, especially in the case of weakly absorbing samples, has increased to a value of $10^{-10}cm^{-1}$ [38]. Extensive work has been carried out in overtone spectroscopy, trace analysis and pollution monitoring [39-43]. PA spectra give direct and reliable information about the optical absorption bands observed in materials like insulators and semiconductors, which is impossible using conventional absorption technique [6].

The study of de-excitation processes in materials is also possible using this technique. The selective sensitivity of the PA technique to non-radiative de-excitation channel can be used to study fluorescence and photosensitivity of materials. After optical excitation four decay branches such as luminescence, photochemical reaction, photoelectric phenomenon and generation of heat by energy transfer processes, are

generally possible. Then by PA monitoring of the heat branch, the quantum efficiency of luminescence under various conditions can be deduced [45-47]. A combination of conventional fluorescent spectroscopy and PAS can provide information about the relative strengths of the radiative and non-radiative deexcitation processes in solids.

Photovoltaic deexcitation processes can be studied using PA technique. In this process, a part of the incident radiation is converted into electrical energy resulting in a corresponding reduction in the thermal energy produced and hence the PA signal depends upon the energy conversion efficiency of the process. First demonstration was done by Cahen in 1978 by measuring the photoelectrical generation efficiency of silicon solar cells as function of load resistance [48]. Similarly it is possible to determine photoconductive quantum efficiency of a thin organic dye film [49] and photocarrier generation quantum efficiency of a Schottky diode [50]. The PA method has been used to find possible damage resulting from laser irradiation, to investigate laser annealing of semiconductor surfaces and to monitor its dopant concentration [51,52]. It has also been used to study recombination processes in semiconductor along with photoconductivity studies [53,54].

The PA technique can be very useful in non-destructive testing of defects in materials. It offers also a possibility for performing a depth profiling analysis of layered materials because the thermal diffusion length is a function of chopping frequency. At high modulation frequencies, the signal only depends on the thermal diffusivity of the top layer. In the low frequency range the signal contains information about the effusivity ratios of the subsequent layers. This unique capability of the PA technique brings some important applications especially in the case of thin films,

layered and opaque samples etc. Depth profiling is also important in the study of doped semiconductors, laser windows etc., whose surface absorption properties are different from that of the bulk.

Another important application of PA effect is the development of Photoacoustic Microscopy (PAM) which can be used in imaging applications [55-58]. In this technique, construct an image, which is characteristic of the optical and thermal properties within a part of the sample, by scanning the amplitude modulated focused light beam across the surface of the sample. Using different chopping frequencies PA images at various depths can be obtained and that image must be due to the spatial variation in the optical and thermal properties of the sample. In detecting flaws in semiconductor chips, this form of imaging technique is ideal. PA microscopy is a promising area of research because of its potential application in thin film technology, chemical engineering, biology and medicine, semiconductor industry etc.

Detection of acoustic waves after absorption of modulated optical radiation provides informations such as sound velocity, elasticity, flow velocity, specific heat, thermal diffusivity, thickness of thin films ,sub-surface defects and so on. This is because the generation and propagation of thermal waves in a sample depend not only on the optical properties of the sample but also on its thermal, geometrical and elastic properties. The amplitude and phase variations of the PA signal against modulation frequency are used to monitor the phase transition phenomenon occurring in materials.

Another important non-spectroscopic application of PA effect is the measurement of thermal diffusivity of samples. During the last decade, several methods have been developed to determine thermal diffusivities with high precision.

The most widely used method is based upon the photoacoustic effect. In order to measure thermal diffusivity by PA method it is necessary to study the variation of phase or amplitude of the dynamic pressure generated, as a function of the modulation frequency. A lot of works have been reported in this field [59-67]. Since this application has special relevance in respect of the work presented in this thesis, a detailed account of setup and experimentation are described in the following chapters.

4.6. REFERENCES

[1]. Bosquet.P. "Spectroscopy and its Instrumentation" Crane-Russack, NewYork (1971)

[2]. W.W. Wendlandt and H.G.Heat, "Reflectance Spectroscopy" Wiely & Sons: NewYork (1966).

[3]. P.A.Wills and T. Hirshfeld, Appl. Spectroscopic Rev. 1, 99 (1968).

[4]. W.D.Ashtry," Development in Applied Spectroscopy" , Plenum: NewYork (1962).

[5]. G.B. Wright, " Light Scattering of Solids" Spring - Verlag : Berlin, (1969).

[6]. A.Rosencwaig, Opt.Commun. ,7, 305 (1973).

[7]. A.Rosencwaig, Anal.Chem. ,47, 592A (1975).

[8]. A.Rosencwaig, In Advances in Electronics and Electron Physics, Vol.46 (L.Marton, Ed.) pp.207-311, Acadmic Press NewYork, (1978).

[9]. A.Rosencwaig, " Photoacoustics and Photoacoustic Spectroscopy" Wiely & Sons : NewYork, (1980).

[10]. S.K.Vikram Singhe, R.C.Bray, V.Gipson, C.F.Quate and H.R.Saludo, Appl. Phys.Lett., 33, 923 (1978).

[11]. A.Rosencwaig and G. Busse, Appl. Phys. Lett., 36, 725 (1980).

[12]. A.G.Bell, Am. J.Sci., 20, 305 (1880).

[13]. M.L.Veingerov, Dokl. Akad. Nank SSSR. , 19, 687 (1938).

[14]. A. H. Pfund, Science, 90, 326 (1939).

[15]. K.F.Luft, Z. Tech. Phys. 24, 97 (1943).

[16]. M.L.Viengerov, Dokl. Akad. Nank SSSR 54, 182 (1945).

[17]. G.Gordic, Dokl Akad. Nank SSSR, 54, 779 (1946).

[18]. P.V.Slobodskaya, Izv. Akad. Nank.SSSR, Ser.FIz. 12, 656 (1948).

[19]. Rayleigh (Lord), Nature, 23, 274 (1881).

[20]. M.E.Mercadier, Phil. Mag., 11, 78 (1881).

[21]. W.H.Preece, Proc. Roy. Soc. 31, 506 (1881).

[22]. J.G.Parker, Appl. Opt. 12, 2974 (1973).

[23]. A. Rosencwaig and A. Gersho, Science, 190, 556 (1975).

[24]. A.Rosencwaig and A.Gersho, J.Appl. Phys. 47, 64 (1976).

[25]. H.S.Bennett and R.A. Forman, J Appl. Phys., 48, 1432 (1977).

[26]. F.A.McDonald and G.C.Wetsel Jr., J. Appl. Phys., 49, 2313 (1978).

[27]. R.S.Quimby and W.M. Yen, Appl. Phys. Lett. 95, 43 (1979).

[28]. Guli, Appl Opt., 5, 955 (1982).

[29] M.J.Adams, G.F.Kirkbright & K.R.Menon, Anal. Chem., 51, 508 (1979).

[30]. J.F.McClell and R.N.Knisely, Appl.Phys. Lett., 28, 467 (1976).

[31]. G.C.Wetsel Jr. and F.A.McDonald, Appl.Phys.Lett., 30, 252 (1977).

[32]. E.M.Monahan Jr. and A.W.Nolle, J.Appl.Phys., 48, 3519 (1977).

[33]. L.C. Aamodt, J.C.Murphy and J.G.Parker, J.Appl.Phys.48, 927 (1977).

[34]. A. Hardwik & Schlossberg, Appl.Opt. 16, 101 (1975).

[35]. A. Rosenwaig, Phys. Today 28, 23 (1975).

[36]. A.Rosenwaig, Science 181, 657 (1973).

[37]. A.Rosencwaig & S.S.Hall, Anal. Chem. 47, 548 (1975).

[38]. C.K.N.Patel and R.J.Kerl, Appl. Phys. Lett. 30, 578 (1977).

[39]. R.G.Bray and M.J.Berry J.Chem. Phys. 71, 4909 (1979).

[40]. G.Stella, J.Getland and W.H.Smith, Chem.Phys. Lett. 146 (1976).

[41]. C.K.N Patel, Science 220, 157 (1978).

[42]. T.H.Vansteenkiste, F.R.Faxvog and D.M.Roessler, Appl. Spectrosc.35, 194 (1981).

[43]. P.C.Claspy, C.Ha and Y.H.Rao, Appl.Opt. 16, 2972 (1977).

[44]. W.Lahman and H.J.Ludewig, Chem. Phys. Lett. 45, 177 (1977).

[45]. M.J.Adams, J.G.Highfield and G.F.Kirkbright, Anal.Chem. 49, 1850, (1977).

[46]. J.C.Murphy and L.C. Aamodt, J.Appl.Phys. 48, 3502 (1977).

[47]. R.S. Quimby and W.M.Yen, Opt. Lett. 3, 181 (1978).

[48]. D.Cahen, Appl.Phys.Lett. 33, 810 (1978).

[49]. A.C. Tam, Appl.Phys. Lett. 37, 978 (1980).

[50]. W.Thieleman and H.Neumann, Phys.Stat.Solidi.(a) 61, K123 (1980).

[51]. J.F.McClelland and R.N. Kniseley, Appl. Phys.Lett. 35, 121 (1979).

[52]. J.F.McClelland and R.N.Kniseley, Appl. Phys. Lett. 35, 585 (1979).

[53]. V.A.Sablikov and V.B.Sandomirskii, Sov.Phys. Semi.Cond., 17, 50 (1983).

[54]. A.Mandelis and E.K.M.Sin, Phys.Rev. B 34, 7209 (1986).

[55]. G.F.Kirkbright and R.M.Miller, Analyst, 107, 798 (1982).

[56]. A.Rosenwaig and G.Busse, Appl. Phys.Lett. 36, 725 (1980).

[57]. Y.H. Wong, R.L Thomas and G.F.Hawkins, Appl.Phys Lett. 32, 538 (1978).

[58]. H.K. Wickramasinghe, R.L.Brag, V.Jipson, C.F.Quate and J.R.Saleeda, Appl.Phys.Lett., 33, 923 (1978).

[59]. M.J.Adams and G.F.Kirkbright, Analyst 102, 28 (1977).

[60]. P.Charpentier, F.Lepoutre and L.Bertrand, J. Appl. Phys. 51, 608 (1982).

[61]. O.Pessoa, C.L.Cesar, N.A.Patel, H.Varges, C.C.Ghizoni and L.C.M.Miranda, J. Appl. Phys., 59, 1316 (1986).

[62]. P.Korpium, R.Tilgner, and D.Schmidt, J.Phys., (Paris) Colloq. 44, C6 (1983).

[63]. A. Torres-Filho, L.F.Perondi and L.C.M.Miranda, J.Appl.Polym.Sci. 35, 103 (1988).

[64]. T. Hashimoto, J.Cao and A.Takakn, Thermochem.Acta., 120, 191 (1987).

[65]. B.Bonno, J.L.Laporate and Y. Ronsset ,J.Appl. Phys. , 67, 2253 (1990).

[66]. A.M. Mansanares, H.Vargas, F. Galembeck, J.Buigs and D.Bicanic, J.Appl.Phys. 70, 11 (1991).

[67]. J.Thomas, V.N. Sivasankarapillai, E.Xavier and C.P.G.Vallabhan, J. Mater. Sci.Lett. , 15, 151 (1996).

CHAPTER 5

PHOTOACOUSTIC MEASUREMENT OF THERMAL DIFFUSIVITY IN METAL PHTHALOCYANINES

5.1. ABSTRACT.

Thermal diffusivity values in iron, nickel, manganese, zinc phthalocyanines and in a metal free phthalocyanine as well as in their iodine doped samples have been determined using photoacoustic (PA) technique. Samples in the form of a pressed pellet have been used along with an Ar^{+} laser for exciting the PA effect in a suitable photoacoustic cell and the amplitude of the PA signal was measured with a lock-in amplifier. The method involves the determination of the characteristic frequency f_c obtained by measuring the variation of the amplitude of the photoacoustic signal as a function of the chopping frequency of the laser beam. The results indicate that doping with iodine enhances the thermal diffusivity in a substantial manner in Metal Phthalocyanines (MPcs). It is also found that the thermal diffusivity values obtained for metal phthalocyanines are comparable with that of zinc naphthalocyanines which are also organic semiconductors like phthalocyanines.

5.2. INTRODUCTION.

Phthalocyanines have received more attention recently because of their chemical flexibility, charge transport properties and technological applications. Most of this work has been carried out on polycrystalline samples, owing to the difficulties encountered in obtaining single crystals of sufficient size. Porphyrin like structure with high chemical and thermal stability makes phthalocyanine compounds a very attractive class of materials in the field of organic semiconductors. Metal phthalocyanines have found wide use as paint pigments and dyes. Because of their extremely good stability to acids, alkalis and solvents phthalocyanines are particularly useful in spin dyeing. Phthalocyanine pigments in the form of aqueous dispersions are used in pad dyeing with resin emulsions. Many of these metal phthalocyanines can be used as catalysts. Cobalt, Nickel and Iron phthalocyanines catalyse the oxidation of many organic compounds. Similarly, the photoconducting property of MPcs has been extensively studied for use in electrophotographic systems, diodes, laser printers, photovoltaic cells and photoelectrochemical devices [1-5].

However, metal phthalocyanines such as FePc, NiPc, MnPc and ZnPc are of considerable interest as new candidates for optical, electronic, photoelectric, electrochemical and photovoltaic applications. Recent reports show that organic dyes such as phthalocyanines are very good material for optical data storage (ODR) applications in place of metallic substances because of their chemical stability and feasibility for synthetic engineering [6,7]. It has also been reported that phthalocyanines posses non-linear optical properties and many of these exihibit large χ^3

values [8]. Highly conjugated π - electron system has been considered as the most suitable organic materials for third- order non-linear optics. As a result measurement of their thermal, chemical and optical properties has acquired great significance.

Photoacoustic technique (PA) is a versatile method for the measurement of thermal and optical properties of materials of various kinds. It is also a very reliable technique which yields fairly accurate values for the above parameters when only small sample volumes are available. In PA method the energy of intermittent optical radiation incident on a sample surface generates periodic heating which is finally converted into a sound signal. The composite nature of the acoustic signal generation with definite amplitude as well as phase constitutes the main feature of the PA effect in comparison with other measurement methods. The signal produced is sensitive only to the absorbed radiation which is converted to PA signal by nonradiative processes. This chapter describes the photoacoustic measurements of thermal diffusivity in metal free phthalocyanines (H_2Pc), metal phthalocyanines and their iodine doped forms using front surface excitation technique. A knowledge of the thermal diffusivity of these molecular electronic materials will be very useful in situations involving heat flow problems encountered in device fabrication and application.

5.3. THEORY.

As seen in chapter 4 , following the one dimensional model of Rosencwaig and Gersho [9], the pressure variation δP at the front surface of an optically thick sample irradiated with a chopped beam of monochromatic radiation depends on the thermal diffusivity α_s of the sample. The theoretical expression of δP may be written as

$$P = X.Y$$

In the above relation,

$$X = \left[1 + g\frac{h^+ + h^-}{h^+ - h^-}\right]^{-1}\left[g + \frac{h^+ + h^-}{h^+ - h^-}\right]\frac{1}{\alpha_s^{\,2}\, l_s^{\,2}} \qquad \text{----------(5.1)}$$

where,

$$h^+ = \exp.(\sigma_s . l_s)$$

$$h^- = \exp.-(\alpha_s . l_s)$$

$$\sigma_s = (1 + j)\left[\frac{\pi f}{\alpha_s}\right]^{\frac{1}{2}}$$

$$g = \frac{e_b}{e_s} = \left[\frac{K_b}{K_s}\right]\left[\frac{\alpha_s}{\alpha_b}\right]^{\frac{1}{2}},$$

the ratio between the effusivities of the backing material (e_b) and the sample (e_s),

and $$Y = \frac{P_0 \gamma W_a l_s^{\,2}}{2 l_g T_0 K_s}\left[\frac{\alpha_g}{\alpha_s}\right]^{\frac{1}{2}} \qquad \text{----------(5.2)}$$

Here l, K, ρ and C are length, thermal conductivity, mass density,and specific heat, and subscripts g, s, and b refer to the gas (air), sample and backing material respectively. $P(T_0)$ is the ambient pressure (temperature), γ is the specific heat ratio for air, Wa is the absorbed power of light. The effusivity of the gas in the cell has been neglected compared to the effusivity of the sample, since their ratio is always less than 1%. The term X depends on the modulation frequency f_c through the product $\sigma_s l_s$, which can be written as

$$\sigma_s\, l_s = (1+j)\left[\frac{\pi f}{f_c}\right]^{\frac{1}{2}} \qquad \text{----------(5.3)}$$

where the characteristic frequency f_c is given by

$$f_c = \frac{\alpha_s}{l_s^{\,2}} \qquad \text{----------(5.4)}$$

It can be found out by plotting log A against log f where A is the amplitude of the PA signal (which is directly proportional to δP). When chopping frequency f becomes equal to f_c, a change in slope occurs in the above plot.

5.4. EXPERIMENTAL.

5.4.1. Synthesis, Purification and Characterisation of Phthalocyanines.

Phthalocyanine metal complexes may be prepared by various methods. The technological importance of the phthalocyanine pigments has generated renewed interest in their synthesis, purification and characterisation. One

of the important methods available for the synthesis of metal phthalocyanines is the reaction of phthalonitrile with a metal or metal salt in a high boiling liquid like nitrobenzene or quinoline. In this method phthalonitrile and metal chloride with mole ratio 4:1 is heated to 180^0-190^0 C for two hours in quinoline or in a mixture of quinoline and tricholrobenzene. Iron, Nickel,Manganese and Zinc phthalocyanines have been synthesised by this method [10,11]. The reaction may be written as,

$MeCl_2$ + 4 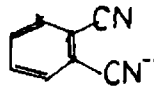 ----------> MPc Cl + Cl^-

This reaction takes place in the presence of urea, or quinoline act as accepters for the halogen atoms which enter the phthalocyanine molecule to an appreciable extent when the accepters are not present.

A formidable hurdle in phthalocyanine chemistry is the isolation of phthalocyanine in its purest form. Every method of synthesis of phthalocyanines results in the contamination of the product with unreacted materials such as phthalic anhydride, urea, phthalimide or phthalonitrile. The phthalocyanine formed itself is a mixture of oligomers. Classical purification techniques such as acid and alkali washing, solvent washing, solvent extraction, regeneration by concentrated H_2SO_4 , vacuum sublimation and chromatography are used to purify the crude phthalocyanines.

The first step in the purification of phthalocyanine involves washing with 10% caustic soda, 2M HCl, methanol and benzene successively. The solid mass so obtained is slurried in concentrated sulphuric acid and dropped on ice. The precipitate which is essentially a mixture of various polymorphs of metal phthalocyanines is washed with water and dried. Though this method is sufficient for the removal of

unreacted materials, the different polymorphs and oligomers cannot be separated. The unreacted phthalonitrile was removed by soxhlet extraction with benzene. It is again purified by vacuum sublimation.

The method of preparation of metal free phthalocyanines is quite different. Magnesium phthalocyanine that is already prepared is dissolved in concentrated sulphuric acid and the solution thus obtained is poured over ice. Metal free phthalocyanines precipitate and which can be purified by the procedure described above.

The whole samples prepared were characterised by elemental analysis ; UV-Vis and IR Spectroscopy.

5.4.2. Structure of Phthalocyanines.

Phthalocyanines are macrocyclic compounds containing four pyrrole units and structurally similar to porphyrins and tetraazaporphins. More generally, they include tetraazaporphins in which the four pyrolle units are fused to an aromatic structure. In addition to the structural similarity of phthalocyanines to porphyrin, they are closely related in many other respects. Both are stable to alkalis, less so to acids, both are highly coloured, and form complex metallic compounds, both are degraded by oxidation to the imides of dibasic acids. The order of stability of the metallic derivatives of the two classes are also similar.

The compound usually referred to under the phthalocyanine class consists of metal derivatives of phthalocyanine. The two hydrogen atoms attached to the two isoindole group can be replaced by metal atoms from every group of the periodic table

to form the metal phthalocyanines (Fig.5.1). Also, each of the sixteen peripheral hydrogen atoms on the four benzene rings can be substituted by a variety of atoms and groups.

The Phthalocyanine can be considered as a weak dibasic acid and the metal derivatives as its salts. For example, in metal phthalocyanines, the metal atom supplies one electron to the nitrogen atoms of the isoindole groups and these isoindole nitrogen atoms in turn supplies an electron to the metal atom, forming a covalent bond. The unshared pairs of electrons in the remaining two isoindole nitrogen atom presumably form coordinate covalent bonds with the metal atom. The unusual stability of these metal complexes can be explained by the coordintion of the central metal atom.

5.4.3. Doping in Metal Phthalocyanines.

The effect of doping on the electrical and photoconductivity of molecular solids is well known. The electrical and photoconductivities of phthalocyanines are also found to be increased by the addition of dopants like iodine. A study of the doping effect on the organic semiconductors give a clue to the electronic processes such as charge carrier generation upon irradiation, the process being essential in photosynthesis and solar energy conversion [12]. However, by doping with iodine, the conductivity of phthalocyanines can be markedly increased [13,14]. Because of the high stability of I_3^- polar environments,and its ability to accommodate itself into channels in one dimensional lattices, iodine is an advantageous dopant for

(A)

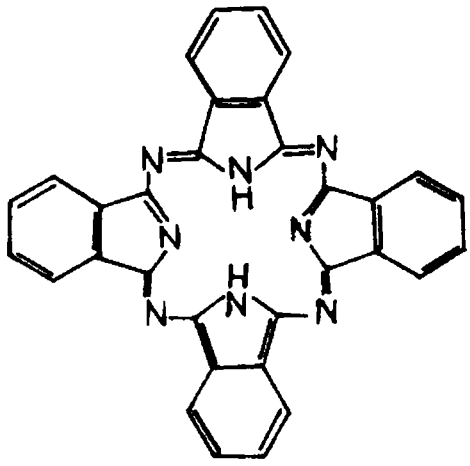

(B)

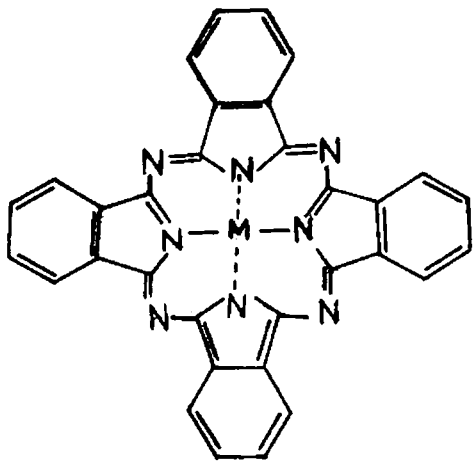

Fig.(5.1). Structures of (A) Phthalocyanines and (B) Metal Phthalocyanines.

the oxidation of planar organic molecules. Iodine doping forms stacks of partially oxidized metal phthalocyanine units and parallel chains of I_3^- counter ions [15]. The oxidation of purified metal phthalocyanines and metal free phthalocyanines by iodine vapour or solutions results in dark coloured solids with a range of stoichiometries [16], the exact composition obtained depending on the conditions,

$$M\,Pc + 1/2 \times I_2 \text{ ----------} > M\,Pc\,(I)_x$$

FePc, NiPc, MnPc ZnPc and H_2Pc samples were doped with iodine in the solution phase as reported in the case of cobalt phthalocyanine earlier [17,18]. 200mg each of the samples was stirred with a saturated solution of iodine in carbon tetrachloride (CCl_4) for 48h. The doped materials were filtered, washed with CCl_4 till there was no extraction of iodine. These samples were dried at 800° C in vacuum for 2h before pelletising the same. The measurements were made on pressed (2000 kg cm^{-2}) pellets of the samples having thickness 0.065 cm. The saturation pressure (2000 kg cm^{-2}) was determined by pressing the sample to a level at which the density remains unaltered with further increase in pressure.

5.4.4. Instrumental.

Block diagram of the experimental set up is shown in Fig.(5.2). Fig. (5.3) shows a photograph of the experimental set up. The light source used is the 488 nm radiation from an Ar^+ laser (Liconix -5000 series) at a power level of 30 mW. The laser beam is chopped by a mechanical optical chopper (Stanford Research System model SR 540). The non-resonant type PA cell used for the measurement is shown in Fig.(5.4). It has a cylindrical cavity of length 0.5cm and diameter 1cm made in a

solid block of stainless steel. The glass window and the microphone are sealed with 'O ' rings and air at atmospheric pressure acts as the coupling gas medium . The signal is detected by Knowle' s 1753 electret microphone kept inside the PA cell and the output is analyzed using a digital lock-in amplifier (EG & G model 5208). The response of the PA cell to the incident radiation was evaluated using carbon black as the sample [Fig.(5.5) and Fig.(5.6)].

5.5. RESULTS.

The amplitude of the PA signal A is measured as a function of the chopping frequency f which ranged from 20 to 200 Hz for all the five samples and for their iodinated forms. The log A vs log f plots obtained for FePc, NiPc, MnPc , ZnPc and H_2 Pc and their iodine doped forms are shown in Figures (5.7a, 5.7b, 5.7c, 5.7d, 5.7e.). The characteristic frequency (frequency at which sudden change in slope occurs) for each of the substance was obtained from these graphs. The calculated values of thermaldiffusivity are given in the Table 1. The results can be considered as reliable within 2% .

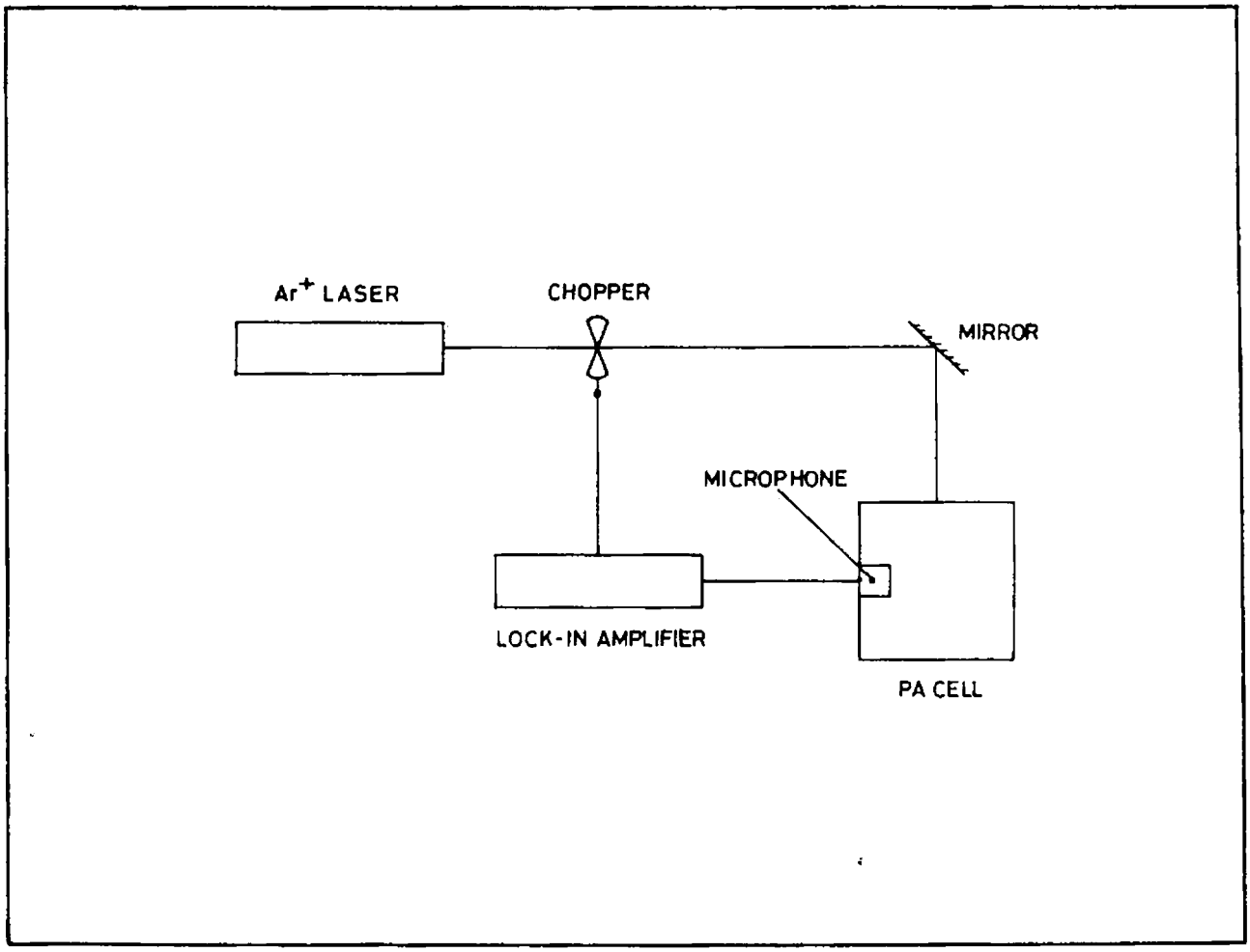

Fig.(5.2). Block diagram of the experimental set up.

Fig.(5.3). Photograph of the experimental set up.

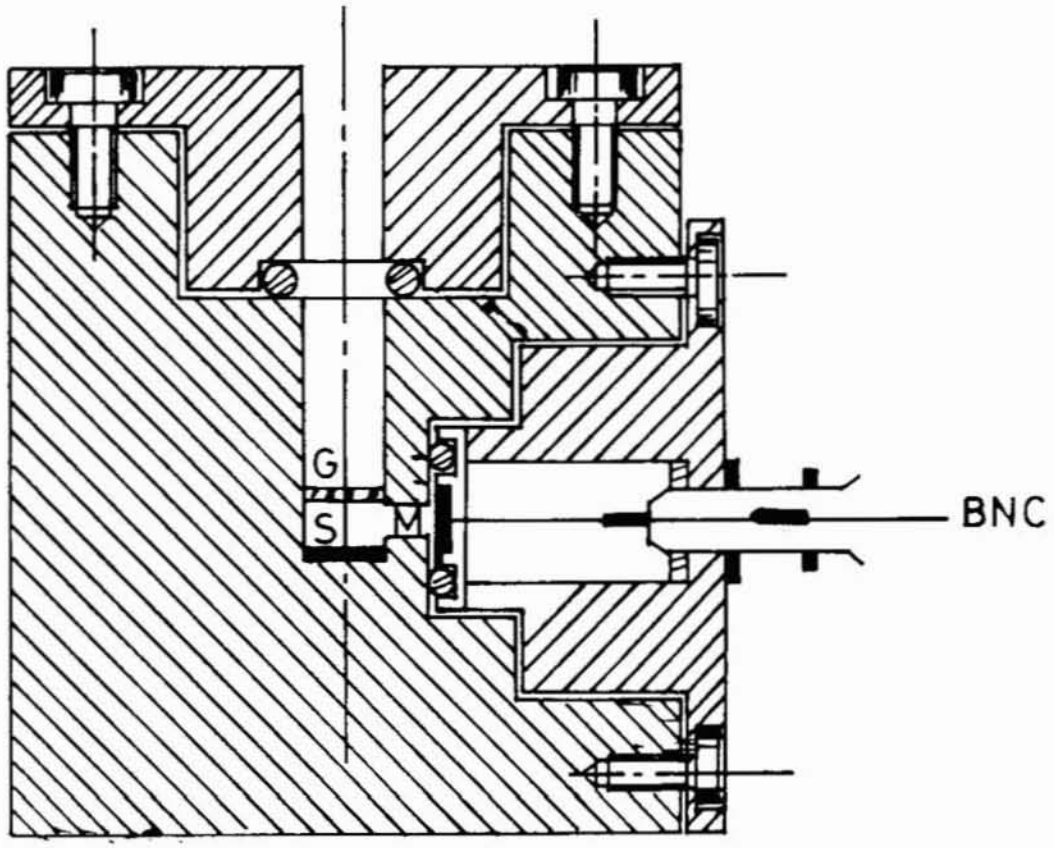

G - GLASS WINDOW
S - SAMPLE
M - MICROPHONE

Fig.(5.4). Schematic diagram of the PA Cell.

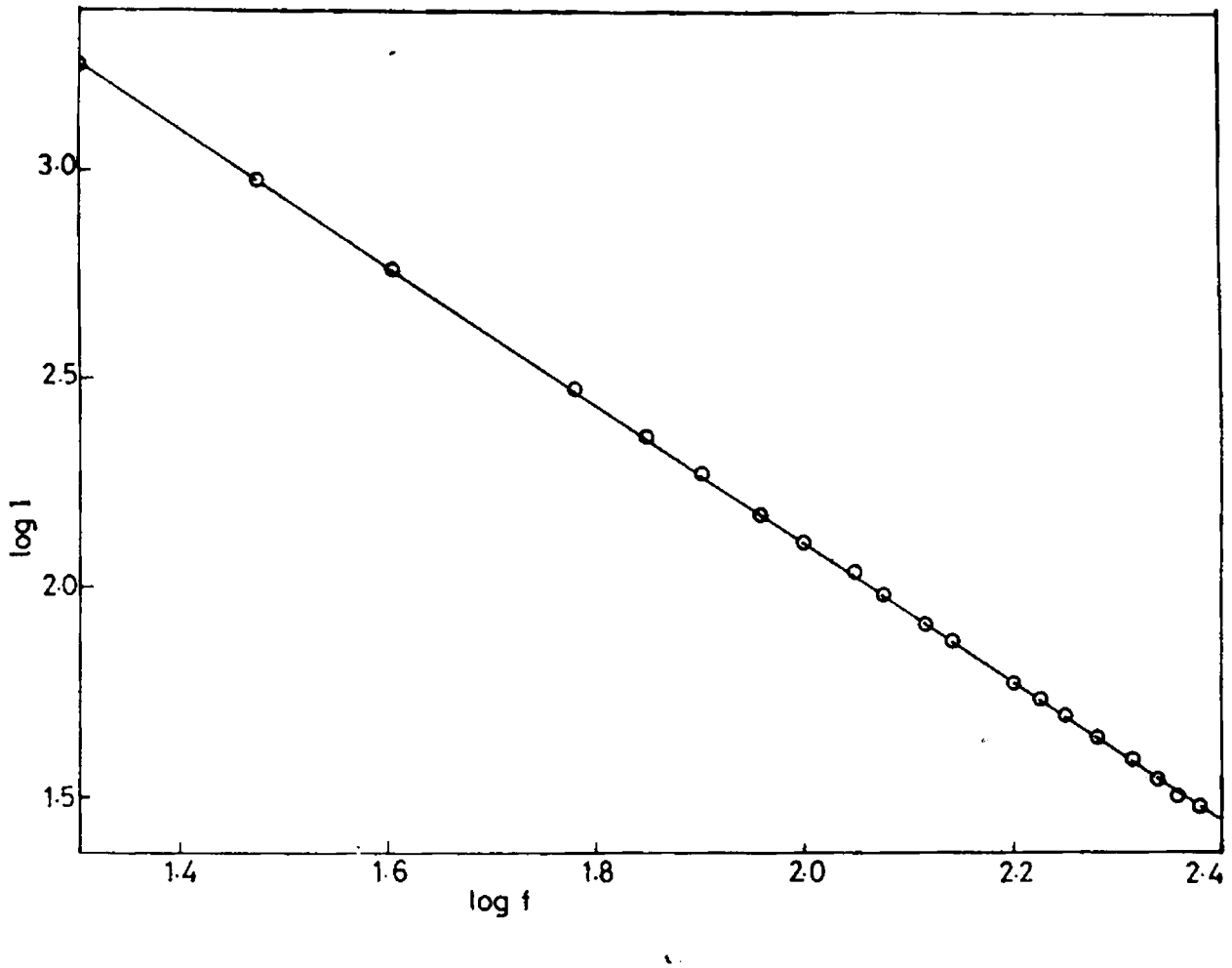

Fig.(5.5). log-log plot of the PA signal amplitude versus chopping frequency of carbon black.

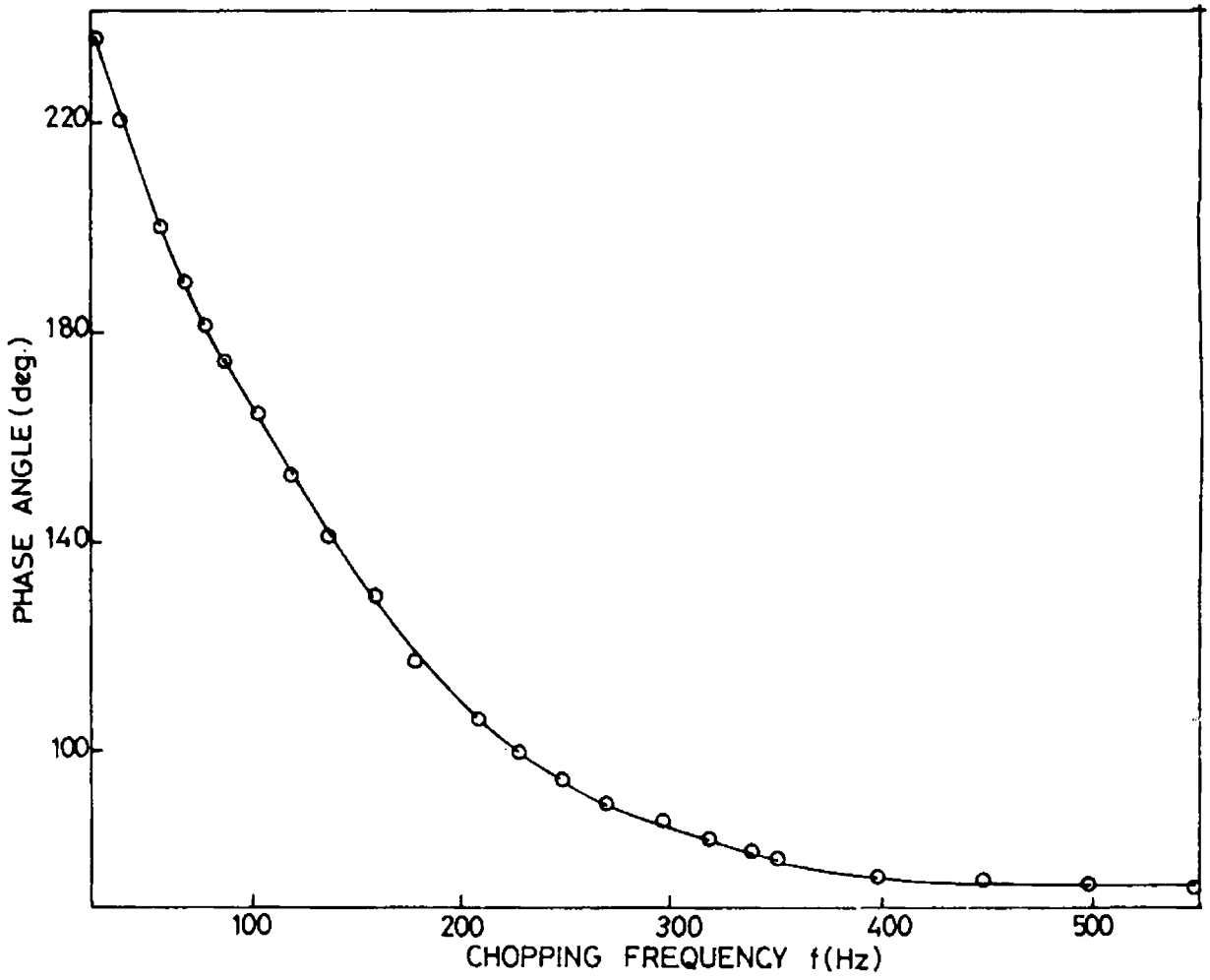

Fig.(5.6). Variation of the PA phase with chopping frequency for carbon black.

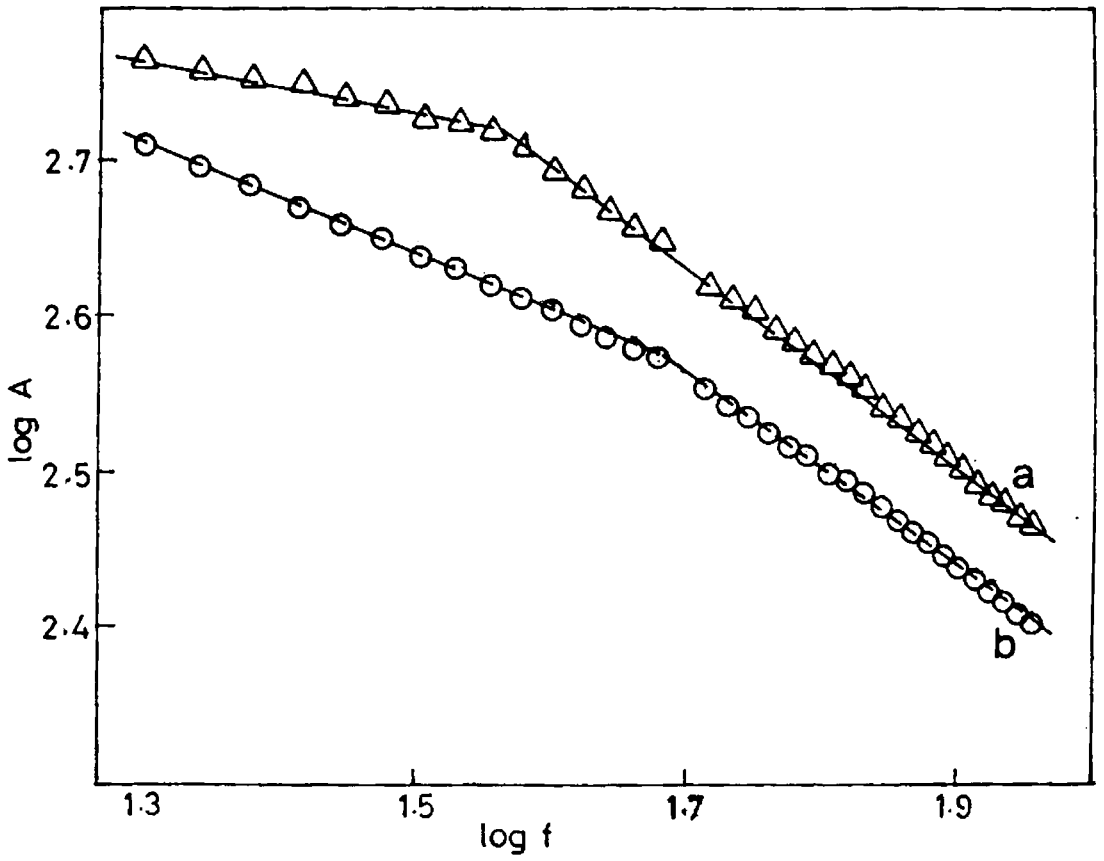

Fig.(5.7a). log-log plot of the PA signal amplitude versus chopping frequency for FePc (a) and FePcI (b)

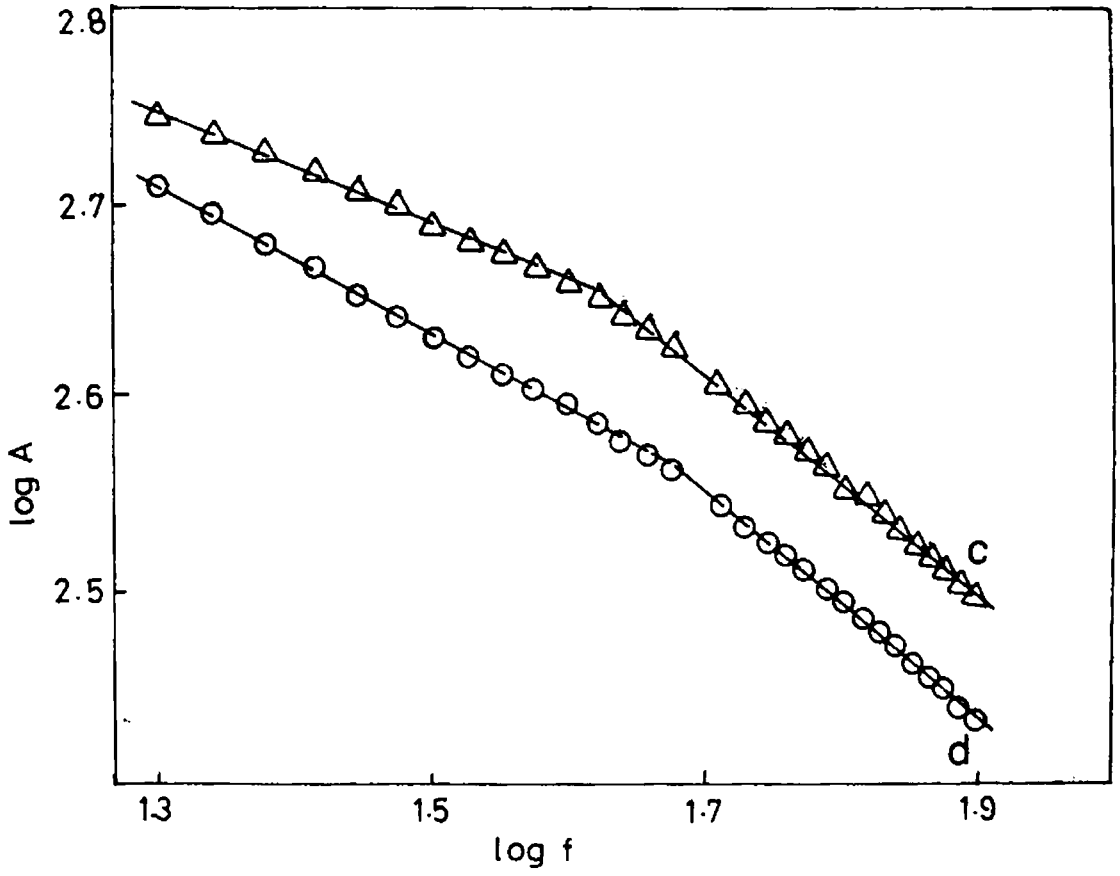

Fig.(5.7b). log-log plot of the PA signal amplitude versus chopping frequency for NiPc (c) and NiPcI (d)

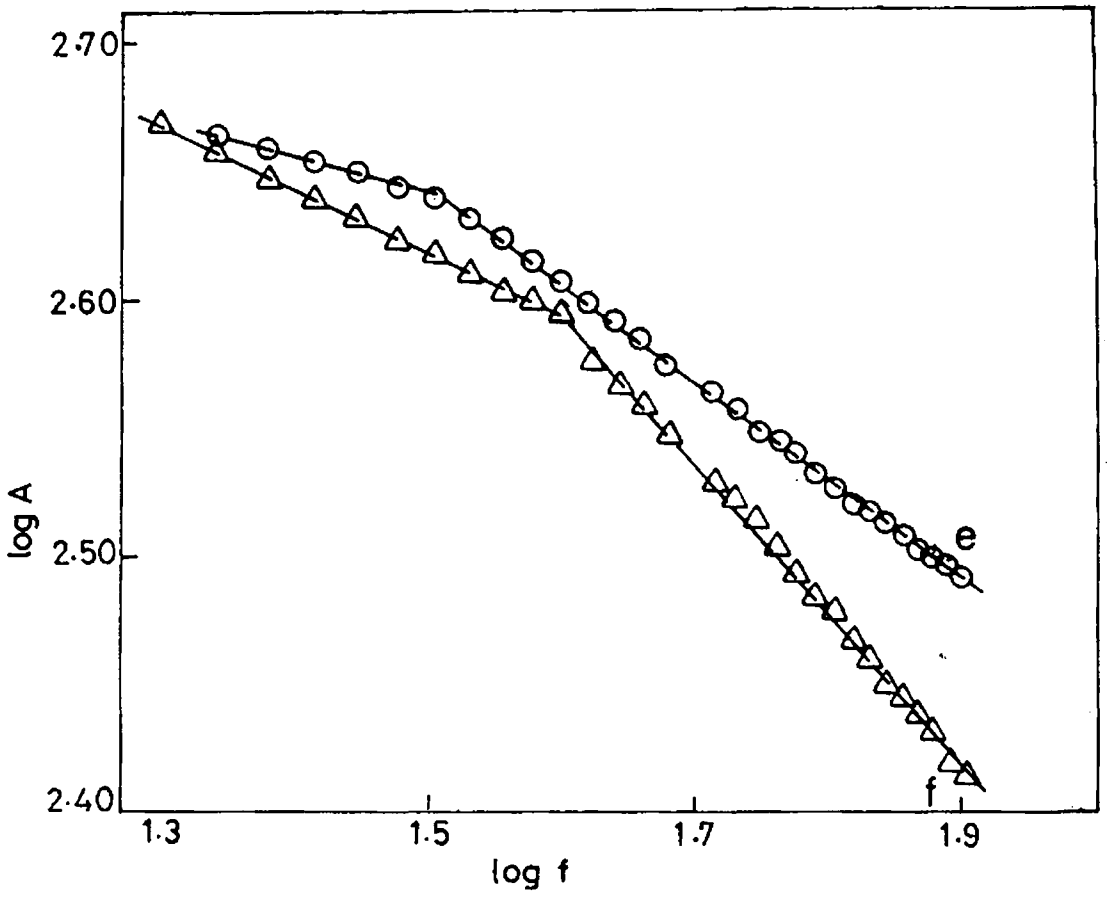

Fig.(5.7c). log-log plot of the PA signal amplitude versus chopping frequency for MnPc (e) and MnPcI(f)

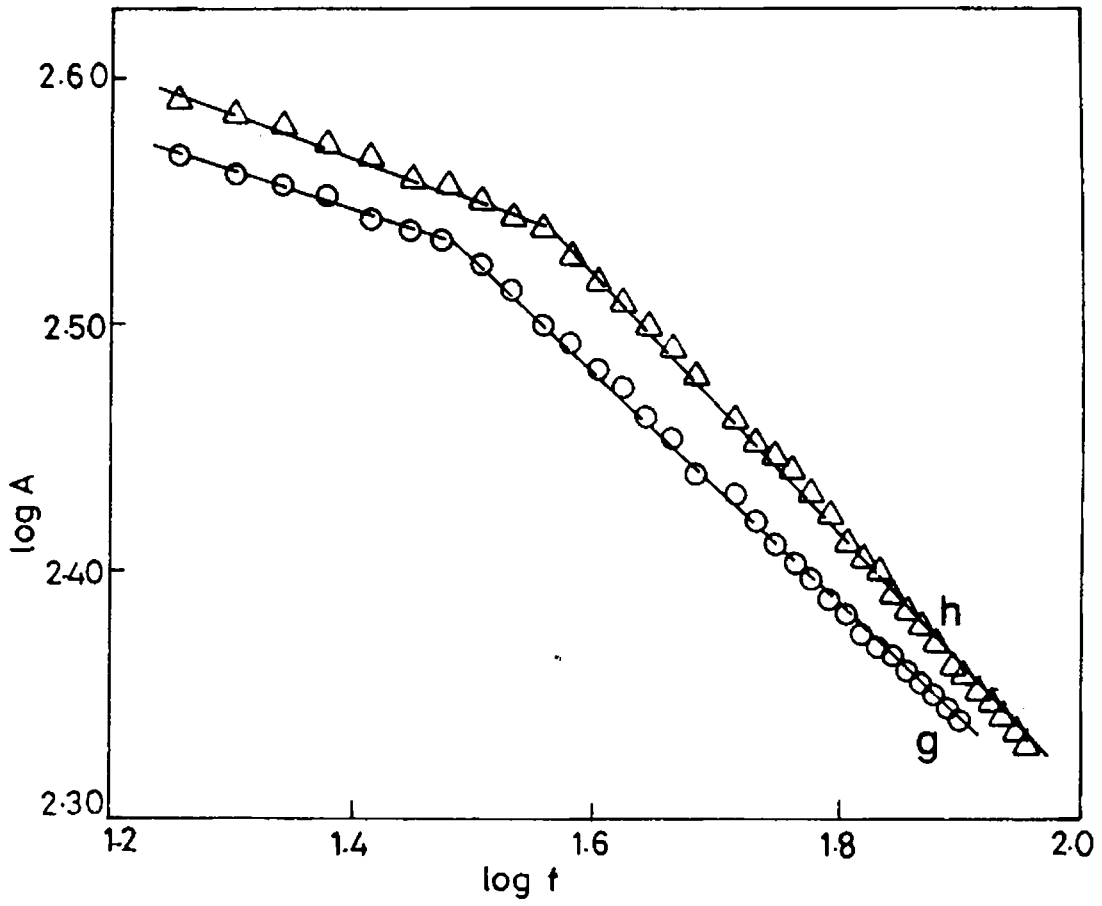

Fig.(5.7d). log-log plot of the PA signal amplitude versus chopping frequency for Zn Pc (g) and ZnPcI (h)

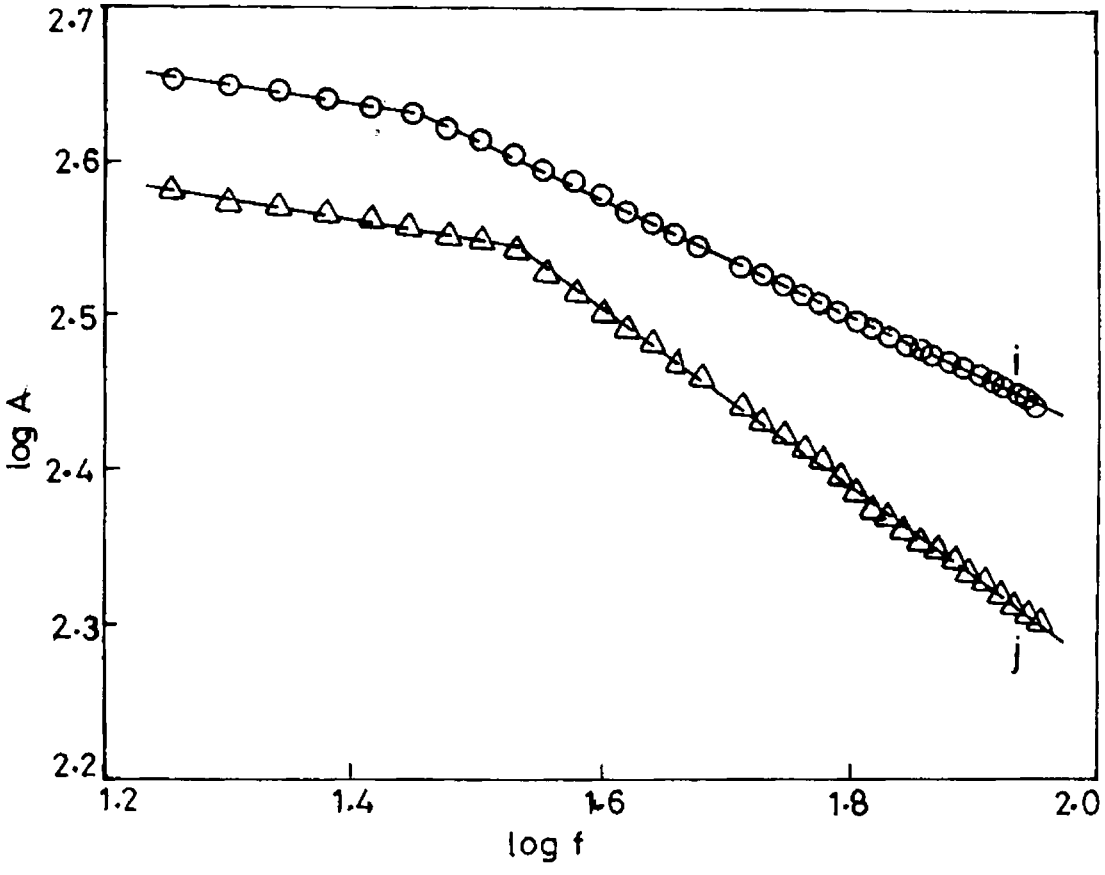

Fig.(5.7e). log-log plot of the PA signal amplitude versus chopping frequency for H_2 Pc (i) and H_2PcI (j)

TABLE 1. Thermal diffusivity values of pristine and iodine doped phthalocyanines .

Samples	Characteristic frequency(f_c)Hz	Thermal diffusivity α_s cm^2 /sec.
FePc	36.76	0.17.
FePcI	49.74	0.23
NiPc	33.14	0.14
NiPcI	49.70	0.21
MnPc	32.35	0.14
MnPcI	39.81	0.17
ZnPc	31.12	0.13
ZnPcI	36.48	0.15
H_2Pc	28.18	0.12
H_2PcI	33.81	0.14

5.6. DISCUSSION.

From the result presented here it may be noted that the thermal diffusivity values are substantially higher in the case of iodine doped metal phthalocyanines in comparison with iodine free samples. It may also be noted that the magnitude of thermal diffusivity values obtained here for phthalocyanines are comparable with the values reported for zinc naphthalocyanines which is also an organic semiconductor like phthalocyanines [19].

Since the thermal diffusivity $\alpha = K/\rho C$ where K, the thermal conductivity, ρ the density, and C, the specific heat capacity of the sample, the variation in α may be contributed by any of the above three quantities. Studies have shown increased value of density in iodinated metal phthalocyanines [17]. As the structure of the metal phthalocyanines considerably changes on doping with iodine, the variation in specific heat capacity should also be taken into account [15]. Specific heat capacity of metal phthalocyanines increases on iodination because the thermal activation energy of the iodinated sample is 50 fold greater than the undoped complexes [20]. Nevertheless we see a substantial increase in the thermal diffusivity value on iodination. As a result we can safely conclude that there must be a significant increase in thermal conductivity of MPcs on iodination and the increase in thermal diffusivity in MPcs on doping with iodine arises mainly from a change in thermal conductivity of the materials. It must be added here that a very large increase in electrical conductivity values also has been observed in these materials on doping with iodine [18]. This points to the significant role of electronic carriers in

contributing to the heat conduction mechanism in organic semiconductors like phthalocyanines.

The simplicity and convenience of the experimental set up together with non contact nature of measurement strongly favour the present technique for determining thermal diffusivity of solid samples. The PA method has the added advantage that accurate measurement of thermal diffusivity is possible for sample materials available in small quantities.

5.7. CONCLUSION.

In conclusion the thermal diffusivity values for five MPcs and their iodinated forms have been determined from PA measurements. The iodinated MPcs. are found to exhibit higher values for the thermal diffusivity. These results point to a substantial enhancement of thermal conductivity of these materials on iodination.

5.8. REFERENCES.

[1]. Grammatica and Mort, J.Appl.Phys.Lett. 38, 445 (1981).

[2]. A.Kakuta, Y.Mori, S.Takano, M.Sawada and I.Shibuya, J.Imag.Technol. 11, 7 (1985).

[3]. A.K.Ghosh, D.L.Morel, T.Feng, R.F.Shaw and C.A.Rowe, J.Appl.Phys. 45, 230 (1974).

[4]. M.Shimura and A.Toyoda, Jpn.J.Appl.Phys. 23, 1462 (1984).

[5]. R.O.Loutfy and L.F.McIntyne, Energy Mater. 6, 467 (1982).

[6]. H.Yanagi, M.Ashida, J.Elbe and D.Wohrle, J.Phys.Chem. 94, 7056 (1990).

[7]. H.Yanagi, T.Kouzeki, M.Ashida, T.Noguchi, A.Manivannan, K.Hashimoto and A.Fujishima, J.Appl.Phys. 71, 5146 (1992).

[8]. Hari Singh Nalwa, Atsushi Kakuta and Akio Mukoh, J.Phy.Chem. 97, 1097 (1993)

[9]. A.Rosencwaig and A.Gersho, J.Appl.Phys. 47, 64 (1976).

[10]. W.J.Kroenke and M.E.Kenney, J.Inorg.Chem. 3, 25 (1964).

[11]. K.Kasagua and M.Tsutsin, Coord. Chem. Rev. 32, 67 (1980).

[12]. R.F.Chaiken and D.R.Keams, J.Chem.Phys. 45, 3966 (1970).

[13]. A.D.Ghosh, D.L.Monel, T.Feng, R.S. Shaw and Rowe Jr., J.Appl.Phys. 1, 230 (1974).

[14]. T.Gleizer, T.J.Marks and J.A.Ibers, J.Am.Chem.Soc. 97, 3545 (1975).

[15]. T.J.Marks,. Science 227, 881 (1985).

[16]. S.W.Pelletier and N.U.Mody, J.Am.Chem.Soc. 99(1), 286 (1977).

[17]. C.J.Schramm, R.P.Scaringe, D.R.Stogakovic, B.M.Hoffman, J.A.Ibers and T.J.Marks, J.Am.Chem.Soc. 102, 6702 (1990).

[18]. P.S.Harikumar and V.N.Sivasankara Pillai, J.Mater.Sci.Letters. 9, 1324 (1990).

[19]. J.Thomas, V.N.Sivasankara Pillai, E.Xavier and C.P.G.Vallabhan,, J.Mater.Sci.Letters. 15, 151152 (1996).

[20]. J.Simon and J.J.Andre, Molecular Semiconductors ; Photoelectrical Properties and Solar Cells. Springer Verlag, New York, (1985).

CHAPTER 6.

PHOTOACOUSTIC MEASUREMENTS OF THERMAL ANISOTROPY: AXIS-WISE MEASUREMENTS OF THERMAL DIFFUSIVITY IN KDP CRYSTAL.

6.1. ABSTRACT.

Axis-wise measurements of thermal diffusivity in single crystals of Potassium Dihydrogen Phosphate (KDP) using Photoacoustic (PA) technique have been presented in this chapter. The calculated values of thermal diffusivities along different crystallographic axes (a or b and c axes) at various temperatures show clearly the anisotropy in thermal conductivity of KDP crystals. Heat conduction is higher along a/b axis and it is lower along c axis and it has also been found that thermal diffusivity decreases with temperature along a/b as well as c axes.

6.2. INTRODUCTION.

Potassium Dihydrogen Phosphate (KDP) is a scientifically important photonic material that has a tetragonal structure with space group D_{2d}^{12} in the piezoelectric phase .It is known to undergo a ferroelectric transition to the orthorhombic structure with space group C_{2v}^{19} at 123 K [1]. More precise values of the atomic coordinates to a tetragonal cell are a = b = 7.434A and c = 6.945A [2]. The large piezoelectric values in ferroelectric phase especially near the transition temperature, make them attractive in several applications. The non-linearity at optical frequencies results in a large electrooptic effect which makes these crystals very useful for control of the beams of coherent light now commonly available from different laser sources. One of the most striking nonlinear effects is the phenomenon of second harmonic generation for which KDP crystals is an ideal material.

For second harmonic generation of picosecond Nd:YAG laser radiation, use is mainly made of KDP crystals. To obtain an optimum efficiency of SHG for powerful laser radiation, large aperture laser beams must be used. This calls for large aperture crystals [3]. At present KDP crystals can be grown possessing a high optical quality and having an aperture of several tens of centimeters. Since the polarisation vectors of the first and second harmonic after frequency doubling are orthogonal, crystal possessing type II phase matching can be easily used for Third harmonic Generation (THG). In particular, KDP crystals satisfy this condition and, therefore, they have found wide application as second and third harmonic generation in commercial laser system.

Fourth harmonic generation of Nd:YAG laser radiation at λ = 266 nm has also been achieved in KDP crystals. It has sufficiently large non-linear coefficients, small coefficients of linear and two photon absorption at the fourth harmonic frequency, and high optical breakdown thresholds. In some papers harmonic generation of Q-Switched Nd:YAG laser radiation was studied with the use of fundamental radiation at λ=1318 nm. Generation of higher order harmonics with a peak power of 0.2 - 85 kW was obtained with KDP [4]. Recently considerable advances have been achieved in harmonic generation, especially in the case of diode laser pumped solid state lasers. As KDP has sufficiently large non linear coefficients and high optical breakdown threshold, it becomes an attractive material for the generation of higher order harmonics in many of these laser systems.

In view of the above aspects, it was considered worthwhile to study the heat conduction properties along different crystallographic axes of such an important crystal. The present chapter explains the thermal diffusivity measurements using PA technique along different crystallographic axes of a single crystals of KDP. It is the first time that a non-contact method has been used for such measurements.

PA measurement of thermal diffusivity has been shown to be capable of demonstrating the thermal anisotropy usually observed in anisotropic crystals. This method is nondestructive, fast, accurate and requires only sample with smaller dimensions. The detailed discussions of the PA effect and its applications had already been presented in chapter IV. PA techniques have found increasing use as a nondestructive method for the determination of thermal diffusivity of solid samples in different forms. The advantage offered by photoacoutics over other

conventional spectroscopic techniques due to the two of its unique features viz; the insensitivity to the nonabsorbed light and the nondependence of the detection of photons, need to be specially emphasized here. The axis-wise measurements of thermal diffusivity in anisotropic crystals can be conveniently carried out using PA technique and it directly gives the information on heat conduction along different crystallographic axes. Thermal diffusivity α is of direct importance in heat flow studies, as it determines the rate of periodic heating or transient heat propagation through the medium, a situation often encountered in experiments with pulsed or chopped laser radiation.

6.3. EXPERIMENTAL DETAILS.

6.3.1. Temperature varying Photoacoustic cell.

The most important part of any PA spectrometer is the PA cell which contains the sample and the microphone. Depending upon the nature of investigations to be carried out, various cell designs have appeared in literature [5,6]. The common type of cell designs adopt cylindrical geometry in which the light beam is centered along the axis. They are of two types; resonant and non resonant. A resonant type cell, in which the microphone is separated from the sample chamber by a long narrow tube, has been used for the present investigations [7]. Such a cell shows acoustic resonances at frequencies which are well within the range used in the particular PA measurements. For temperature varying studies this type of PA cells are most convenient. Frequency response of this cell very closely follows the predictions of RG theory [8].

A schematic diagram of the temperature varying cell is shown in Fig. (6.1). The sample compartment, made out of steel, is in the form of a cylindrical cavity of inner diameter 6 mm and depth 6 mm.. The cell volume can be varied by putting circular buffer metallic discs inside the sample cell. This cavity is sealed onto the cell body with a copper flange using indium O-ring. The copper flange is provided with a highly polished circular glass plate which is fixed on to it using proper epoxy. The sample is maintained in the cavity by inserting a concentric SS hollow cylinder with a transverse opening which is directed towards the microphone chamber. The rearside of the sample compartment is threaded and it is screwed to a cold finger provided with heater windings (60W) used for heating the sample. The cold finger is permanently joined to an SS tube through an L-joint such that the sample cavity is pointed towards one of the window ports. The length of the SS tube is so adjusted that the center of the sample cavity is on the axis of the window ports. The top end of the SS tube is permanently fixed to an MS flange which is vacuum sealed to the top flange of the main chamber. The temperature of the sample is monitored by inserting a chromel alumel thermocouple on the rearside of the sample cavity by drilling 1mm bore on the PA cell assembly. The microphone compartment is acoustically coupled to the sample cell through a thin walled stainless steel tube of inner diameter 1mm and of length 19 cm. The microphone compartment is firmly fixed to the top flange of the main chamber. The electrical connections to the heaters, thermocouples and microphone biasing are made through teflon insulations fixed on the top plate of the chamber. The whole PA cell is kept within a main chamber which can be evacuated as this chamber is sealed by two MS flanges

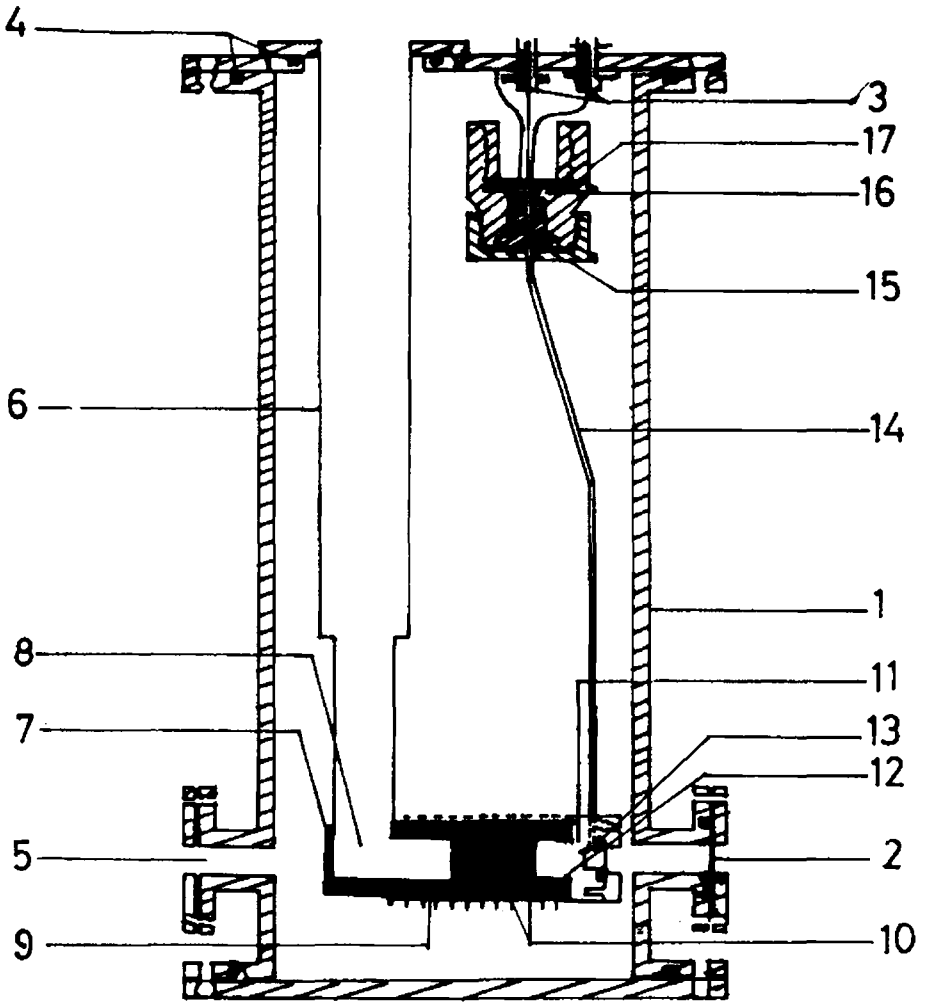

1 MS OUTER CHAMBER
2 GLASS WINDOW
3 BNC
4 NEOPRINE O RINGS
5 TO VACUUM PUMB
6 SS TUBE
7 COPPER BLOCK
8 LN_2 CAVITY
9 MICA INSULATION
10 HEATER WINDINGS
11 SS PA CELL
12 SAMPLE CHAMBER
13 INDIUM O RINGS
14 SS PIPE
15 MICROPHONE ASSEMBLY
16 MICROPHONE
17 EBONITE MICROPHONE HOLDER

Fig.(6.1). Schematic diagram of the temperature varying cell.

fixed at the top and bottom by using neoprene O-rings.

Four window ports are provided to the main chamber for different purposes. One port is used for connecting rotary pump for evacuating the chamber so that the background noise can be reduced. Through another window port light beam enters the cell for optical excitation of the sample. The PA cell configuration is thus that of an Helmholtz resonator [10-12], which for several reasons is an appropriate design for variable temperature PA cells, whether heated [13] or cooled [14]. This configuration permits large variations in the sample temperature without altering the microphone temperature appreciably.

The major advantages of this cell are:

(i) It can be operated in the temperature range 80K to 420K

(ii) Liquid nitrogen consumption is very low and

(iii) It has extremely good temperature stability.

6.3.2. Calibration of the PA cell.

The experimental setup used for the measurements of thermal diffusivity is shown in Fig.(6.2). Fig (6.3) shows a photograph of the experimental set up. In order to characterise the performance of the cell, both the modulation frequency and temperature response of the cell have been studied using a carbon black as the standard. Fig.(6.4) shows the frequency response of the PA amplitude at four different temperatures 100K, 200K, 302K and 400K. The amplitude shows an ω^{-1} dependence at low frequencies away from the resonance. The effect of resonance can be clearly seen on all the curves. The calculated resonance frequency at room

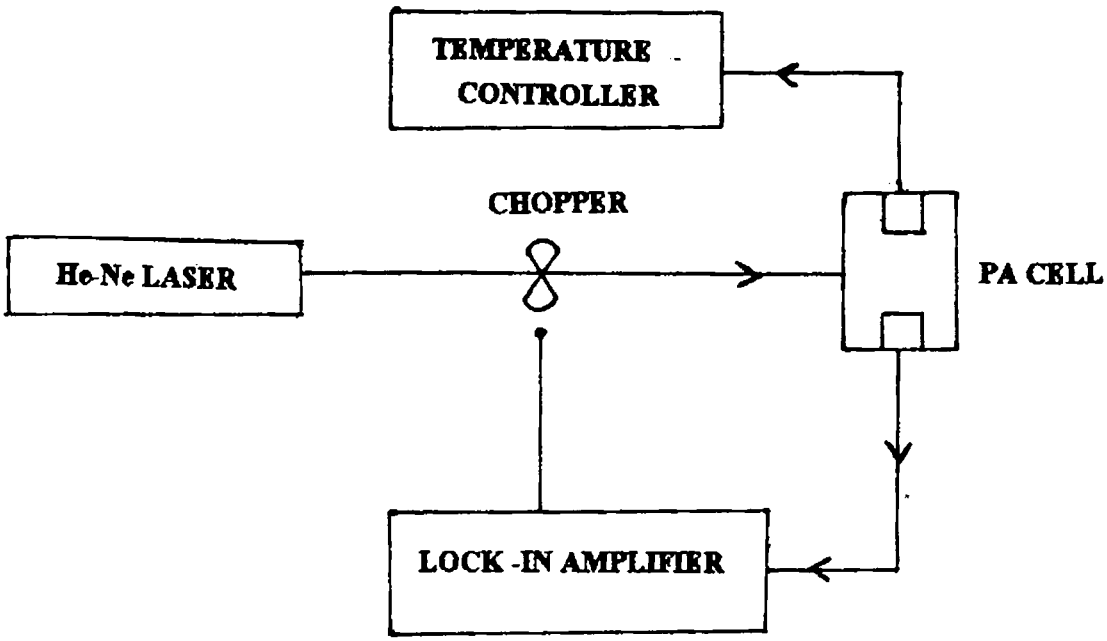

Fig. (6.2). Block diagram of the experimental set up used for the measurement of thermal diffusivity.

Fig. (6.3). A Photograph of the experimental set up.

temperature is 344 Hz. This theoretical value is in reasonably good agreements with the experimentally observed value. The resonance peak of the low temperature curve is slightly shifted towards low frequencies due to the decrease in sound velocity in air at low temperatures. Figures (6.5) and (6.6) show the dependence of the PA signal (both amplitude and phase) as a function of temperature, at modulation frequency 325 Hz, for carbon black sample which is used as the standard. It is observed that both the amplitude and phase of the PA signal decrease with increase in temperature.

6.3.3. PA measurements of thermal diffusivity.

The above PA set up has been used for axis-wise measurements of thermal diffusivity and its temperature dependence systematically in KDP crystals. For our experiments single crystals of pure KDP were grown by slow evaporation from a saturated solution prepared with triply distilled water. Samples of the typical sizes 5 x 5 x 0.4 mm^3 were cut along three crystallographic axes from the large single crystals. As the pure crystals of KDP is a weak absorber of light (optically thin specimen), the front surfaces of each sample, on which the light is made to fall, were deposited with a very thin layer (0.05 μm.)of carbon black changing the sample to an optically thick one. The light source used is a He-Ne laser at a power level of 10 mW and wavelength 632 nm. The laser beam is chopped by a commercial light beam chopper (Standford Research System Model SR540). The measurements are made on single crystal slabs of KDP with edges cut along three crystallographic axes having thickness 0.040 cm. The signal is detected by Knowle's (model 1753) electret

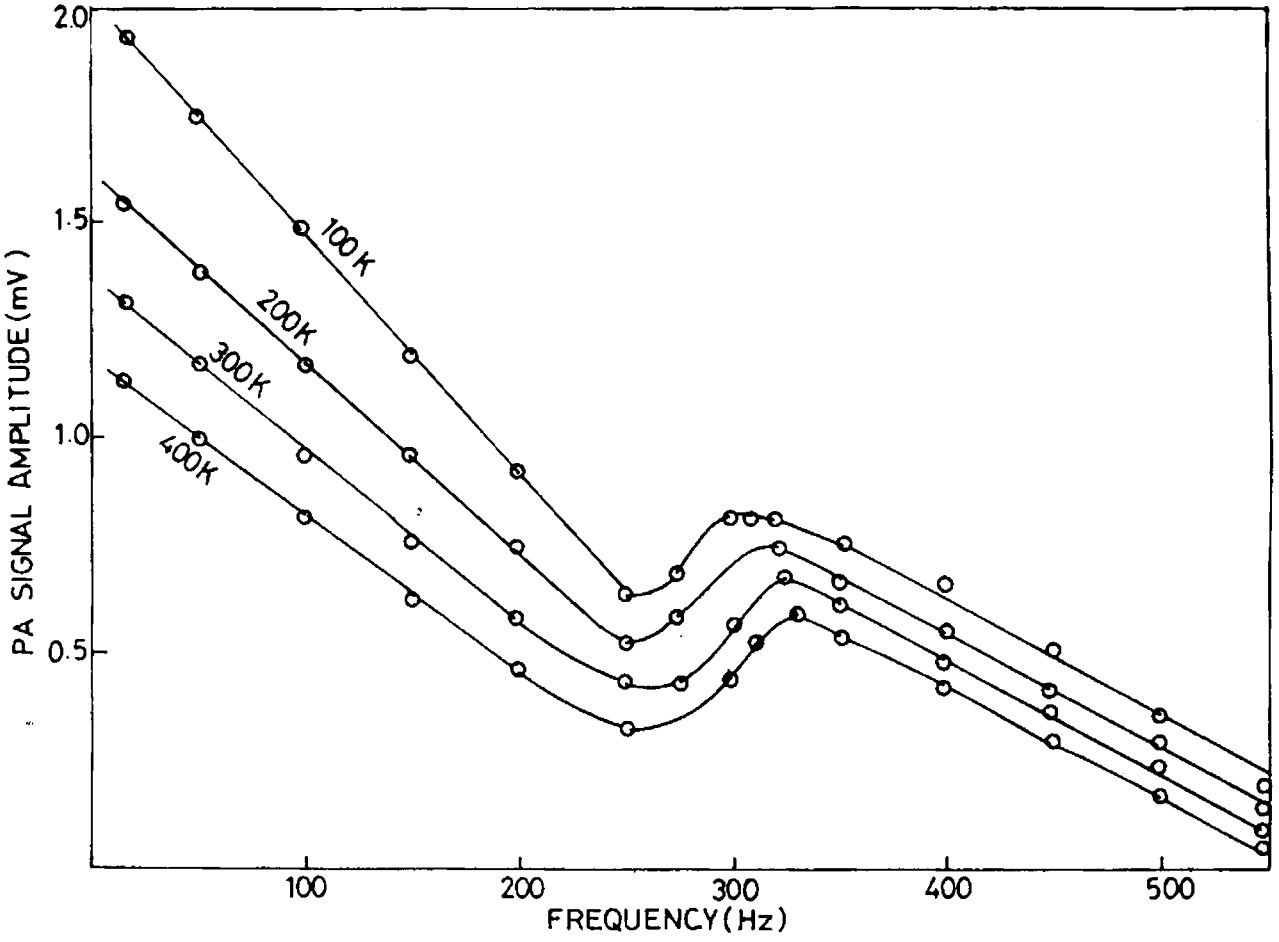

Fig.(6.4). Frequency response of PA amplitude at different tempertures (carbon black).

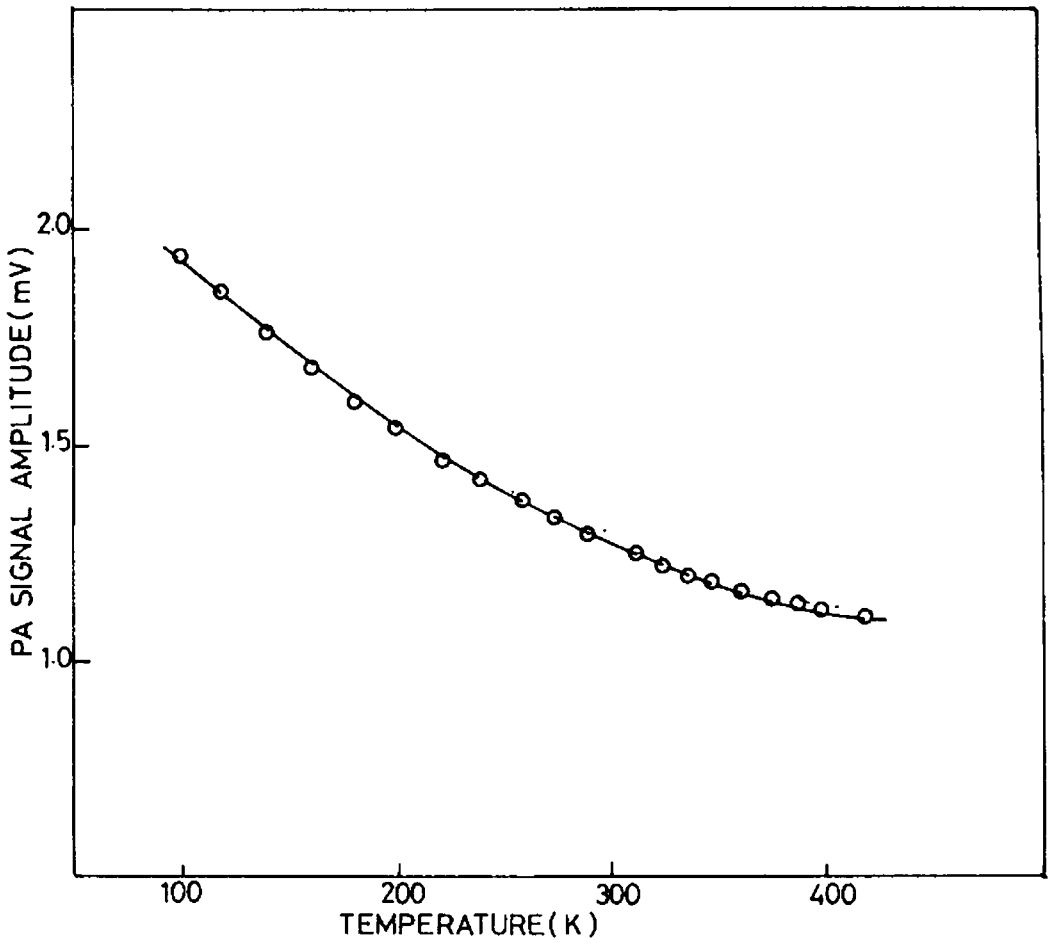

Fig.(6.5). Variation of PA signal amplitude as a function of temperature (carbon black).

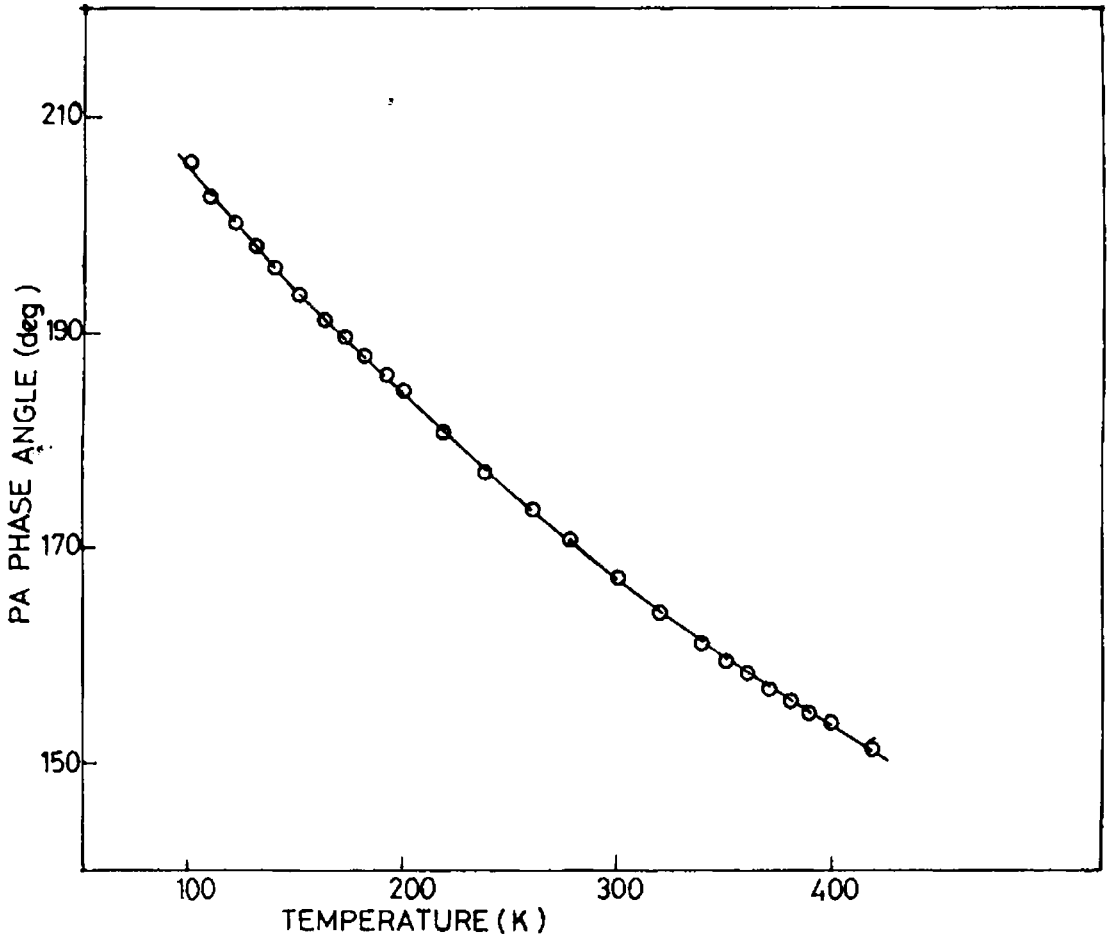

Fig.(6.6). Variation of PA phase with temperature (carbon black).

microphone kept inside the PA cell and analyzed using a lock in amplifier (EG&G Model 5208). The method involves the determination of the characteristic frequency f_c by measuring the variation in the amplitude A of the photoacoustic signal as a function of the chopping frequency f of the laser beam. The characteristic frequency f_c can be obtained from the intercept of the two straight line regions of the log A against log f plot. Thermal diffusivity α_s is related to the characteristic frequency f_c by expression given by Charpentier et.al. [15]. For an optically thick sample, when irradiated with a monochromatic light beam, thermal diffusivity, $\alpha_s = f_c\, l_s^2$ where l_s is the thickness of the sample. In this way the thermal diffusivity along different axes are determined at various fixed temperatures 50^0 C, 60^0 C, 70^0 C, 80^0 C, 90^0 C and 100^0 C.

6.4 RESULTS.

The values of thermal diffusivities thus obtained along the crystallographic axes a or b and c at different temperatures are given in the Table 1. Log-Log plot of the PA signal amplitude versus chopping frequency along a/b-axis and c-axis of the KDP at the room temperature is shown in Fig.(6.7). The log A vs. log f plot drawn for different temperatures along a or b and c axes of KDP are given in Figures (6.8) and (6.9) respectively. Fig.(6.10) also gives the variation of thermal diffusivity with temperature along different crystallographic axes. From both the figures it is quite evident that f_c decreases as temperature increases i.e. the crystals thermal diffusivity values decrease as temperature increases in the case of

KDP. Fig.(6.11) shows the variation of the ratio $\alpha_{a/b}$ / α_c with temperature, where $\alpha_{a/b}$ is the thermal diffusivity value along a or b axis and α_c, that along c-axis.

TABLE 1. Thermal Diffusivity values of KDP along a/b as well as c-axes at different temperatures.

Temp.(K)	a / b -axis		c - axis		$\frac{\alpha_s(a/b)}{\alpha_s(c)}$
	f_c Hz	α_s cm^2/sec	f_c Hz	α_s cm^2/sec	
304	37.58	0.060	21.13	0.034	1.765
323	32.36	0.052	20.18	0.032	1.625
333	30.55	0.049	19.72	0.032	1.531
343	29.51	0.047	19.28	0.031	1.516
353	28.51	0.045	19.05	0.030	1.500
363	27.23	0.044	18.62	0.029	1.466
373	25.70	0.041	17.78	0.028	1.464

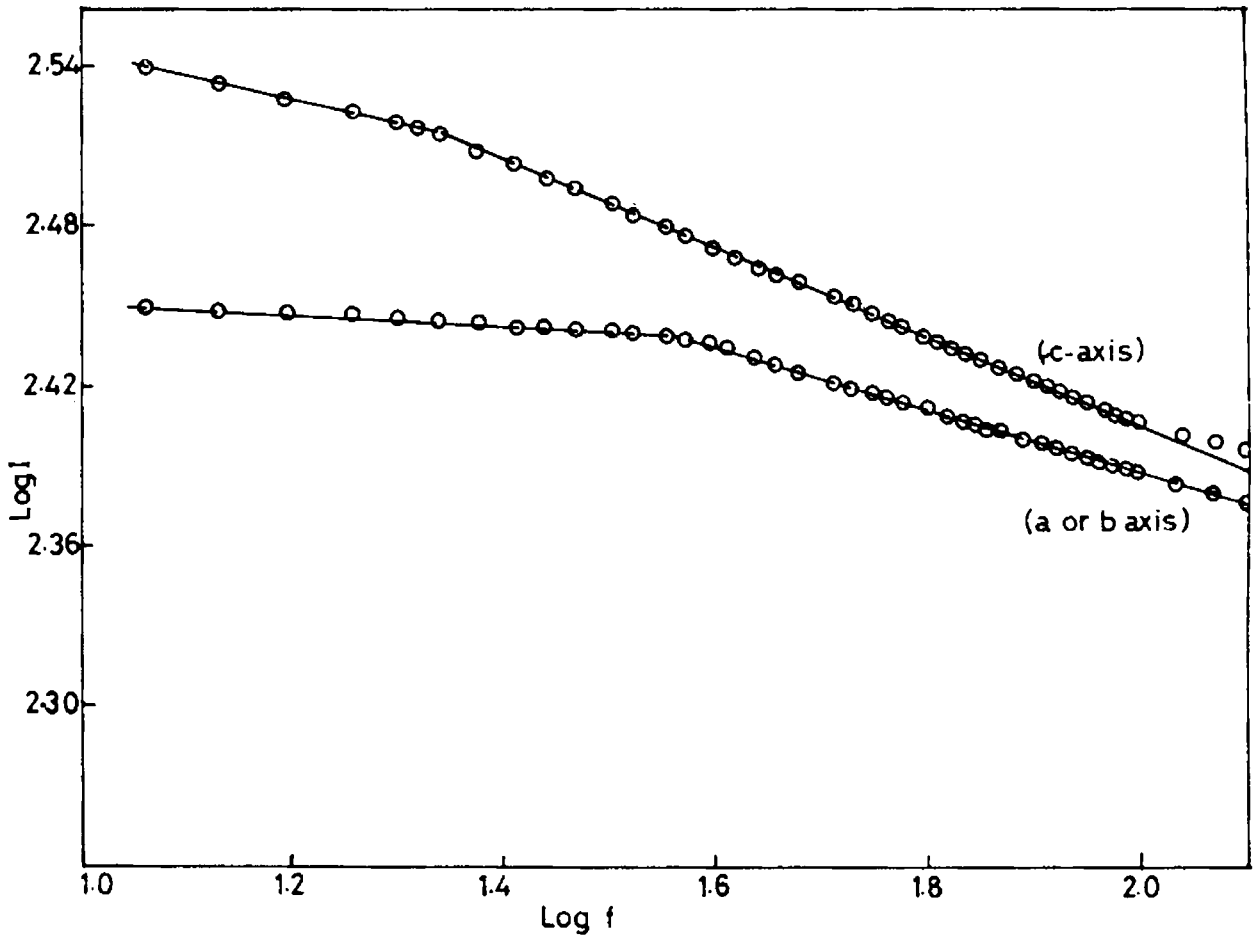

Fig.(6.7). log- log plot of the PA signal amplitude versus chopping frequency of KDP along a or b and c-axes at room temperature.

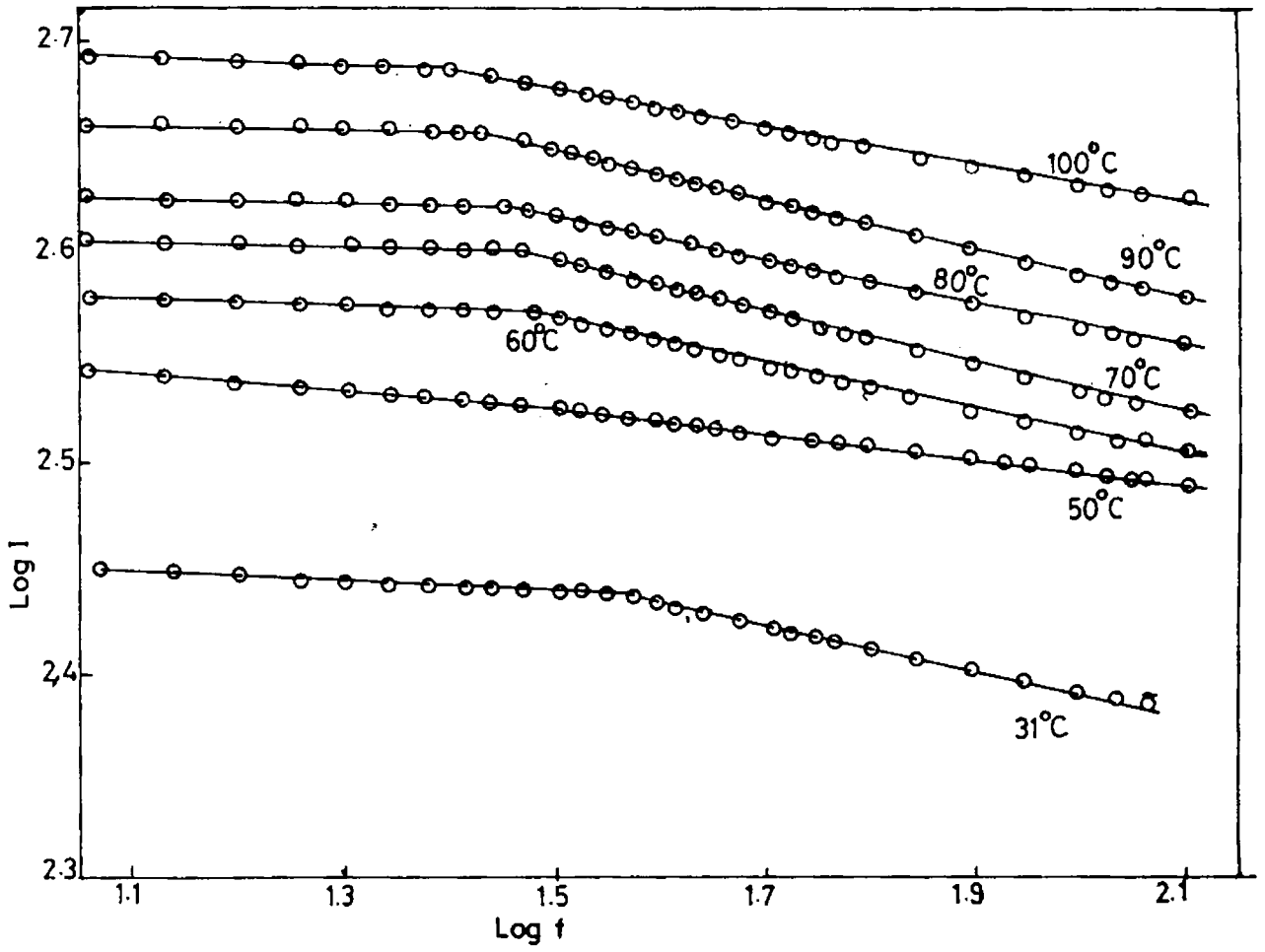

Fig.(6.8). log-log plot of the PA signal amplitude versus chopping frequency of KDP along a or b axis at different temperatures.

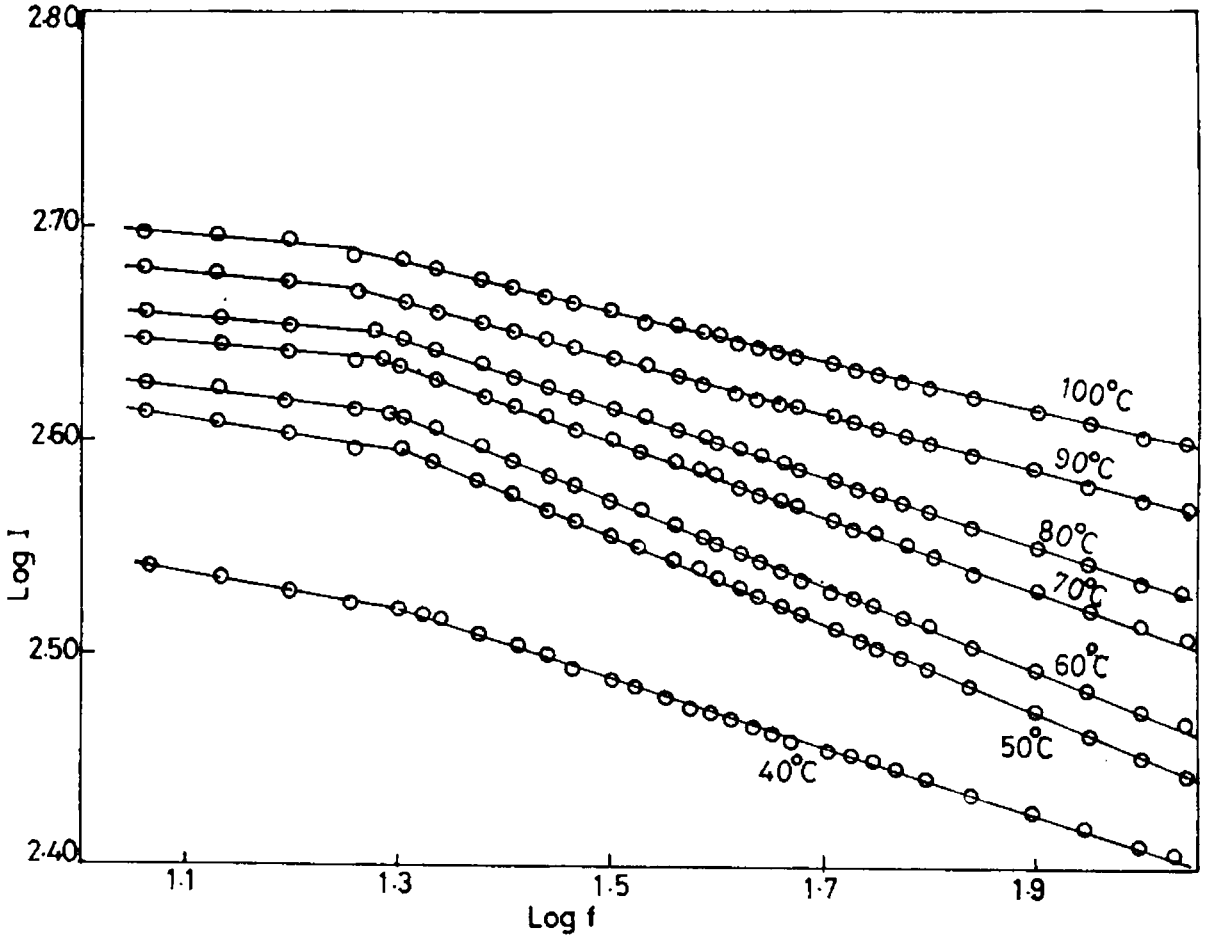

Fig.(6.9). log-log plot of the PA signal amplitude versus chopping frequency of KDP along c-axis at different temperatures.

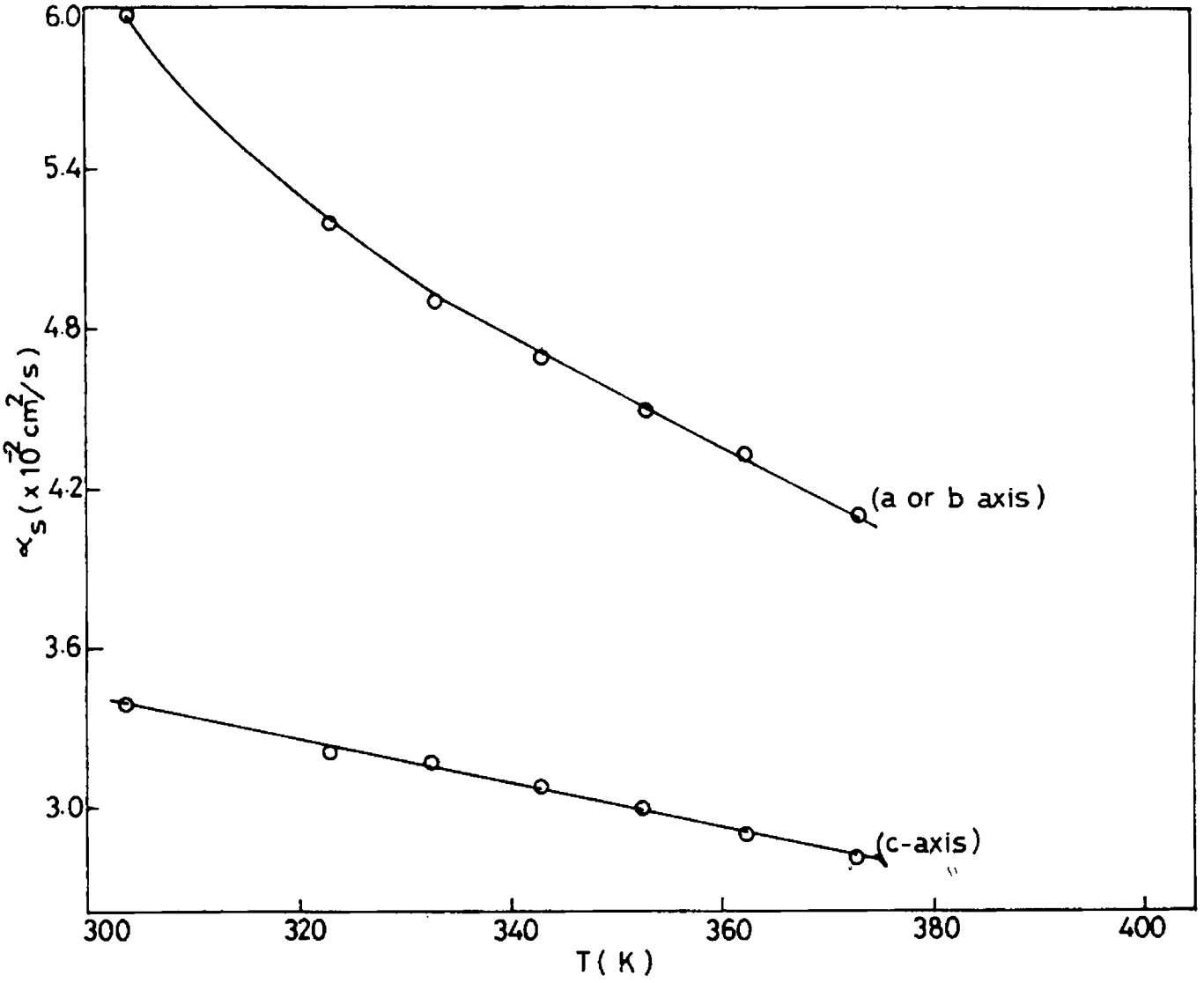

Fig.(6.10). Variation of thermal diffusivity with temperature along different axes of KDP.

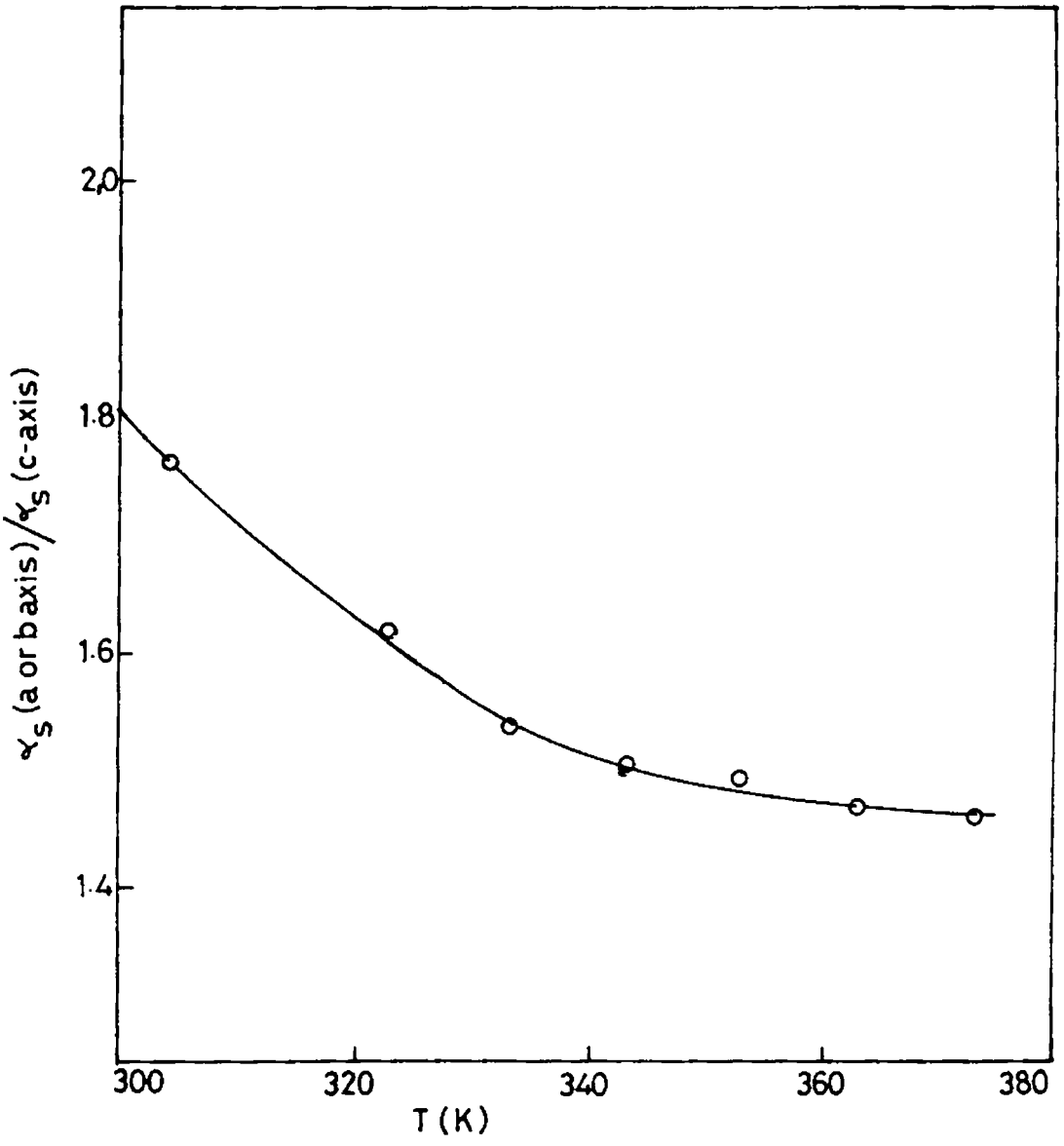

Fig.(6.11). Variation of thermal diffusivity ratio $\alpha_{a/b}$ / α_c with temperature.

6.5. DISCUSSION.

The striking result is that, the thermal diffusivity shows higher value along a or b axis of the KDP crystal; while it shows lower value along c-axis. The thermal diffusivity $\alpha_s = K / \rho C$, where K is the thermal conductivity, ρ, the density and C the specific heat capacity of the material. Since the density and specific heat capacity are direction independent parameters the present observation gives an idea of thermal conductivity along different axes of the crystal and hence the thermal anisotropy of the material. Heat conduction is maximum along a or b axis and it is minimum along c-axis . Since generally heat is conducted by both electrons and phonons, measurement of thermal conductivity yields valuable information about the interactions between them. In KDP crystals, at room temperature or above the phononic contribution will be the dominant mode of heat transport because of the near total absence of free electrons. As the variation in density and specific heat capacity is negligibly small in the range of temperature considered here the explanation for the observed thermal diffusivity variation with temperature can very well be attributed to the corresponding thermal conductivity variation.

A brief consideration of the crystal structure will facilitate the discussion of thermal conduction mechanism in KDP crystal (Fig.6.12). The phosphate lattice is consisting of $(H_2 PO_4)^-$ ions that are linked by ionic bonds to K^+ ions. Each phosphate group is linked by four hydrogen bonds. However, pairs of these bonds are at levels separated by a distance c/4. In the entire crystal one has layers of hydrogen bonds lying losely in a-b planes, spaced at a separation of c/4 [16]. Therefore, the number of scattering of thermal phonons is maximum along c-axis,

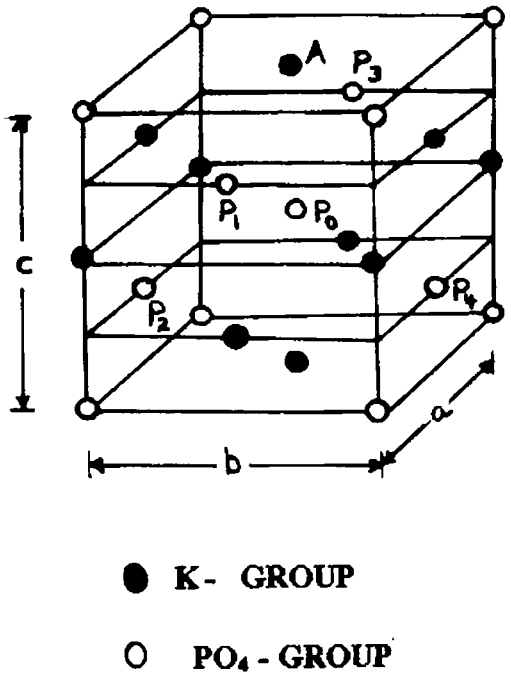

Fig. (6.12). Structure of KDP.

thus reducing the phonon mean free path along that direction. Hence a low value of thermal diffusivity is observed along c-axis.

Each hydrogen bond of the phosphate lattice has two positions for its proton, each located towards the end of the bond. Each phosphate group associates with an average of two near neighbour protons to form an $H_2 PO_4$ ion. As temperature increases, a proton may jump from one position to the other along the same bond. This is an intra bond jump, giving rise to ionisation defects: HPO_4 , H_3PO_4 . In addition it is possible for protons to jump from one bond to another bond on the same phosphate group called inter bond jumps. In general, such an inter bond jump leaves a hydrogen bond without a proton which is known as L defect and it produces a bond with a proton in each of its two proton positions. Such a doubly occupied bond is a D defect. In KDP crystals, the defect concentration increases with temperature and the possible number of phonon scattering due to defects increases and as a consequence the phonon mean free path reduces. Hence a corresponding decrease in thermal diffusivity can be expected. It is quite evident from Fig. (6.11) that the ratio $\frac{\alpha(a/b)}{\alpha(c)}$ reduces as temperature increases. So it has been concluded that the defect concentration increases as temperature increases and at a fairly high temperature this cause the phonon scattering to become uniform in all different directions. In such situation we can expect the value of this ratio as 1.

6.6. CONCLUSION.

In conclusion the anisotropy in thermal conductivity of KDP crystal has been demonstrated using Photoacoustic technique. It has been found that thermal diffusivity decreases with temperature along a/b as well as c axes.

6.7. REFERENCES

[1]. B.C.Framer and R.Pepinsky, Acta.Cryst. 6, 273 (1953).

[2]. A.R.Ubbelohde and I.Woodward, Proc.Roy.Soc. A188, 358 (1947).

[3]. M.R.Wohlers and K.G.Leib, J.Appl.Phys. 35, 2311 (1964).

[4]. P.D.Maker, R.W.Terhune, M.Nisenoff and C.M.Savage , Phys.Rev.Letters. 8, 21 (1962).

[5]. L.G.Rosengren, Appl.Opt. 14, 1960 (1975).

[6]. C.E.Dewey, in Optoacoustic Spectroscopy and Detection (ed: Y.H.Pao) Academic Press, New York (1977).

[7]. A.Rosencwaig, 'Photoacoustic Spectroscopy of Solids' Rev.Sci.Instrum. 48, 1133 (1977).

[8]. A.Rosencwaig and A.Gersho, J.Appl.Phys. 47, 64 (1976).

[9]. C.P.G.Vallabhan, J. Instru.Soc.India 21, 99 (1993).

[10]. N.C.Fernelius and T.W.Hass, Appl.Opt. 17, 3348 (1978).

[11]. N.C.Fernelius, Appl.Opt. 18, 1784 (1979).

[12]. R.S.Quimby, P.M.Selzer and W.M.Yen, Appl.Opt 16, 2630 (1977).

[13]. P.S.Bechthold, M.Campagna and T.Schober, Solid State Commun. 36, 225 (1980).

[14]. J.C.Murphy and L.C.Aamodt, J.Appl.Phys. 48, 3502 (1977).

[15]. P.Charpentier, F.Lepoutre and L.Bertrand, J.Appl.Phys. 53, 1 (1982).

[16]. L.B.Harris and G.J.Vella, J.Chem.Phys. 58, 4550 (1971).

CHAPTER 7.

A PHOTOACOUSTIC CELL FOR REAR SIDE ILLUMINATION OF THIN FILM SAMPLES.

7.1. ABSTRACT.

A Photoacoustic (PA) cell which can be used for the measurement of thermal diffusivity of thin films using rear surface illumination method has been fabricated. Thin / thick films of Indium, Aluminium, Silver and CdS having thicknesses of the order of 18-690μm. prepared from vacuum coating technique have been used for measurements. The experimental method involves the determination of the variation of the phase of the photoacoustic signal as a function of the chopping frequency for a monochromatic incident beam. The thermal diffusivity values obtained for each of the samples using this cell show close agreement with the previously reported results.

7.2. INTRODUCTION.

The PA technique has been recently revived as very useful tool for the spectroscopic investigation of samples where the conventional optical absorption and reflectance spectroscopy can not be used. The main factor behind the interest in photoacoustic spectroscopy is that it can be used as a powerful tool for studying the thermal properties of samples in any form. Detection of acoustic waves after absorption of modulated optical radiation provides information of thermal properties of the material in a very elegant way. As shown by several authors [1-6] thermal waves are very sensitive to a change in thermal characteristics of the materials. The thermal properties , especially, those of thin films, are of growing interest in microelectronics and microsystems, because the heat removal from highly integrated devices becomes a serious problem requiring practical solutions. Knowledge of thermal diffusivity value in thin films helps one to select microelectronic materials systematically and to get precise input data for microelectronic device modelling. In particular, CdS is a II-VI group semiconductor and it has received considerable attention as an important photonic material because of its potential use in the fabrication of solar cells [7-11] as well as in other areas of photonics. CdS is a prominent photoconductive material used in photoconductive detectors. Photoconducting property of CdS opens up the possibility of the use of this material in image recording technology. In photoconductivity process, photoinduced charges create a space-charge distribution that produces an internal electrical field, which inturn, alters the refractive index by means of the electro-optic effect. Thus the material can be used to record and to store optical images, much like a photographic emulsion storing an image. CdS is also known as the low

cost visible radiation sensor. It was thought worthwhile to investigate the thermal diffusivity in this important photonic material using PA technique.

Various methods have been developed to measure the thermal diffusivity by means of the PA effect [12-14]. In the rear surface illumination method, chopped light is allowed to fall on the thin substrate (copper), the farther side of which is deposited with sample, and the PA signals are generated on its free surface. The principle of the rear surface excitation is illustrated in Fig. (7.1). Here, the thermal wave generated at the surface , where the light beam is incident, starts propagating through the sample, and it eventually generates the acoustic signal in the gas medium. Therefore the PA signal amplitude and phase directly depends on the thickness of the sample and its thermal diffusivity. Thus the sample thickness is found to be an important parameter in these measurements. In order to find the thermal diffusivity of thin film samples, the films are deposited on a copper substrate. The phase of the PA signal with the copper substrate alone and that with thin film on copper substrate for different modulation frequencies ω are measured using a lock-in amplifier. Thus from the relative phase difference between the substrate and substrate + thin film, the thermal properties of the thin film alone can be determined. In the present investigation, the thermal diffusivity values of the thin films of Indium,Aluminium,Silver and CdS deposited on copper substrate are measured by the rear surface illumination method.

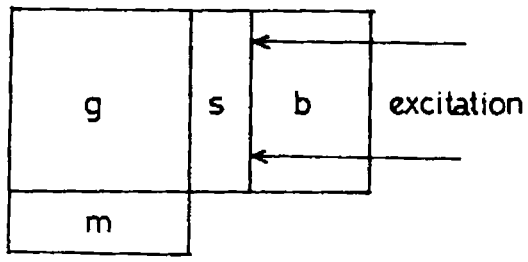

m — microphone
g — gas medium
s — sample
b — backing

Fig.(7.1). Schematic representation of rear surface illumination.

7.3. OUTLINE OF THE THEORY.

When an intensity modulated light beam falls on the rear surface of the sample, which is optically opaque, localised heat centers are produced at the surface of the sample. This results the propagation of thermal waves through the thickness l_s of the sample. The thermal diffusion equation along the thickness can be expressed as

$$\frac{d^2\theta_s}{dx^2} - \frac{1}{\alpha_s}\frac{d\theta_s}{dt} = 0$$

where θ_s is the temperature at the sample surface and α_s, the thermal diffusivity of the sample. The real part of the solution of above equation is

$$\theta_s(x,t) = \theta_0 e^{-a_s x} \cos(\omega t - a_s x)$$

This expression represents the temperature distribution along the thickness of the sample and it is evident that the thermal wave gets attenuated exponentially as it traverses through the sample. The term which represents the phase of the thermal wave is a_s x where a_s is the thermal diffusion coefficient of the sample and 'x' is the position where the temperature is found to be θ_s. θ_0 is the complex amplitude of the periodic temperature of the sample sample gas boundary. Therefore the total phase difference between the front surface and rear surface of the sample is expressed as

$\Delta\phi = a_s l_s$

The thermal diffusion coefficient $a_s = \left(\frac{\omega}{2\alpha_s}\right)^{\frac{1}{2}}$, ω being the angular frequency of the intensity modulated light beam. Thus the graph between $\sqrt{\omega}$ and $\Delta\phi$ will be a straight line and its slope is $\left(\frac{1}{2\alpha_s}\right)^{\frac{1}{2}} l_s$. The thickness l_s of the thin film is measured using optical method [15].

7.4. EXPERIMENTAL METHOD.

The experimental set up used for the measurements of thermal diffusivity of thin film samples is same as described in chapter V. A photograph of the experimental set up is shown in Fig. (7.2). An Ar^+ laser beam (Liconix - 5000 Series) at a power level of 30 mW is used as the light source and targets are Indium, Aluminium, Silver and CdS thin films deposited on identical copper discs (0.3 mm thick). The materials were obtained in the form of thin/ thick films by means of thermal evaporation process. Copper was used as the substrate material so that rear surface illumination method can be conveniently adopted for PA measurements. For the present measurements we have made use of a PA cell which is capable of measuring thermal diffusivity of thin films using rear surface illumination method. The signal is detected by highly sensitive electret microphone (Knowel's model BT 1753) and analysed using lock-in amplifier (EG&G Princeton Applied Research model -5208). The phase of the photoacoustic signal is measured for various chopping frequencies in between 20 and 150 Hz.

Fig (7.2). A photograph of the experimental set up.

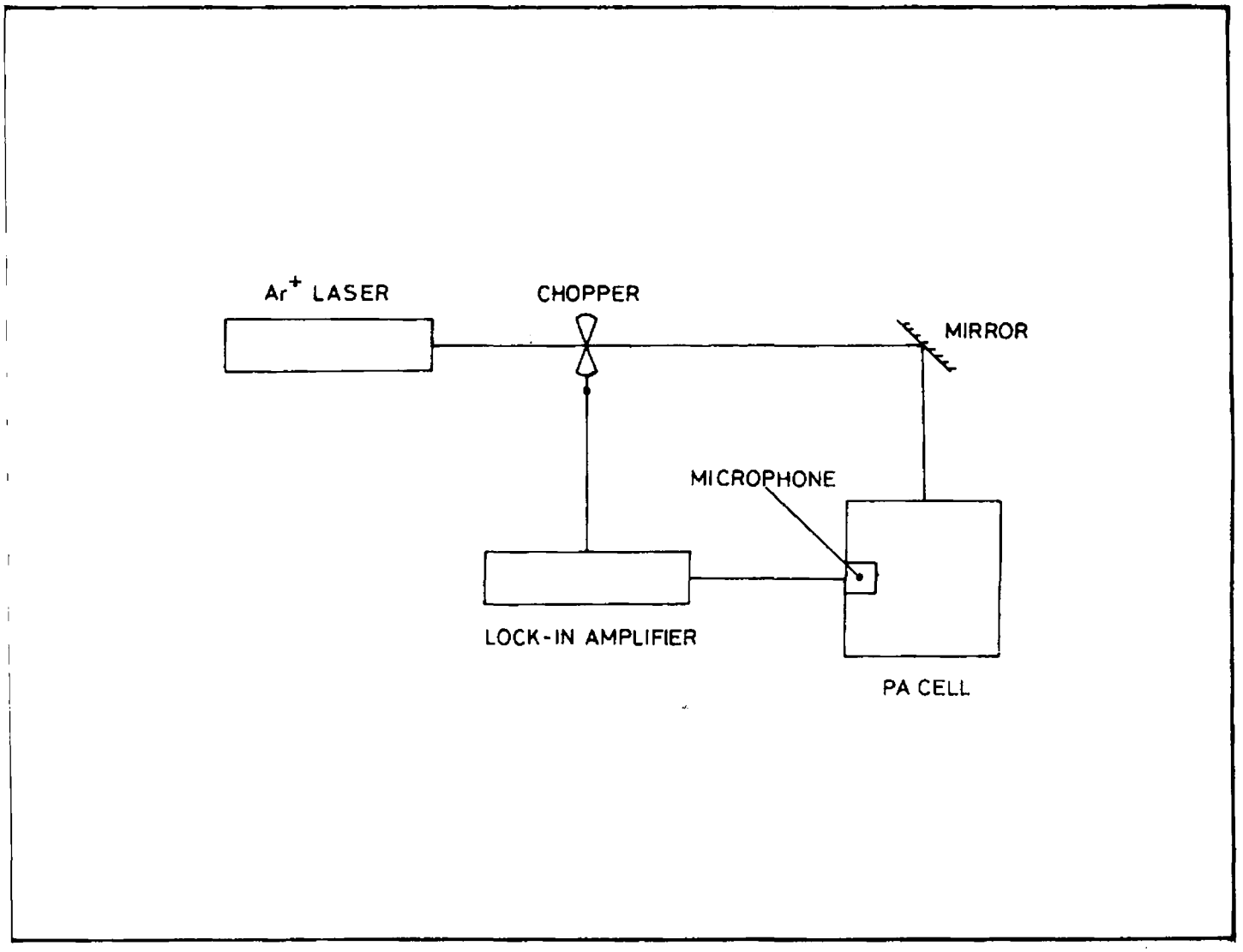

Fig. (7.3). Schematic diagram of the rear side illumination cell.

Schematic diagram of the small volume rear side illumination cell used for room temperature measurements is shown in Fig. (7.3). It has a cylindrical cavity of height 1cm and diameter 0.8 cm made in a solid block of stainless steel. Window holders and microphone compartment are also made up of using stainless steel. Two windows are provided, one for front side illumination and another for rear side illumination of the sample. The cell volume is acoustically isolated from outside using 'O' rings on the window holders. The electret microphone used in the cell is also kept in a separate port which can be removed from the cell body. It has got a flat frequency response in the range 10 to 2000 Hz. The microphone output is taken using a BNC connector attached to the microphone port and is fed to the lock-in amplifier. Microphone is also sealed with 'O' rings and air at atmospheric pressure acts as the coupling gas medium. In order to avoid "drum effect" the sample is rigidly fixed in the PA cell using 'O' ring seal.

7.5. RESULTS AND DISCUSSION.

Fig. (7.4) shows the variation of PA phase difference $\Delta\phi$ (between copper and copper + Indium thin film) with the square root of the modulation frequency ($\sqrt{\omega}$) at two different thicknesses of Indium thin films (240μm. and 630μm). From the straight line graphs the slopes are found to be 2.416×10^{-2} and 6.463×10^{-2} respectively for 240μm. And 630μm. and the corresponding α_s values obtained are 0.4935 cm^2/ sec and 0.4755 cm^2/sec.

By following the same procedure, the thermal diffusivity value of Aluminium, Silver and CdS has been determined (Figures. 7.5, 7.6and 7.7). Measured values and

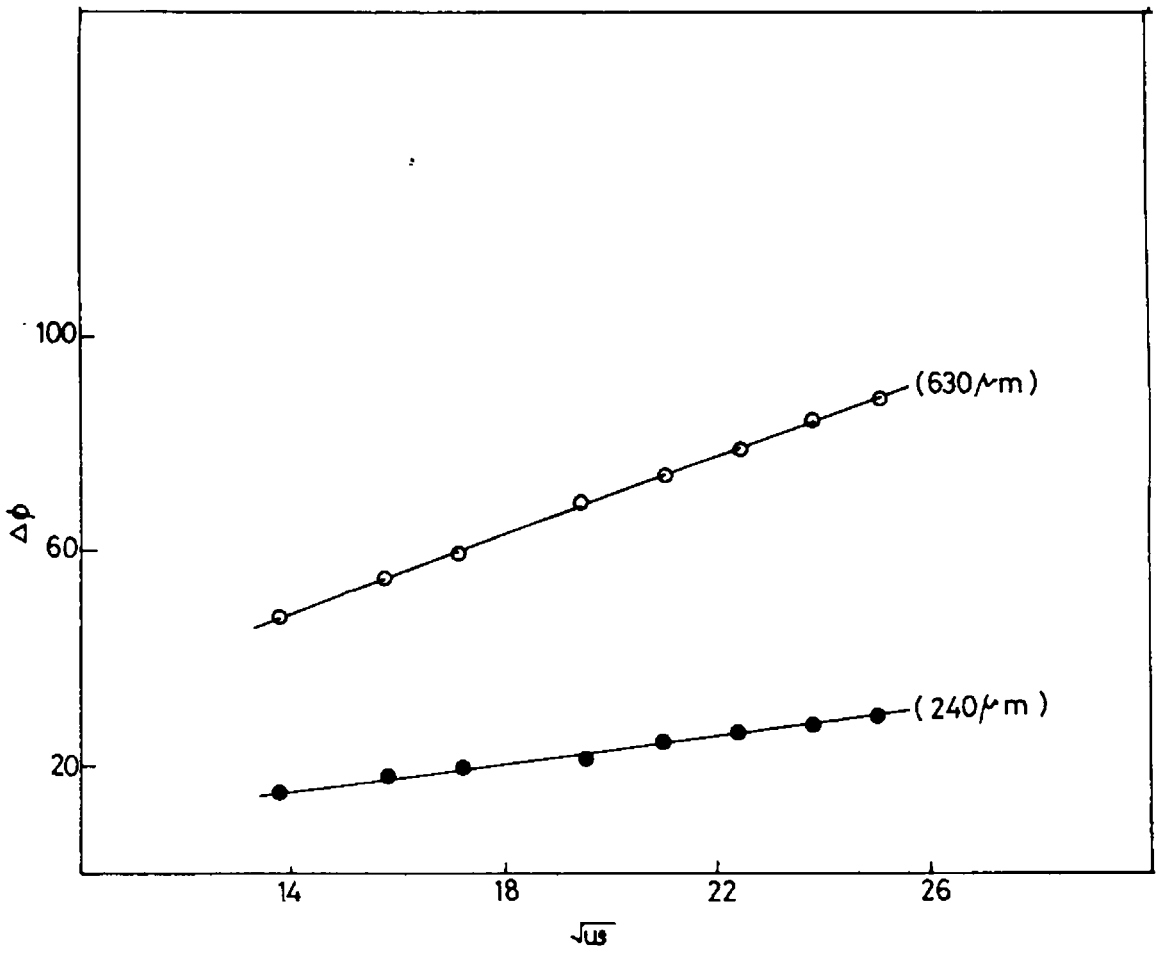

Fig.(7.4). Phase difference versus square root of the angular frequency plot for Indium thin films having two different thicknesses.

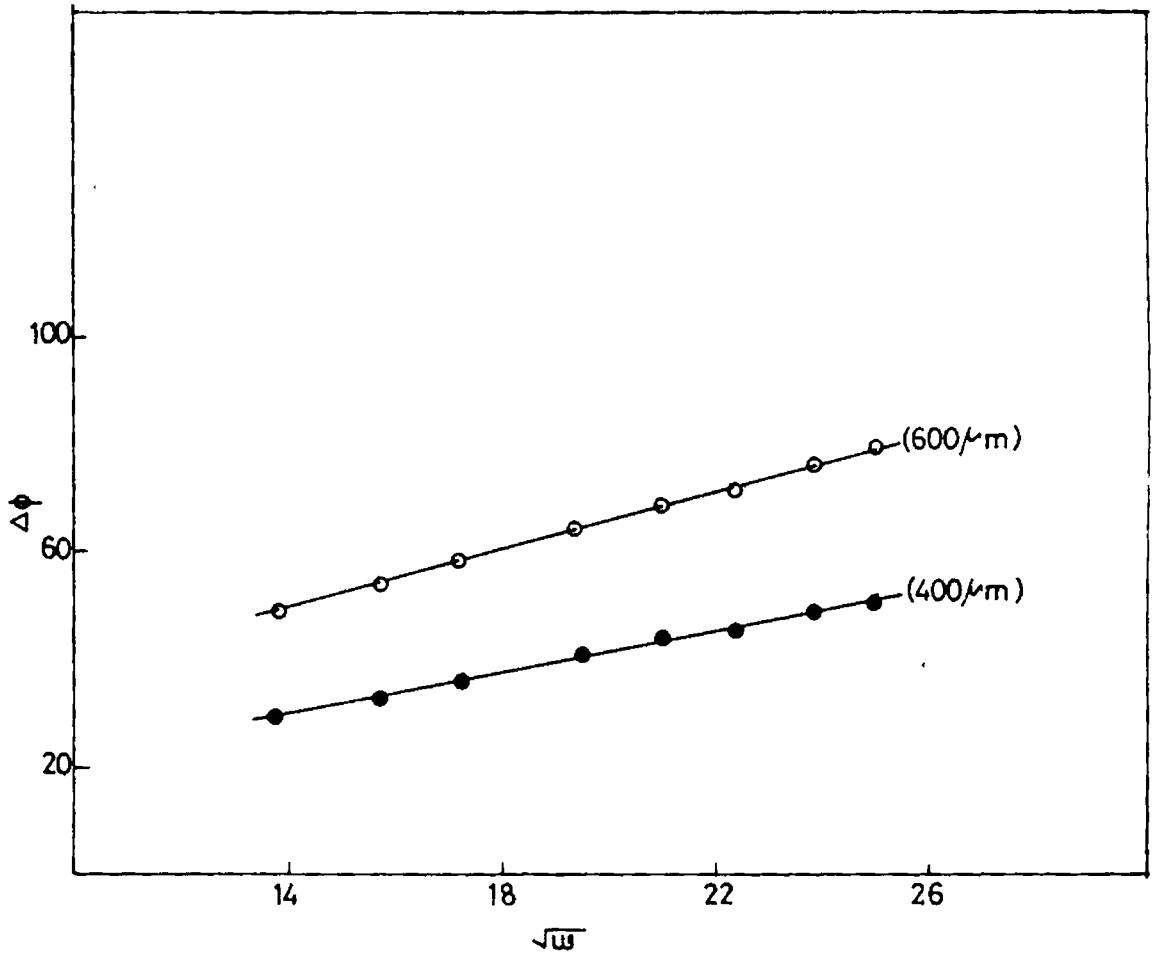

Fig.(7.5). Phase difference versus square root of angular frequency plot for Aluminium thin films having two different thicknesses.

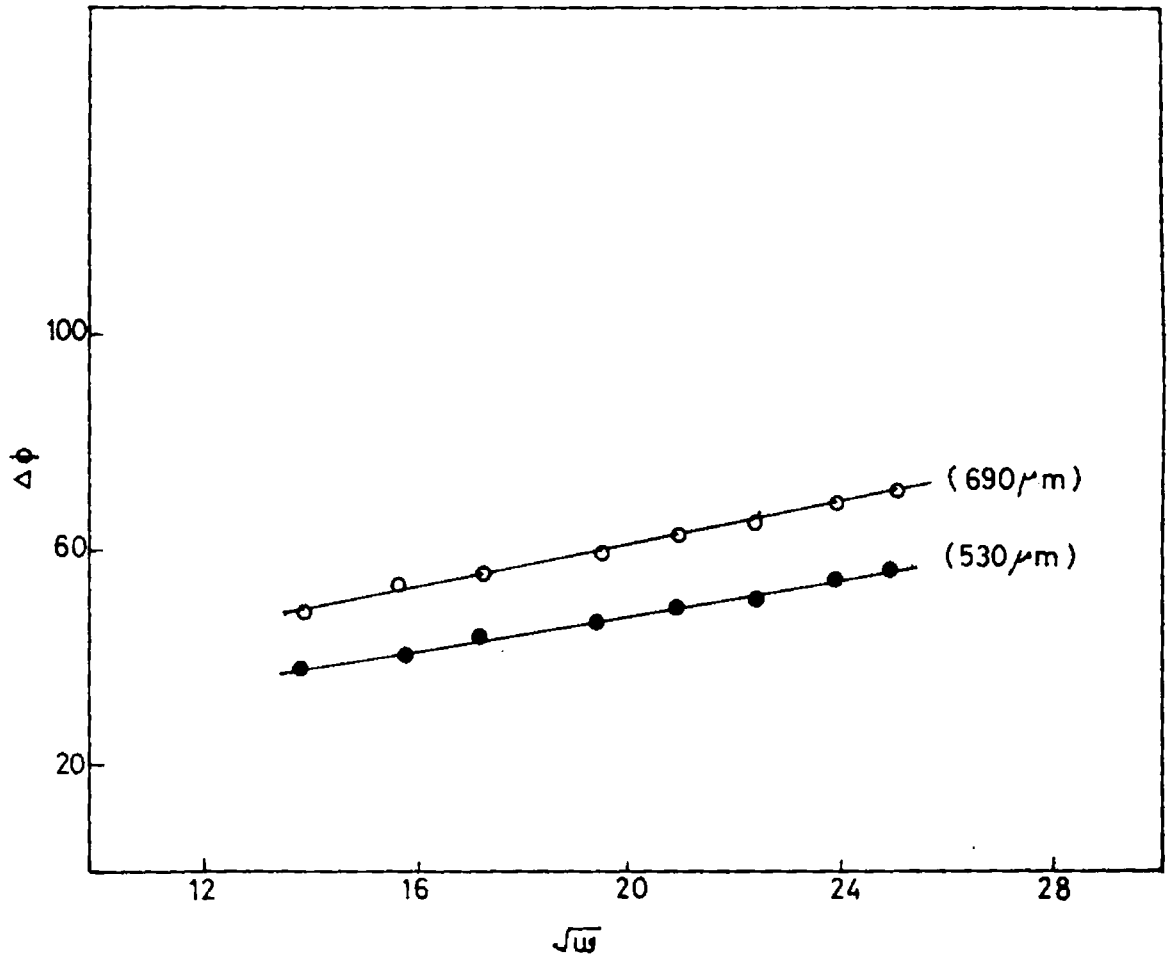

Fig.(7.6). Phase difference versus square root of angular frequency plot for Silver thin films having two different thicknesses.

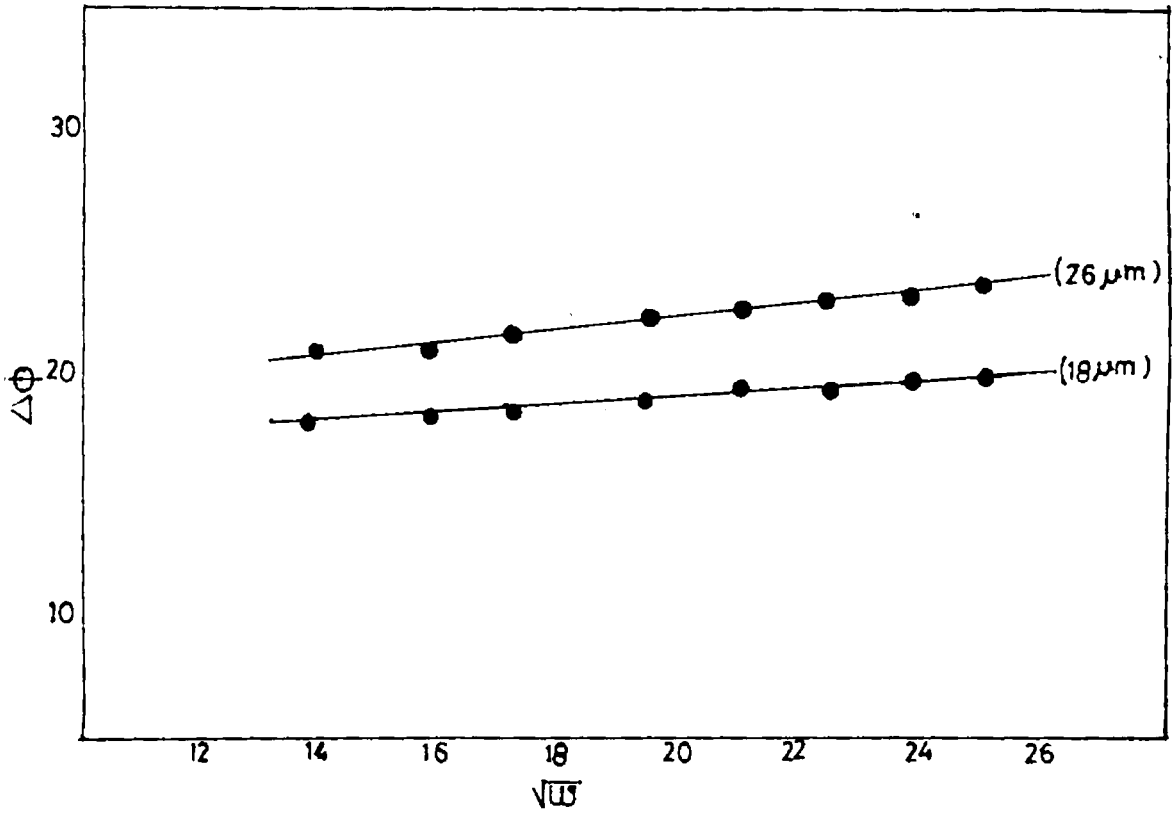

Fig. (7.7). Phase difference versus square root of angular frequency for Cadmium Sulphide thin films having two different thicknesses.

literature values are shown in Table I. In our view, this shows extremely good agreement between the calculated value of α_s and its known value[16,17]. In view of the simplicity of the experimental set up, one can strongly recommend the present technique for determining the thermal diffusivity of thin films. However, the sample thickness is found to be an important parameter in these measurements. This doesnot pose any serious problem since their exists a number of standard methods for fairly accurate determination of sample thickness. Alternatively, with known values of thermal diffusivity it is possible to estimate the sample thickness with fair amount of accuracy using the PA technique described above.

7.6. CONCLUSION.

Thermal diffusivities of thin films can be accurately measured by the photoacoustic method. Because of its controlling effect and common occurrence in heat flow problems, thermal diffusivity determination is often necessary, and knowledge of it can inturn be used to calculate the thermal conductivity.

TABLE . 1. Measured and literature values of thermal diffusivity of different samples.

Material	Thickness of thin films. (l_s) μm.	Measured value of α_s cm^2/ sec.	Literature value of $\alpha_s cm^2$/sec.
Indium	240	0.4935	0.4787.
	630	0.4755	
Aluminium	400	0.8156	0.8200
	600	0.8072	
Silver.	530	1.7460	1.75
	690	1.7680	
CdS	18	0.1412	0.153
	26	0.1440	

7.7. REFERENCES.

[1]. D.R.Green, J.Appl.Phys. 37, 3095 (1966).

[2]. M.J.Adams and G.F.Kirkbright, Analyst. 102, 281 (1977).

[3]. P.Korpiun, B.Merte, G.Fritch, R.Tilgner and E.Luscher: Coll.& Pol.Sci. 261, 312 (1983).

[4]. C.A.Bennett and R.R.Patty, Appl.Opt. 21, 49 (1982).

[5]. R.T.Swimm, Appl.Phys.Lett. 42, 955 (1983).

[6]. A.Lachaine and P.Poulet, Appl.Phys.Lett. 45, 953 (1984).

[7]. N.Nakayama, H .Matsumoto, A.Nakano and S. Ikegami, H. Uda and T. Ymashita, Jpn. J. Appl. Phys. 19, 703 (1980).

[8]. J.S Lee and H.B.Im, J.Mat. Sci. 21, 980 (1986).

[9]. J.S.Lee, H.B.Im, A.L.Fahrenbruch and R.H.Bube, J.Electrochem. Soc. 134, 1790 (1987).

[10]. Y.Y.Ma, A.L.Frhenbruch and R.H.Bube , Appl. Phys. Lett. 30, 423 (1977).

[11]. H.J. Hovel, in Semiconductors and Semimetals, Eds. R.K. Willardsin and A.C.Beer, Vol.II, Academic Press, Newyork (1975).

[12]. M.J.Adams and G.F.Kirkbright, Analyst. 102, 281 (1977).

[13]. P.Charpentier, F.Lepoutre and L.Bertrand, J.Appl.Phys. 53(1), 608 (1982).

[14]. C.L.Ceaser, H.Vargas, Mendes Filho Jr. and L.C.M.Miranda, Appl.Phys.Lett. 43(6), 555 (1983).

[15]. R.Glang and L.V.Greor, "Hand book in thin film technology" , Leon.I.Maisel and Reinhard Glang (Ed.), McGraw Hill : New York (1970).

[16]. Edwin K.M. Sui and Andreas Mandelis Phys. Rev. B. 34 (10), 7222 (1986)

[17] A Rosencwaig, " Photoacoustics and Photoacoustic Spectroscopy " Wiely & Sons: NewYork (1980).

CHAPTER 8

SUMMARY AND CONCLUSION

The present thesis is centered around the study of electrical and thermal properties of certain selected photonic materials. The thesis contains two parts **A** and **B.** The first phase of measurements, which is included in Part-A, involves the study of mechanisms of electrical conduction in pure single crystals of Ammonium Dihydrogen Phosphate and pressed pellets of Ammonium Iodate in various phases and those associated with different phase transitions occurring in them. DC conductivity and dielectric constant measurements were used to chracterise the materials under investigation. These measurements were carried out in a cell described in the first chapter. Some important merits of the cell are

(i) It can be used in the temperature range 80K to 420K without disturbing the vacuum conditions,

(ii) The electrical properties like electrical conductivity and dielectric constant measurements have been carried out using the same cell and

(iii) Liquid nitrogen consumption is found to be very low.

For conductivity measurements, we have used highly sensitive electrometers (Keithley model 642 & 617) .The capacitance was measured as a function of frequency as well as temperature using LF Impedance Analyser (Hewlett Packard Model 4192A.) and the dielectric constant was derived from the measured values of capacitance after eliminating the lead and fringe capacitance using standard method.

DC electrical conductivity measurements were done in single crystal of $NH_4H_2PO_4$ (ADP) along c-axis in the temperature range 80 K to 400 K. The log σ vs 10^3/ T plot obtained for ADP shows a single unmistakable peak at 147 K on cooling the sample. In the heating run it again occurs but is found to be shifted to a temperature of 148.1 K with a clear reversal in the direction of variation. It has been concluded that the anomalous variations at 147 K(148.1 K) in the conductivity plot are directly related to the paraelectric to antiferroelectric transition occurring in ADP at this temperature. It should be noted that below 400 K the conductivity plots have two straight line regions characteristics of ionic crystals. The activation energy values evaluated by making use of the straight line regions are 0.7 eV and 0.08 eV. The mechanism of phase transition and of the electron conduction process can be understood by making use of the peculiar structure configuration of the PO_4 and NH_4 tetrahedra in this material. Several authors felt doubt about the co-existence of two phases at the low temperature transition point in the case of ADP crystals. This observation undoubtfully confirms that at the transition point the crystal shows pyroelectric behaviour in addition to the antiferroelectric behaviour. Thus explains the directional change observed in the conductivity plot at the transition point.

Another important investigation made in the first phase of measurements is the dc electrical conductivity and dielectric constant measurements carried out in polycrystalline NH_4IO_3 The conductivity measurements carried out in NH_4IO_3 samples in the temperature range 300 K to 450 K show distinct λ - shaped anomaly with two straight line regions characteristics of ionic crystals. The activation energy values obtained from the two straight line regions are 1.07 eV and 0.0478 eV.

The sudden jump in the conductivity plot resulting in a λ - shaped anomaly at 363 K indicates a phase transition. On the other hand the dielectric measurements carried out in the sample at 1 kHz show that the dielectric constant increases gradually from its room temperature value of 27 and at 90^0C, its value rises sharply to 31.6 and on further increase in temperature the dielectric constant decreases forming a peak around 90^0C. The variation of dielectric constant as a function of temperature for different frequencies has also been investigated. It is observed that dielectric constant value increases as frequency increases and at the transition point these values are higher compared to its room temperature value. The anomalous change observed in the dielectric constant at the transition point is attributed to the re-orientation of the NH_4 ions in a slightly different hindered potential barrier which is in full agreement with the results of spin lattice relaxation time measurements. Such a variation of NH_4 group will make a major contribution to the orientational polarizability and explains the high value of dielectric constant at the phase transition point.

The second set of measurements involve the determination of the absolute value of the thermal diffusivity in metal phthalocyanines and its iodinated forms, in single crystals of KH_2PO_4 and in certain metallic thin films using photoacoustic technique. PA technique has found increasing interest as a non-destructive method for the determination of thermal diffusivity of solid samples in any forms. The important elements of the experimental set up for the determination of thermal diffusivity are laser beam source, an electromechanical light beam chopper, a variable temperature (resonant) PA cell, two room temperature (non-resonant) PA cells of which one can be operated using front

surface illumination and the other using rear surface illumination method and a lock-in amplifier. The above mentioned PA cells have been fabricated and using these measurements can be done successfully. Every cell incorporates a sensitive electret microphone for detecting the acoustic signal. Characterisation of cells have been done over the frequency range of interest.

Metal Phthalocyanines are important photonic materials whose thermal diffusivity measurements have been carried out using front surface excitation technique. Phthalocyanines and its metal complexes play a key role in the field of molecular semiconductors. Because of its high thermal and chemical stability phthalocyanines have become the focus of recent research. Iodine doped metal phthalocyanines are also taken up for investigation. For finding the thermal diffusivity value the amplitude of the PA signal is measured as a function of the chopping frequency for a sample of appropriate thickness l_s. The characteristic frequency f_c above which the PA signal is independent of the thermal properties of the backing material is determined from the amplitude frequency plot and thermal diffusivity α_s is calculated using the relation $\alpha_s = f_c\, l_s^2$. The results indicate that doping with iodine enhances the thermal diffusivity in a substantial manner in metal phthalocyanines.

Axis-wise measurements of thermal diffusivity carried out for the first time in single crystals of Potassium Dihydrogen Phosphate (KDP) as a function of temperature is another work presented in this thesis. Temperature varying PA cell is used for the measurements. The anisotropy in thermal conductivity of KDP crystal has been

demonstrated using PA technique. It has been found that thermal diffusivity decreases with temperature along a/b as well as c - axes.

Another important work presented in this thesis is the thermal diffusivity measurements in thin films using rear surface illumination method. In this method, if $\Delta\phi$ is the total phase difference of the phase of signals from the front surface and rear surface of the thin film sample, the graph between $\sqrt{\omega}$ and $\Delta\phi$ will be a straight line and its slope is given by $\left(\frac{1}{2\alpha_s}\right)^{\frac{1}{2}} l_s$, ω being the angular frequency, α_s, the thermal diffusivity of the sample and l_s, the sample thickness. Thin films of indium ,aluminium , silver and cadmium sulphide prepared from vacuum coating technique have been used for measurements. Thermal diffusivity values obtained using this cell show close agreement with the previously reported values.

In conclusion, we have studied the electrical conduction mechanism in various phases of certain selected photonic materials and those associated with different phase transitions occurring in them. A phase transition leaves its own impressions on the key parameters like electrical conductivity and dielectric constant. However, the activation energy calculation reveals the dominant factor responsible for conduction process.

PA measurements of thermal diffusivity in certain other important photonic materials are included in the remaining part of the research work presented in this thesis. PA technique is a promising tool for studying thermal diffusivities of solid samples in any form. Because of its crucial role and common occurrence in heat flow problems, the thermal diffusivity determination is often necessary and knowledge of thermal diffusivity can inturn be used to calculate the thermal conductivity. Especially,

knowledge of the thermal diffusivity of semiconductors is important due to its relation to the power dissipation problem in microelectronic and optoelectronic devices which limits their performances. More than that, the thermal properties, especially those of thin films are of growing interest in microelectronics and microsystems because of the heat removal problem involved in highly integrated devices. The prescribed chapter of the present theis demonstrates how direct measurement of thermal diffusivity can be carried out in thin films of interest in a simple and elegant manner using PA techniques. Although results of only representative measurements viz; thermal diffusivity values in Indium, Aluminium, Silver and CdS thin films are given here, evaluation of this quantity for any photonic and / electronic material can be carried out using this technique in a very simple and straight forward manner.